Norwegian University of Life Sciences

Master's Thesis 2018 60 ECTS
Faculty of Chemistry, Biotechnology and Food Sciences

Implementation of a two-plasmid CRISPR/Cas9 system in *Lactobacillus plantarum*: A new approach in the development of a novel vaccine against *Mycobacterium tuberculosis*

Kamilla Wiull
Master of Technology, Chemistry and Biotechnology

Acknowledgements

The work presented in this thesis was carried out at the Faculty of Chemistry, Biotechnology and Food science of the Norwegian University of Life Sciences, supervised by Dr. Geir Mathiesen.

I want to thank everyone who has helped me in my work on this thesis. First and foremost, I would like to thank my supervisor Dr. Geir Mathiesen. I am so grateful for all the conversations and discussions we have had regarding this thesis. Despite all challenges I have met through the experimental work, you have always kept my spirit up. I would also like to thank the rest of the PEP group, and especially former department engineer Lise Øverland. Furthermore, thank you to Dr. Morten Kjos for sharing your knowledge on the CRISPR/Cas system.

Last but not least, I am beyond grateful for the support and encouragement provided by my family and boyfriend. You are all invaluable to me.

Ås, December 2018

Kamilla Wiull

Abstract

Tuberculosis (TB) is the leading cause of deaths from a single infectious agent, and in 2017 1.7 million people died from TB. To date the only available vaccine against the disease is the bacille Calmette-Guèrin (BCG) vaccine. The BCG vaccine does not ensure full protection against the mature form of TB, and is not recommended to immunocompromised patients. Therefore, a new and more effective vaccine is urgently needed. This study is a part of a larger project with a long-term goal to develop mucosal vaccines, utilizing the lactic acid bacteria (LAB) *Lactobacillus plantarum* as delivery vectors of antigens. LAB occurs in a wide range of habitats, ranging from food products such as fruit and dairy, but also human mucosal surfaces such as the small intestine and colon. Lactobacilli are natural inhabitants of the human gastro intestinal tract (GIT) and are generally regarded as safe (GRAS). Some Lactobacilli are believed to have probiotic properties and live in close association with the intestinal epithelium and have shown immunomodulatory effects in human. These properties make Lactobacilli, such as *L. plantarum*, an ideal candidate as a delivery vector of immunogens.

In the present study, pSIP inducible vectors for cytoplasmic and membrane anchoring of the TB fusion antigen Ag85B_TB10.4 in *L. plantarum* were constructed, and production of surface localized antigen was confirmed. Currently, the production of the antigen is plasmid based. To reduce the number of heterologous genes of the recombinant *L. plantarum*, it is desirable to integrate the antigen production into genome of the bacteria. In this thesis, methods for utilization of the CRISPR/Cas system was attempted developed for integration of the antigen. To simplify integration, as it is independent of helper genes unlike the pSIP system, construction of vectors for constitutive production of Ag85B_TB10.4 were attempted. Evaluation of the functionality of the CRISPR/Cas system in *L. plantarum* was performed through experiments of gene editing, replacement and depletion with Cas9, $Cas9^{D10A}$ and dCas9.

In conclusion, Ag85B_TB10.4 was successfully anchored to the cell membrane of *L. plantarum* by using the pSIP system, while construction of a vector for constitutive production of Ag85B_TB10.4 failed. Conceivably due to toxicity of the constitutive production of the antigen in *E. coli*. The CRISPR/dCas9 system was successfully developed, and reduction of transcripts of target genes was confirmed by ddPCR. Gene editing and exchange with Cas9 and $Cas9^{D10A}$ gave the expected phenotype, but no mutations were detected from DNA sequencing. These methods require further optimisations.

Sammendrag

Tuberkulose (TB) er hovedårsaken til dødsfall forårsaket av en infeksjonssykdom. I 2017 døde 1.7 millioner mennesker av TB. Per dags dato er bacille Calmette-Guèrin (BCG) vaksinen den eneste tilgjengelige vaksinen som beskytter mot sykdommen. En stor svakhet ved BCG-vaksinen er at den ikke sørger for full beskyttelse mot den modne og smittsomme formen av TB, og anbefales ikke til immunkompromitterte pasienter. På grunn av dette er utvikling av en ny vaksine mot TB høyst nødvendig. Denne studien er en del av et større prosjekt, hvor langtidsmålet er å utvikle slimhinne vaksiner, ved å utnytte melkesyrebakterien *Lactobacillus plantarum* som leverings vektor av antigener. Melkesyrebakteriene finnes i mange varierte habitater, fra matprodukter som frukt og melkeprodukter, men også som en del av den naturlige tarmfloraen hos mennesker. På bakgrunn av dette regnes melkesyrebakteriene generelt som trygge. Noen Laktobasiller er også kjent for å ha probiotiske egenskaper, nær tilknytning til tarmepitelet, samt immunmodulerende effekter. Disse egenskapene bidrar til at Laktobasiller, som *L. plantarum*, anses som ideelle kandidater som leverings vektorer av immunogener.

I denne studien ble pSIP induserbare vektorer for intracellulær og membranankret produksjon av TB hybridantigenet Ag85B_TB10.4 i *L. plantarum* konstruert, og produksjon av overflate lokalisert antigen ble bekreftet. Foreløpig har produksjonen av antigener vært plasmidbasert. For å redusere antall heterologe gener i rekombinante *L. plantarum*, er det fordelaktig å integrere antigen produksjonen inn i genomet til bakterien. I denne oppgaven ble ulike metoder for bruk av CRISPR/Cas systemet forsøkt utviklet, for integrering av antigenet. For å forenkle integreringen ble det forsøkt konstruert vektorer for konstitutiv produksjon av Ag85B_TB10.4. I motsetning til pSIP systemet, avhenger ikke det konstitutive ekspresjonssystemet av andre gener for aktivering. Funksjonaliteten til CRISPR/Cas systemet i *L. plantarum* ble evaluert ved utførelse av eksperimenter for gen-editering, -utbytte og -nedregulering mediert av Cas9, $Cas9^{D10A}$ og dCas9.

Arbeidet som er beskrevet i denne masteroppgaven viser at en vektor for overflateankret Ag85B_TB10.4 produsert av pSIP systemet ble konstruert, mens konstruksjon av en vektor for konstitutiv produksjon av Ag85B_TB10.4 mislyktes. En mulig årsak til den mislykkede konstruksjon kan være at konstitutiv produksjon av antigenet er toksisk for *Escherichia coli*. CRISPR/dCas9 systemet, for nedregulering av genuttrykk, ble utviklet og nedreguleringen av målgenene ble bekreftet med ddPCR. Gen-editering og -utbytte av gener med Cas9 og $Cas9^{D10A}$ produserte den forventede fenotypen, men sekvensering avslørte villtype sekvens. Disse metodene behøver derfor videre optimering.

Abbreviations

BCG	Bacillus Calmette-Guérin
BSA	Bovine Serum Albumin
Cas protein	CRISPR associated protein
CRISPR	Clustered regularly interspaced palindromic repeats
CRISPRi	CRISPR interference
crRNA	CRISPR RNA
DC	Dendritic cell
ddPCR	Droplet digital PCR
dNTP	Deoxyribonucleotide triphosphate
FITC	Fluorescein isothiocyanate
GIT	Gastrointestinal tract
GRAS	Generally Recognised As Safe
HDR	Homology directed repair
HRP	Horseradish Peroxidase
IgA	Immunoglobulin A
LAB	Lactic acid bacteria
NHEJ	Non-homologous end joining pathway
PAM	Protospacer adjacent motif
PAMP	Pathogen-associated molecular patterns
PCR	Polymerase Chain Reaction
SDS-PAGE	Sodium dodecyl sulphate polyacrylamide gel
SgRNA	Single guide RNA

TALEN	Transcription activator-like effector nucleases
TB	Tuberculosis
tracrRNA	Trans-activating crRNA
ZFN	Zinc-finger nucleases

Table of contents

1 Introduction

Lactic acid bacteria (LAB) are a genetically and ecologically diverse group of Gram-positive bacteria. Due to their role in fermentation and conservation of foods, LAB have been of interest to humans for hundreds of years. However, the last three decades the interest has significantly increased due to their believed health-promoting effects as probiotics. LAB strains are also robust and versatile organisms, able to withstand harsh conditions and even survive through the human gastrointestinal tract (GIT). This has made them attractive candidates as delivery vectors for therapeutic molecules. LAB are the most abundant group of Gram-positive bacteria used in industry and medicine and represent a major economic factor.

Another promising potential of the lactic acid bacteria are as live delivery vectors of medical interesting proteins such as immunogens. To progress from vector produced immunogens, which often also introduce unnecessary heterologous genes, to integration of the expression system into the genome of the bacteria a gene editing system like the CRISPR/Cas system could be utilized.

After the discovery of clustered regulatory interspaced short palindromic repeats (CRISPR), it has revolutionized genomic engineering. The CRISPR-Cas9 system, naturally responsible for adaptive immunity in prokaryotes, can in principle generate double stranded breaks at any genomic locus, making it widely available. The present study describes the construction of recombinant *Lactobacillus plantarum* for antigen production, as well as the development of a CRISPR/Cas system in *L. plantarum* WCFS1.

1.1 Lactic acid bacteria

Lactic acid bacteria (LAB) are gram positive, non-sporulating rods or cocci. They are facultative anaerobe and can perform fermentation of carbohydrates by two different metabolic pathways, either by the homofermentative pathway or the heterofermentative pathway. From the homofermentative pathway, lactic acid is the main end product, while the heterofermentative pathway also produces CO_2, acetic acid and/or ethanol in equal amounts (Kandler, 1983).

LAB occurs in a wide range of habitats, e.g. different food products such as fruit, vegetable, meat and dairy, but also in mucosal surfaces of animals such as the small intestine, colon and

vagina (Makarova et al., 2006). As they are natural inhabitants of animals' gastro intestinal tract (GIT), LAB has not been associated with any pathogenic effect. Rather, they have a "Generally regarded as safe status" (GRAS).

In addition to being GRAS organisms, some specific lactic acid bacterial strains are being marketed as probiotic with health-promoting effect for the consumer. Probiotics are defined as "live microorganisms which administered in adequate amounts confer a health benefit on the host" by the Food and Agriculture Organization/World Health organisation. A key property of probiotic bacteria is the ability to survive the passage through the GIT. To do so, the bacteria must have protection systems against the low pH in the stomach, digestive enzymes and the bile in the small intestine (Jensen et al., 2012).

As well as being able to survive through the GIT, combined with several other properties LAB makes an ideal candidate as a live delivery vector of immunogens. Some of the most important properties are the close association with the intestinal epithelium, immunomodulatory properties and that the consumption of LAB in large amounts are regarded as safe (Mohamadzadeh et al., 2009).

1.2 *Lactobacillus plantarum*

The largest group of lactic acid bacteria are the genus *Lactobacillus,* which comprises of more than 200 different species and subspecies(Sun et al., 2015). One of the most versatile lactic acid bacteria, *Lactobacillus plantarum,* belongs to this genus. *L. plantarum* can be found both in different foods and in the GIT. It is also involved in the spoilage of foods, such as wine, meat and orange juice (de Vries et al., 2006).

L. plantarum was selected as the first to be completely sequenced based on its accessible to high efficiency genetic transformation, as well as it was found to efficiently survive the GIT making it a potentially ideal probiotic or delivery strain (de Vos, 2011). In 2003, Kleerebezem and co-workers sequenced the full genome of *L. plantarum* WCFS1, and it was found to have one of the largest genomes known for lactic acid bacteria. The authors suggested that the flexible and adaptive behaviour of the bacteria was reflected by the relatively large amount of regulatory and transport proteins (Kleerebezem et al., 2003). To date, there are 72 complete genome sequence assemblies of different *L. plantarum* strains available in the NCBI database. There is a lot of genetic variation among the sequenced *L. plantarum* strains (Molenaar et al., 2005), with *L. plantarum* WCFS1 perhaps being one of the best studied strains.

1.3 Gene expression systems in *L. plantarum*

As described in section 1.2 *L. plantarum* is a candidate for delivery of immunogens, since it is GRAS, able to survive GIT and a potential probiotic. However, because over expression of a heterologous protein can lead to a significant amount of stress on the bacteria, it is important to evaluate the gene expression system to be used.

1.3.1 Inducible gene expression systems

Gene expression with an inducible system allows gene regulation controlled by different additives, e.g. lactose and xylose or by other changing parameters such as temperature or pH (Diep et al., 2009). The dependency of an additive for activation of the inducible system can both be an advantage and a disadvantage. If overproduction of a protein to a maximum level is wanted, an inducible expression system is more feasible. For proteins that can be toxic to the host, an inducible expression system allows the biomass of the bacteria to increase before activation of the expression system and production of the protein, which may decrease the toxicity of some proteins (Tauer et al., 2014). Bacteriocin induced expression systems are another method available in LAB and has shown to drive high-level gene expression in *L. sakei* and *L. plantarum* (Mierau & Kleerebezem, 2005; Sørvig et al., 2003; Sørvig et al., 2005a) . The two most exploited bacteriocin inducible systems are the so called NICE-system (nisin controlled gene expression system) (Kuipers et al., 1995) or the pSIP-based inducible system (Mathiesen et al., 2004).

In *Lactobacillus*, the NICE-system is either used as a two-plasmid system, or one plasmid system where the regulatory genes are integrated in the chromosome of a designed host strain. The pSIP system has an advantage over the NICE-system in *Lactobacillus*, as the pSIP-vector in the pSIP system serve as a one plasmid expression system and are built up of cassettes with restriction sites, allowing easy exchange of all parts through restriction enzyme digestion and ligation (Sørvig et al., 2003). The pSIP-vector are based on genes that regulates the production of the bacteriocins sakacin A and sakacin P. The pSIP expression vector (Figure 1.1) contains genes coding for a histidine-kinase (SppK), which senses the SppIP pheromone, and a response regulator (SppR). These genes are under the control of an inducer peptide promoter, P_{sppIP}. However, the gene originally encoding the inducer peptide SppIP are deleted in these expression vectors. The P_{sppIP} therefore only regulates transcription of the genes coding for the histidine-kinase and the response regulator. Genes of interest expressed with the pSIP expression system are translationally fused to the P_{sppA} (Figure 1.1), which is controlled by the peptide pheromone. To start expression of the genes, the inducer peptide SppIP is added to the

growth medium, which ultimately leads to binding between the phosphorylated response regulator and segments of the P_{sppA} and P_{sppIP}. The binding leads to an explosive production of the target protein, the histidine-kinase and the response regulator (Risøen et al., 2000). The pSIP-system has later been further modified for protein secretion (Mathiesen et al., 2008; Mathiesen et al., 2009) and for anchoring of heterologous proteins to the bacterial cell surface (Fredriksen et al., 2010; Fredriksen et al., 2012; Kuczkowska et al., 2017).

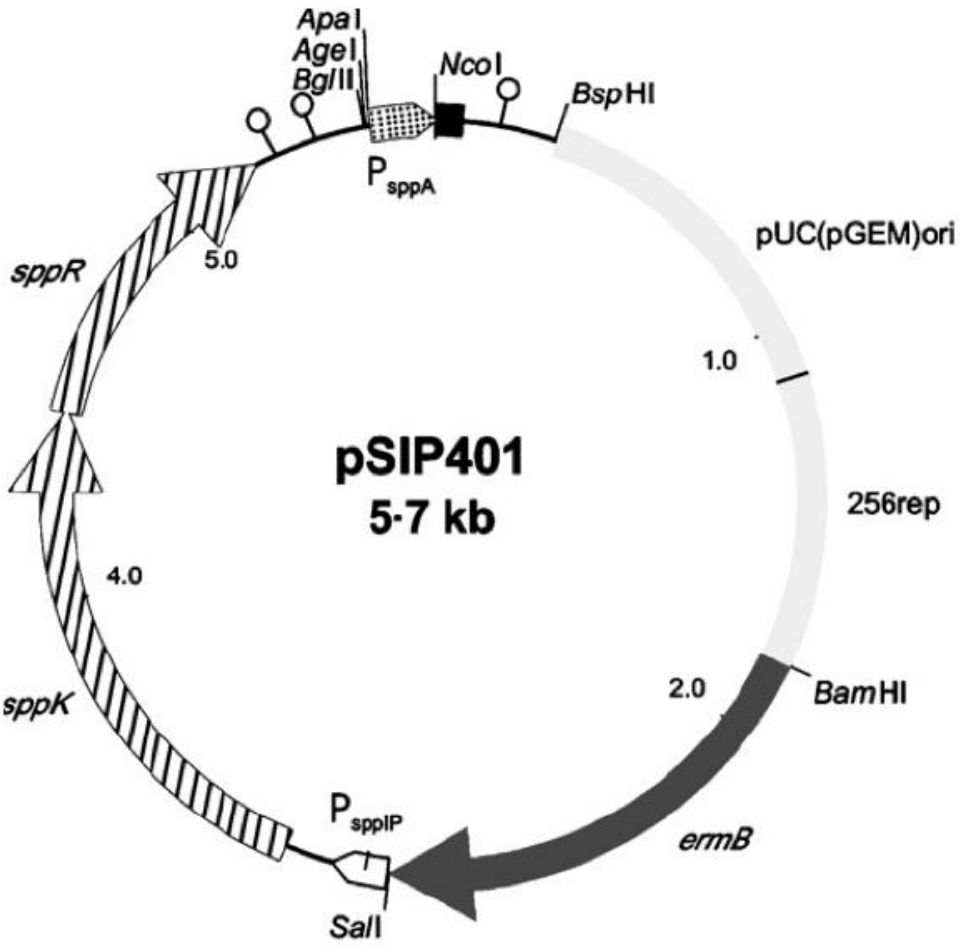

Figure 1.1. Schematic representation of pSIP401. Light grey regions show replicons pUC(pGEM)ori from *E. coli* and 256rep from *L. plantarum*. Dark grey regions mark the Erythromycin (*ermB*) resistance gene. The inducible promoter P_{sppIP} is shown by the white region. The vertically hatched regions show the histidine kinase (*sppR*) and response regulator genes. Dotted region shows the inducible promoter P_{sppA}. The black box is a multiple cloning site region. Target genes will be cloned downstream of the P_{sppA} promoter. The figure is taken from Sørvig et al. (2005).

1.3.2 Constitutive gene expression systems

The strength of a constitutive promoter can vary, which can be used to ensure expression of genes at a suitable level for different applications. For expression of a potential toxic protein, a weak constitutive promoter can be chosen to keep proteins levels at a non-toxic level. For applications where it is desirable to produce as much protein as possible, a strong constitutive promoter can be chosen. Unlike the inducible promoter, the constitutive promoter is not dependent on other genes for activation, thereby making the system less complicated. This might be beneficial e.g. if integration into the chromosome is desirable. Integration of a gene controlled by an inducible promoter would require concomitant integration of the helper genes, while a gene controlled by a constitutive promoter would be expressed on the genome as long as the promoter is integrated. Several constitutive promoters have been exploited in heterologous gene expression studies in *L. plantarum.* Rud et al. (2006) constructed a library consisting of 35 constitutive promoters, where some of the most potent constitutive promoters showed higher activities than those of the inducible pSIP system. Promoters from the synthetic promoter library was constructed in the inducible vector pSIP409 in *L. plantarum* NC8, by replacing the inducible promoter of the vector with synthetic constitutive promoters. Sasikumar et al. (2014) constitutively expressed the heterologous enzyme oxalate decarboxylase, fused to the signal peptide Lp_0373, using the homologous promoter P_{ldhL} in *L. plantarum* WCFS1. Tauer et al. (2014) showed constitutive expression of the model protein mCherry with four different constitutive promoters, where two where homologous, one where heterologous and one where the synthetic promoter P_{11} from the synthetic promoter library made by Rud et al. (2006), in *L. plantarum* CD033.

1.4 Bacteria as vectors for antigen delivery

Most infectious agents enter the body through mucosal surfaces, thus mucosal immune responses are most efficiently induced by immunization through oral, nasal, rectal or vaginal routes. However, most vaccines in use today are administered by injection. The reason for this, is because the amount of antigen delivered into the body by an injection is a known quantity and results in generation of specific antibodies and other immune cells, that can be measured in blood samples. Measurements of the mucosal immune responses on the other hand is more complicated, as the uptake of the antigens can vary depending on the mucosal surface (Neutra & Kozlowski, 2006).

Pathogenic bacteria with reduced virulence have been successfully used as delivery vectors of antigens to mucosal sites. Pathogenic bacteria contain pathogen-associated molecular patterns (PAMPs), which include lipopolysaccharides (LPS), lipoproteins and flagellin. These molecular patterns gives pathogenic bacteria an advantage over other non-pathogenic bacteria as delivery vectors, because the PAMPs are recognized, and activates the immune system (Toussaint et al., 2013). However, there is a risk that attenuated pathogenic bacteria may reactivate their virulence. Although the pathogen used as delivery vectors are attenuated, in immunocompromised patients they still have the potential to proliferate freely and therefore poses a significant health risk (Sartori, 2004).

To overcome the safety problems associated with attenuated pathogenic bacteria, GRAS bacteria such as lactic acid bacteria, have been extensively studied as delivery vectors of therapeutic molecules. In addition to LAB strains having a GRAS status, another advantage is the believed potential for LAB to stimulate both systemic and mucosal immune responses by the mucosal route of administration (Wells & Mercenier, 2008). This may lead to the production of immunoglobulin A (IgA), which can be a controlling factor in bacterial persistence and uptake. These properties make LAB attractive candidates for the delivery of heterologous antigens. Some lactic acid bacteria, such as *L. lactis* and *L. plantarum* are also proved to survive the passage through the GIT and withstand the low pH of the stomach (Wells & Mercenier, 2008).

Recombinant strains can produce heterologous proteins to be localized either in the cytosol, at the cell surface or secreted into the environments. All protein anchoring mechanisms are described in section 1.4. A landmark study by Bermudez-Humaran et al. (2005) performed on mice, revealed the protective effects of live *L. lactis* strains expressing cell wall-anchored E7 Ag and a secreted form of IL-12 to treat HPV-16-induced tumours by mucosal administration. When the mice were challenged with a lethal level of tumour cells expressing E7, the immunized mice showed full prevention of tumour growth. In another experiment, mice received therapeutic immunization with *L. lactis* seven days after tumour cell-injection. The therapeutic immunization showed tumour regression in treated mice (Bermudez-Humaran et al., 2005).

However, the use of recombinant bacteria raises some concerns regarding patient and environmental safety. Clinical reports have also been made on infection with *Lactobacillus* spp. in severely immunocompromised patients, although these cases are rather rare (Doron & Snydman, 2015). Other concerns include how heterologous genes affect LAB, and whether

such genes will affect their status as safe. There are also uncertainties about unwanted host responses to recombinant gene products, like allergenicity or autoimmunity. Other problems associated with recombinant strains are propagation outside the host and gene transfer to other organisms (Wells & Mercenier, 2008). This leads to a strong preference to *L. lactis* as delivery vector, because this lactic acid bacteria is able to survive through the GIT, without colonizing, and therefore limits the concern of propagation in the environment (Song, A. A.-L. et al., 2017).

For live bacteria as delivery vectors surviving through the entire GIT, a solution might be to eliminate essential genes. Steidler et al. (2003) eliminated the thymidylate synthase gene *thyA* in *L. lactis* and replaced it with a gene encoding interleukin-10. As a result, Steidler and co-workers generated bacteria entirely dependent on the presence of thymidine in the environment. These *thyA* depleted bacteria would not survive in the environment without a steady supply of thymidine. In a phase I trial with transgenic bacteria expressing interleukin -10 for treatment of Chron's disease, it was shown that the transgenic bacteria did not survive outside and was safe for the host (Braat et al., 2006).

Although live bacteria as delivery vectors in vaccines are extensively researched, a licensed vaccine is yet to come. However, a genetically modified version of the bacille Calmette-Guérin (BCG) vaccine is currently in phase III of clinical testing. In this version, the immunogenicity of the BCG-vaccine is improved by replacing the intrinsic urease C encoding gene with the listeriolysin encoding gene from *Listeria monocytogenes.* The delivery vector is the live, attenuated bacteria *Mycobacterium bovis* (Nieuwenhuizen et al., 2017).

1.5 Secretion and anchoring of proteins in Gram-positive bacteria

In Gram-positive bacteria, the cytoplasmic membrane is covered with a thick peptidoglycan layer, unlike the Gram-negative bacteria where there is only a thin layer of peptidoglycan. However, to compensate for the thin peptidoglycan layer, Gram-negative bacteria contains an additional outer membrane. All proteins are synthesized at the ribosomes (Balchin et al., 2016), but not all have their function intracellularly. Proteins functioning on the outside of the cytosol has a special, mainly N-terminal, peptide sequence, giving the cell information about the end-localization of the protein (Kleerebezem et al., 2010). Secretion of proteins with a N-terminal peptide sequence are simpler in Gram-positive bacteria than in Gram-negative bacteria, since

they are monoderm. This makes Gram-positive bacteria promising candidates for production of secreted proteins.

There are seven known protein secretion pathways for Gram-positive bacteria: the secretion (sec), twin-arginine translocation (Tat), flagella export apparatus (FEA), fimbrillin-protein exporter (FPE), holing (pore forming), peptide efflux ABC and the WXG100 secretion system (Wss) pathways (Desvaux et al., 2009).

Most proteins are secreted by the Sec translocase (Figure 1.2), which mediates protein transfer across the cytoplasmic membrane in Gram-positive bacteria. Proteins that are translocated by the Sec pathway are targeted through a N-terminal signal peptide, which are removed after translocation, consisting of three distinct parts: a N-domain with 1-3 positively charged amino acids, a hydrophobic domain of 10-15 amino acids (H-domain) and a polar C-domain with a signal peptidase cleavage site (Driessen & Nouwen, 2008). If the cleavage site of the signal peptide contains the motif A-X-X-A the peptide will be cleaved by signal peptidase I, this leads to secretion of the protein (van Roosmalen et al., 2004). However, if the signal peptide contains the motif L-X-X-C (lipobox) it is cleaved by signal peptidase II. Subsequently to the cleavage by signal peptidase II, the protein is covalently attached to the lipid bilayer (Sutcliffe & Harrington, 2002). All *Lactobacillus* genomes encode a single signal peptidase II, while the number of signal peptidase I ranges from one in most species to three in *L. plantarum* (Kleerebezem et al., 2010).

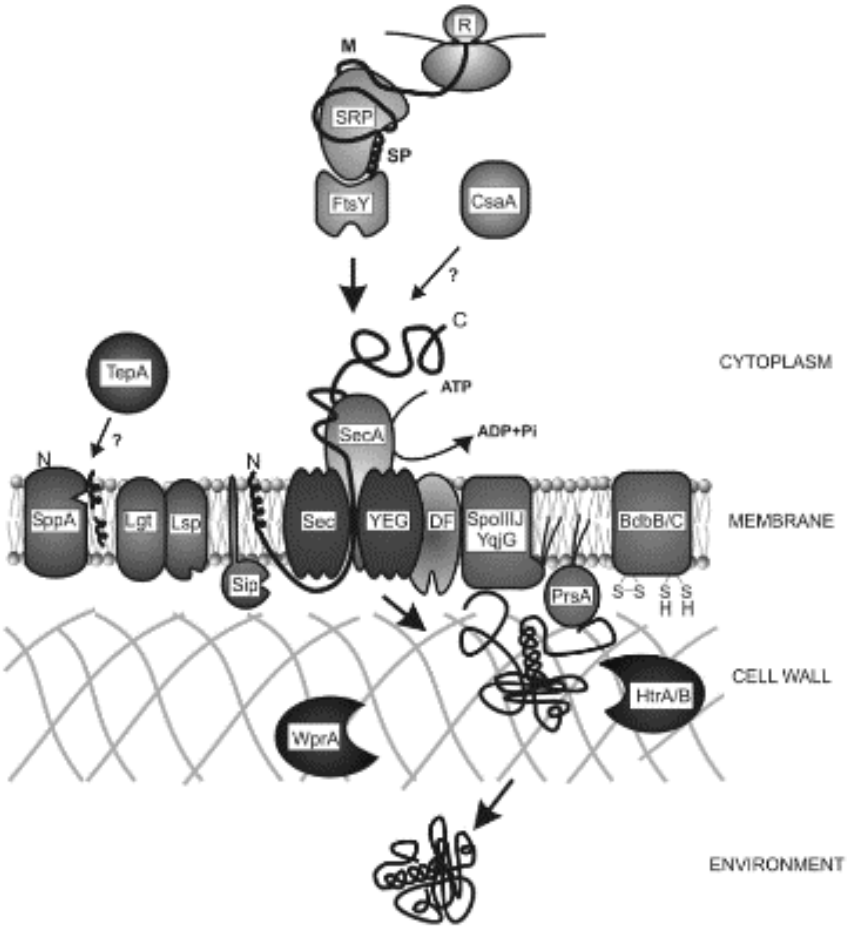

Figure 1.2. Schematic illustration of the Sec secretion system and components involved. Secretory proteins are synthesized on ribosomes in the cytoplasm as preproteins with a N-terminal signal peptide. A signal recognition particle (SRP) binds to the signal peptide of the preprotein. The protein FtsY binds to SRP for stabilisation during the transport of the preprotein to the Sec translocase. The Sec translocase is a protein complex embedded in the cell membrane and consists of an ATP driven motorprotein (SecA) and a protein channel SecYEG. The signal peptide is cleaved by a signal peptidase during or directly after the translocation. For more details about the other components illustrated on the figure see Tjalsma et al. (2014). The figure is taken from Tjalsma et al. (2014).

Gram-positive bacteria employ several different mechanisms for anchoring of protein to the cell surface, either in the membrane or to the cell wall. The anchoring mechanisms can be sorted into four different classes of either transmembrane anchoring, lipoprotein- and LPXTG-anchoring or non-covalent binding to the cell wall. Figure 1.3 shows a schematic illustration of the different anchoring mechanisms.

A protein containing a L-X-X-C motif (lipobox) in the signal peptide leads to lipoprotein anchoring to the plasma membrane. After complete secretion of the protein through the Sec pathway, the enzyme diacylglycerol transferase couples cysteine (C) of the lipobox to a

phospholipid in the plasma membrane by transferring a diacyl-group to the SH-group of the cysteine (Desvaux et al., 2006). Following the lipidation, Signal peptidase II cleaves the Cys-residue N-terminally, which leads to the anchoring of the mature protein to the membrane (Kleerebezem et al., 2010).

This makes it possible to exploit the anchoring of proteins in the development of bacterial vectors for antigen delivery by translationally fusing antigens with anchoring motifs (Desvaux et al., 2006). The choice of anchoring mechanism must be carefully selected when the goal is to anchor a heterologous protein, e.g. a potential immunogen, to Gram-positive bacteria. One aspect to consider is how exposed the protein should be to the extracellular environment. The protein must be able to reach the its interaction partner, but on the other hand, it could be beneficial to be more embedded in the cell membrane to, which may protect the protein from the harsh environment from in the GIT (Michon et al., 2016). In this study, proteins were anchored by lipoprotein anchoring.

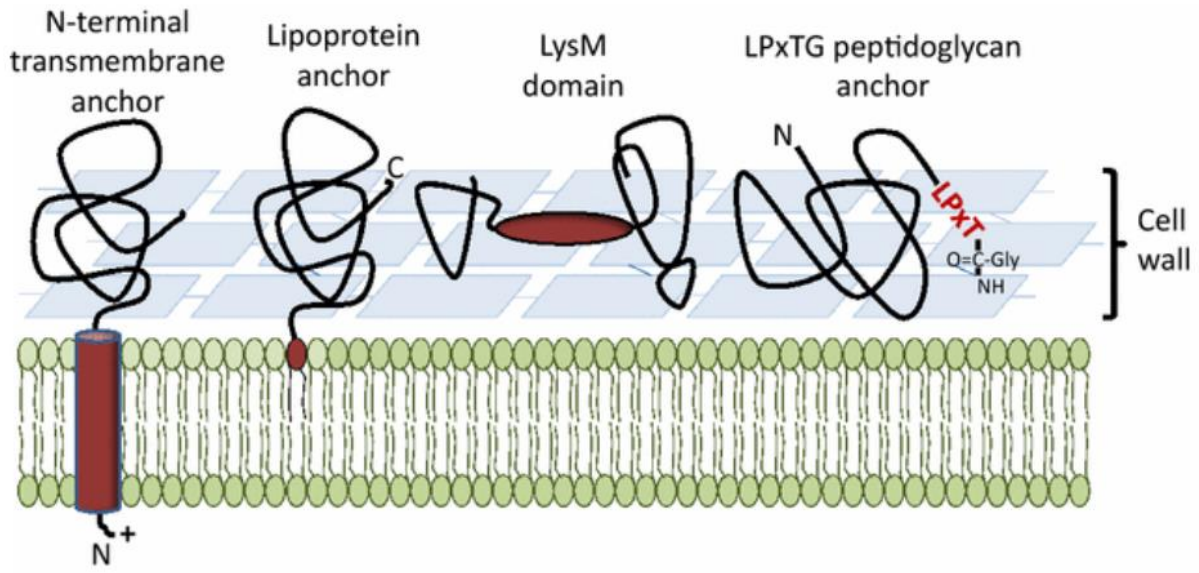

Figure 1.3. Schematic overview of the different anchoring mechanisms. The most common anchoring mechanisms in *Lactobacillus* are illustrated in the figure. All four mechanisms are based on either covalent or non-covalent binding to the cell membrane or the cell wall. Shown in red are the binding motifs/domains. The figure is taken from Michon et al. (2016).

1.6 Tuberculosis

According to the World Health Organization's Global Tuberculosis report from 2017, Tuberculosis (TB) is the ninth leading cause of deaths worldwide and the leading cause of deaths from a single infectious agent, ranking above HIV/AIDS. In 2017 there were an estimated 1.7 million people died of TB and 10.4 million people fell ill with TB in 2017. An increasing threat is the prevalence of drug-resistant TB, with 490 000 million cases of multidrug-resistant TB in 2017. TB is normally treated for six months with antibiotics, but for patients with drug resistant TB, the treatment can take up to twenty months.

Mycobacterium tuberculosis is the causative agent of TB. The *M. tuberculosis* is taken up by phagocytic cells which either leads to destruction of the bacteria, or induction of an inflammatory response which leads to recruitment of immune cells and later the formation of granulomas (Russell et al., 2010). The bacterium can stay latent in granulomas for years. *M. tuberculosis* is released when the granulomas dies and can end up in the lungs and is spread by aerosols.

TB is most common in poor countries and among people who are malnourished, immunocompromised, homeless or imprisoned. The question of why these vulnerable groups have reduced resistance is not yet answered. Vaccination is the most effective tool to defeat TB, and to date the only available vaccine is the bacille Calmette-Guèrin (BCG) vaccine. The BCG vaccine does not ensure full protection against the mature form of TB, pulmonary- or lung-TB, which is the contagious and transmittable form of the disease. Neither is the BCG vaccine recommended for use in HIV-infected or other immunocompromised patients (Crum-Cianflone & Sullivan, 2017). Therefore, a new and more effective vaccine than the BCG-vaccine is urgently needed.

However, research have been done on developing a novel vaccine against TB. According to the World Health Organization Global Report on Tuberculosis from 2017, there are 12 vaccine candidates in clinical trials. In addition to these, the use of lactic acid bacteria (LAB) has been explored as a vector for TB-antigen delivery to mucosal sites. Kuczkowska et al. (2016) successfully surface displayed and expressed a fusion antigen from *M. tuberculosis* on *L. plantarum*. The fusion antigen comprised the two antigens Ag85B and ESAT-6 and was anchored to the bacterial cell by two different mechanisms, a lipoprotein anchor and a covalent cell wall anchor. Proteins from the antigen 85 family are the most commonly used *M. tuberculosis* antigens. Another family of proteins that have shown strong antigenic properties

are proteins from the ESAT-6 family (Armitige et al., 2000; Okkels & Andersen, 2004). The study showed that strains with different anchoring both induced immune response in mice after nasal or oral immunization (Kuczkowska et al., 2016). However, although ESAT-6 have shown strong antigenic properties, it is also a valuable diagnostic reagent. Therefore, finding other antigens inducing strong immune responses are important. A protein that has been raising interest as a substitute for ESAT-6 is the *M. tuberculosis* expressed protein TB10.4, which is strongly recognized in infected humans (Dietrich et al., 2005; Kou et al., 2018). The H4:IC31 BCG booster vaccine comprises the fusion protein Ag85B-TB10.4 and is one of the 12 vaccine candidates in clinical trials. As of 2017, it was in phase II of clinical testing.

1.7 The CRISPR/Cas9-system

The Clustered Regularly interspaced short palindromic repeat (CRISPR) system is an array built up of nucleotide sequences called repeats and spacers and is a defence mechanism against invading agents in bacteria and archaea (Sorek et al., 2008). The first CRISPR array was described by Ishinio and co-workers in 1987, who found 14 repeats of 29 base pairs, interspersed by 32-33 base pairs of non-repeating spacer sequences in *E. coli* (Ishino et al., 1987; Nakata et al., 1989). Similar CRISPR arrays were later found in other bacteria and archaea, for example *Thermotoga maritima* and *M. tuberculosis* (Hermans et al., 1991; Nelson et al., 1999). As sequencing of full genomes became available, researchers were able to perform genome-wide computational searches for CRISPR arrays. These analyses revealed that such CRISPR arrays was found in approximately 40% and 90% of sequenced bacterial and archaeal genomes, respectively (Grissa et al., 2007). Simultaneously, four genes encoding the CRISPR associated protein (Cas protein), located adjacent to the repeat arrays was identified (Jansen et al., 2002). Later, another 25-45 additional Cas encoding genes was found in multiple prokaryotic genomes. These genes are not found in genomes lacking the CRISPR arrays (Haft et al., 2005). Several hypotheses were made regarding the function of the CRISPR arrays. The repeats were suggested to be involved in replicon partitioning, that they were mobile elements or involved in DNA repair (Jansen et al., 2002; Makarova et al., 2002; Mojica et al., 1995). However, in 2005 three individual research groups reported that the spacer sequences often contained plasmid- or phage-derived DNA. Based on these findings, they suggested that the CRISPR arrays mediated immunity of the host against invading agents (Sorek et al., 2008).

The Cas proteins (Figure 1.4) has since its discovery been established as important components for simplifying genome engineering. An advantage the CRISPR-system holds over previously used genetic editing tools, such as zinc-finger nucleases (ZFN) and transcription activator-like effector nucleases (TALEN), is it simplicity. ZFN and TALENs requires labourous engineering of target specific proteins for each new experiments, while the Cas-protein in CRISPR can remain the same (Kim & Kim, 2014). The Cas-protein is an endonuclease that induces double stranded break in DNA. Several different Cas9-proteins exists in prokaryotes, but the proteins are highly variable in sequence and size. However, all known Cas9 enzymes have two domains: the HNH and RuvC domains. The HNH domain cleaves the DNA strand complementary to the single guide RNA (SgRNA) sequence, while the RuvC nuclease domain cleaves the non-complementary strand. Together, the HNH and RuvC domains assure double-stranded DNA breaks (Jinek et al., 2014). While the HNH and RuvC domains is responsible for cleavage of the DNA, Cas9 enzymes also contains a highly conserved arginine-rich region, which is thought to mediate binding of DNA (Sampson et al., 2013).

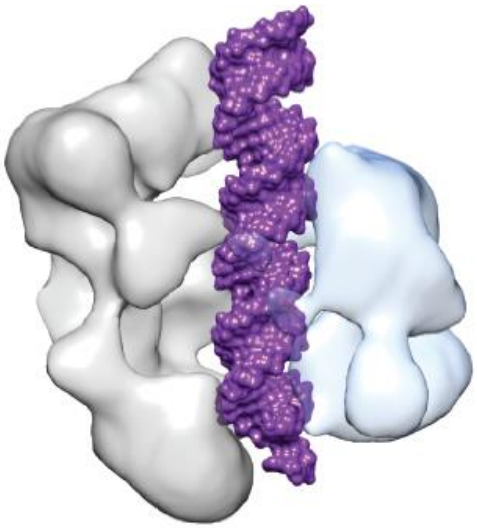

Figure 1.4. The 3-D structure of the CRISPR-associated (Cas) protein. The Cas9 protein consists of two catalytical domains, the RuvC and the HNH domains, which together with the SgRNA induced double stranded breaks in the DNA. If one of the domains are mutated, the protein will only induce single stranded break of the DNA. In catalytically inactive dead Cas (dCas), both RuvC and HNH are mutated. The Cas protein contains a conserved, arginine-rich region which is believed to mediate the binding of the DNA. The figure is taken from (Kim & Kim, 2014).

Several mutants have been made from the model Cas9 enzyme, derived from *Streptococcus pyogenes* (Sp). In the SpCas9 mutant $Cas9^{D10A}$, an Aspartate residue in position 10 of the protein has been changed to Alanine, resulting in inactivation of the RuvC domain. With only

one functioning endonuclease domain in $Cas9^{D10A}$, only single stranded DNA breaks are induced when binding DNA. In the catalytical inactive Cas, so-called dead Cas9 (dCas9), the HNH domain is also inactivated by introduce a substitution of a Histidine to an Alanine at position 840 (Jinek et al., 2012). Because both enzymatic domains (HNH and RuvC) are inactivated in dCas9, the dCas9 protein will not digest DNA. However, dCas9 still binds to the DNA, and thereby blocking transcription by acting as a repressor.

CRISPR mediates protection of prokaryotes against invading viruses through events of capturing DNA fragments of about 20 base pairs from the invading virus. These fragments are inserted as spacers into a CRISPR locus of the bacterial chromosome. RNA transcribed from these spacers, are responsible for guiding the Cas-protein to its target. In bacteria harbouring a CRISPR system, the CRISPR locus of spacers and repeats are first transcribed to make CRISPR RNA (crRNA). From the same locus, the *trans*-activating crRNA (tracrRNA) is also transcribed. *In vitro,* the crRNA and tracrRNA can be fused together to form a single guide RNA (SgRNA). The crRNA is the target-specific part of sgRNA, with its 20 nt complementarity to the genomic DNA. The complementarity guides the Cas-protein to potential cutting sites on the genome. The role of the tracrRNA on the other hand, is to assure binding between sgRNA and the Cas-protein through the Cas-handle (Deltcheva et al., 2011).

An active Cas9 endonuclease is obtained by formation of a complex between the Cas9 and the sgRNA (Figure 1.5). Binding of sgRNA to the Cas9 induces conformational changes in Cas9, forming a central channel that may accommodate target DNA (Jinek et al., 2014). The activated endonuclease Cas9 is then able to cleave a 23 bp target DNA sequence. As previously described, the first twenty base pairs are complementary to the crRNA, however, the last three base pairs on the targeted DNA sequence are the so called protospacer adjacent motif (PAM) site (Jiang et al., 2013). For Cas9-proteins derived from *S. pyogenes,* the PAM site is normally 5'-NGG-3', but can also be 5'-NAG-3'. The PAM site is recognized by the Cas9 itself (Sternberg et al., 2014). Before the discovery of CRISPR, a widely used editing tool was the *loxP*/Cre system, which is used several times for knock out of genes in *L. plantarum* (Chen et al., 2018; Lambert et al., 2007; Yang et al., 2017; Yang et al., 2015). The system consists of the recombinase Cre, that recombines specific *loxP* restriction sites. The *loxP* restriction sites are defined sites of 34 bp, which are not commonly found in the genome, or in all genomes. The CRISPR/Cas system however, can target any site on the genome containing the 3 bp PAM-site, which makes it a more available tool compared to its precursors (Maizels, 2013).

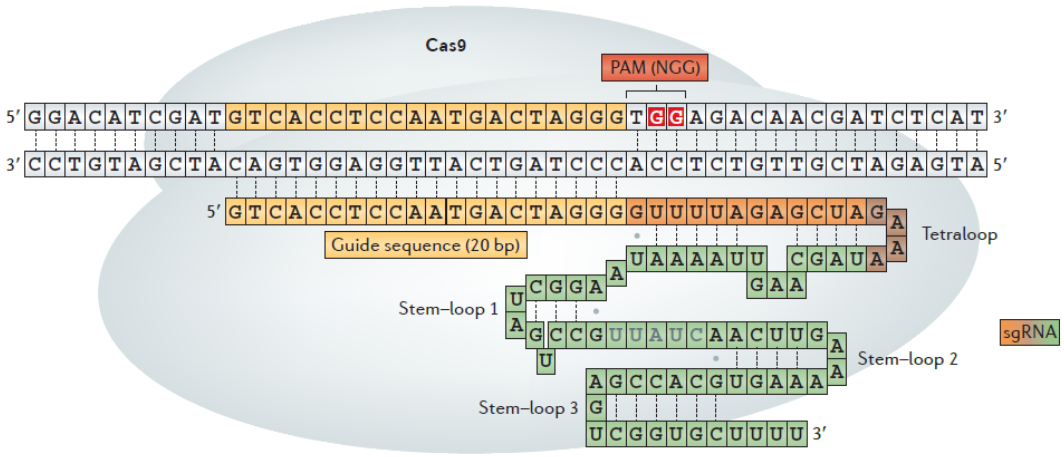

Figure 1.5 Schematic overview of the CRISPR/Cas9 system. An active endonuclease is achieved by complex formation between Cas9 and SgRNA, which induces conformational changes of Cas9. The Cas9-SgRNA complex is guided to the target DNA by the target specific crRNA-part of SgRNA. Through the conformational change, a central channel is formed, where the target DNA can be cleaved. Illustration is taken from (Kim & Kim, 2014).

1.7.1 Repair systems in bacteria

Double or single stranded breaks induced by Cas-proteins must be repaired by the cell. For bacteria unable to repair DNA damage, the CRISPR-system will be lethal. Double stranded breaks induced by Cas9 can be repaired in one of two ways. Either by the non-homologous end joining pathway (NHEJ) or by homology directed repair (HDR) (Figure 1.6). The NHEJ pathway is used in the absence of a DNA template. This repair mechanism is often error-prone and can create insertion or deletion mutations at the junctional site. This results in a frameshift, and thereby disruption of the targeted gene. However, NHEJ pathways are not prevalent in prokaryotes (Su et al., 2016).

In a second strategy, HDR, the genetic information at the break is restored by utilizing an undamaged template. Because HDR uses a template, this repair mechanism is not mutagenic. By taking advantage of this repair mechanism, precise editing can be obtained by cutting with a Cas-protein and relying on HDR (Hiom, 2009). To perform precise editing with HDR the insertion, e.g. of a desired mutation or a new gene must have sequences homologous to the target site (homologous arms) on each side. These homologous arms will then act as the template in the repairing mechanism, and the region between the template regions will be inserted into the genome through homologous recombination. Reparation of single stranded breaks can also be obtained by HDR (Song, X. et al., 2017).

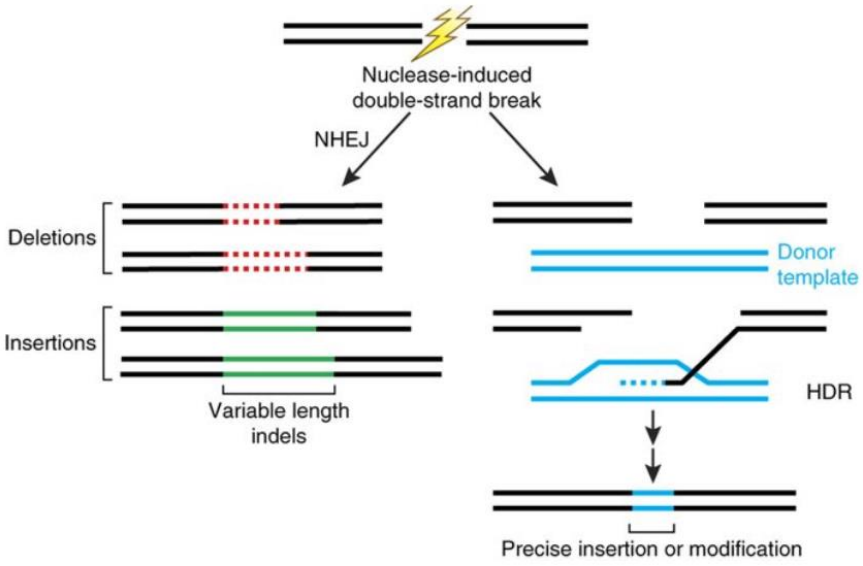

Figure 1.6. The two main pathways for repairing double-stranded DNA break in bacteria. Double-strand breaks induced by the endonuclease Cas9 can either be repaired by nonhomologous end joining (NHEJ) or homology-directed repair pathways. The NHEJ repair is an imprecise mechanism which often produce insertion or deletion mutations of variable length. The precise mechanism HDR can introduce point mutations or insertions from a DNA donor template. The figure is taken from (Sander & Joung, 2014).

All homologous recombination pathways are dependent on the recruitment of a recombinase. The Red/RecET dsDNA recombination system in *E. coli* is a well-known system of recombinases. However, a homolog recombination system to the Red/RecET system has been identified in *L. plantarum* WCFS1. Yang et al. (2015) identified an exonuclease encoded by *lp_0642* and a potential host-nuclease inhibitor encoded by *lp_0640* from a prophage P1 locus in *L. plantarum* WCFS1. They discovered that these two proteins combined with the previously characterized single strand annealing protein encoded by *lp_0641*, could perform homologous recombination between a heterologous dsDNA substrate and host genomic DNA. Unlike the Red/RecET recombineering system in *E. coli*, which only requires homologies of 50 bp for maximum recombination efficiency, the lp_0640-41-42 system in *L. plantarum* WCFS1 required long homologies of >1 kb between the heterologous substrate and the host genome, for efficient recombination. It was also found that recombination is more favoured in WCFS1 when the sequence to be inserted on the recombination substrate is shorter than the region on the genome being deleted. The lp_0640-41-42 system have previously been used in combination with the *loxP*/Cre system for disruption of D-lactate dehydrogenase (l*dhD*) gene, and concomitant insertion of the *gusA* gene and a Chloramphenicol resistance gene (Yang et al., 2015).

1.7.2 Use of CRISPR systems in Gram-positive bacteria

The catalytically inactive dCas9 is often used to study the functionality of genes. As dCas9 interfere with the transcription of the gene it is bound to, this type of experiment is often termed CRISPR interference (CRISPRi). In a recent study by Stamsås et al. (2018), the CRISPRi system was developed in *Staphylococcus aureus* to study the functionality of the cell division proteins CozEa and CozEb. A homolog to these two proteins, CozE, in *Streptococcus pneumoniae* has previously been found to be an essential regulator of cell elongation in the oval shaped cocci bacteria. Stamsås and co-workers found that CozEa and CozEb played overlapping roles to control proper cell cycle progression in the spherical *S. aureus* cells. Using the CRISPRi system, they showed that knock down of one of the proteins only had a minor effect. However, knock down of *cozEa* and *cozEb* simultaneously affected the cell division drastically. *S. aureus* cells normally divide in consecutive, perpendicular planes, meaning that the new septum is formed perpendicular to the previous and thereby splitting daughter cells. In bacterial cells were both *cozEa* and *cozEb* were knocked down, cell division was not performed according to this intricate system, resulting in elongated daughter cells (Stamsås et al., 2018).

Other LAB strains with successful development of a CRISPR/Cas-system is e.g. *Lactobacillus reuteri*, *Lactobacillus casei* and *Lactococcus lactis* (Oh & van Pijkeren, 2014; Song, X. et al., 2017; van der Els et al., 2018). In *L. casei* systems has been developed to use for both gene deletion and insertion. This was achieved using the mutated version of Cas9, $Cas9^{D10A}$, which induces single stranded breaks. The expression of $Cas9^{D10A}$ was optimized by exchanging the wild type promoter with the strong constitutive promoter P_{23}. Deletions or insertions of fragments were performed by using homologous arms and taking advantage of the endogenous repair system of the bacterial cell. One of the aspects investigated in *L. casei* was the impact of deletion size. When a fragment of 1.1 kb was deleted from the gene *LC2W_2179*, the editing efficiency was 36 %. However, the efficiency was reduced drastically when the deletion size increased to 3 kb and for a deletion size of 5 kb, no colonies were obtained. The protein eGFP was also successfully inserted into the genome of *L. casei*, although the fluorescence intensity was about 33% lower than if the bacteria harboured a multicopy plasmid with eGFP (Song, X. et al., 2017).

1.8 Aim of this study

This study is part of a larger project, where the goal is to produce mucosal administrated LAB-based vaccines against *Mycobacterium tuberculosis*. The three goals for the study was (1) to express and display the tuberculosis antigen hybrid Ag85B_TB10.4 on the surface of *Lactobacillus plantarum* WCFS1. (2) to implement the CRISPR/Cas system for use in *Lactobacillus plantarum* WCFS1. (3) To utilize the CRISPR/Cas system to integrate constitutive expression of the tuberculosis antigen into the genome of *Lactobacillus plantarum* WCFS1.

In previous research, the antigens have been produced using the pSIP system, which the gene expression is induced by addition of the pheromone SppIP. Recombinant *Lactobacillus* constructed for production of the novel fusion antigen Ag85B_TB10.4 were made using the pSIP vectors. The antigen production and localization of the constructed strains was characterized. As another goal was integration of the antigen into the genome, a constitutively expression system where thought to simplify the integration process, as briefly described in section 1.3.2. Therefore, attempts at construction of plasmids constitutively producing Ag85B_TB10.4 were conducted. The purpose of implementing the CRISPR/Cas system in *L. plantarum* was to potentially utilize the system to mediate integration of the hybrid antigen into the genome of the bacteria. The CRISPR/Cas system was developed as a two-plasmid system, where the Cas-gene were inducible expressed on one plasmid and the SgRNA was constitutively expressed on the second plasmid. The starting point for all vector constructions in this study was derivatives of the pSIP 401 vector (Table 2.4). The ultimate goal of this study was to develop the CRISPR/Cas system in *L. plantarum* and use the system to integrate the tuberculosis antigens into the genome.

The experimental work of this study was carried out in the following steps:

- Construction of inducible vectors for expression of Ag85B_TB10.4
- Construction of vectors for constitutive expression of Ag85B_TB10.4
- Investigation of production and surface localization of the antigen in *L. plantarum* using western blotting, flow cytometry and confocal laser scanning microscopy.
- Construction of the two-plasmid CRISPR/Cas-system in *L. plantarum*, using three different variants of the Cas-protein: Cas9, Cas9^{D10A} and catalytically inactive dCas9
- Transcription analyses of genes depleted with the CRISPR/dCas9 system by droplet digital PCR and confocal laser scanning microscopy

2 Materials

2.1 Laboratory Equipment

Laboratory equipment	Supplier
Cryovials, 1.5 mL	Sarstedt
Various glassware	
Electroporation cuvette, Gene Pulser®, 0.2 cm	Bio-Rad
Disposable cuvette, 1.5 mL	Brand
1 mm cuvette	Bio-Rad
Eppendorf tube, 1.5 and 2.0 mL	Axygen
Falcon 2059 Polypropylene Round Bottom tube, 14 mL	Becton Dickinson
FastPrep® tube	Fisher Scientific
Glass beads	Sigma
Microwell plate, 96 wells	Thermo Scientific
Nunc tube, 15 and 50 mL	Nunc
Slides and cover slip, Menzel-gläser	Thermo Scientific
PCR tube, 0.2 mL	Axygen
Pipetboy comfort	Integra
Serological pipette, 5, 10 and 25 mL	Sarstedt
Syringe, 10-60 mL	Plastipak
Sterile filter, 0.20 µM in pore size	Sarstedt
Water bath	Julaba
8- well strips	VWR
Multiplate Unskirted 96-Well PCR Plates	Bio-Rad
DG8™ Cartridges	Bio-Rad
DG8™ Gaskets	Bio-Rad
Pierceable Foil Heat Seals	Bio-Rad
Lysing matrix 2 tubes, 2 mL	MP Biomedicals

Instrument	Supplier

Azure c400	Azure biosystems
CertoClav	OneMed
Electrophoresis electricity supplier	Bio-Rad
FastPrep® -24 Tissue and Cell Homogenizer	MP Biomedicals
GelDoc EZ imager	Bio-Rad
Gene Pulser II	Bio-Rad
Incubator	Termaks
Inverted Light Microscope, Leica DM IL	Leica Microsystems
Leica TCS SP5 Confocal laser scanning microscope	Leica Microsystems
MacsQuant®Analyser	Miltenyi Biotec
PCR machine	
Mastercycler gradient	Eppendorf
SimpliAmp Thermal Cycler	Applied Biosystems
pH-meter	Metrohm
Pulse Controller Plus	Bio-Rad
Centrifuge	
Allegra X-30R Centrifuge	Beckman Coulter
Eppendorf centrifuge 5418R	Eppendorf
Heraeus Pico 21 centrifuge	Thermo Scientific
Micro centrifuge MiniStar silverline	VWR
SNAP i.d. Protein Detection System	Millipore
Ultrospec 10 Cell Density Meter	Amersham Biosciences
QX200 Droplet Generator	Bio-Rad
QX200 Droplet Reader	Bio-Rad
Multiskan FC	Thermo Scientific
BioPhotometer D30	Eppendorf
PX1™ PCR-Plate sealer	Bio-Rad
NanoDrop	Thermo Fisher

Software	Supplier
AzureSpot Analysis Software	Azure Biosystems
CLC DNA Main Workbench 7	Qiagen

ImageJ	Fiji
MacsQuantify™ Software	Miltenyi Biotec
pDRAW32	www.acaclone.com
QuantaSoft Software	Bio-rad
CRISPR Primer designer	www.plantsignal.cn

2.2 Chemicals

Chemical	Supplier
Acetone, C_3H_6O	Merck
Acetonitrile, C_2H_3N	Sigma-Aldrich
Ammonium Citrate Tribasic, $C_6H_{17}N_3O_7$	VWR
Ampicillin, $C_{16}H_{19}N_3O_4S$	Sigma-Aldrich
Brain-Heart Infusion (BHI)	Oxoid
Chloramphenicol, $C_{11}H_{12}Cl_2N_2O_5$	Merck
De Man, Rogosa, Sharpe (MRS)	Oxoid
Dithiothreitol (DTT), $C_4H_{10}O_2S_2$	Sigma-Aldrich
Ethylenediaminetetraacetic acid (EDTA), $C_{10}H_{16}N_2O_8$	Merck
Erythromycin, $C_{37}H_{67}NO_{13}$	Merck
Ethanol, C_2H_5OH	Sigma-Aldrich
D-(+)- Glucose, $C_6H_{12}O_6$	VWR
Glycerol, $C_3H_8O_3$	Merck
Glycine, $C_2H_5NO_2$	Duchefa Biochemie
Kanamycin, $C_{18}H_{36}N_4O_{11}$	Sigma-Aldrich
Magnesium Chloride, $MgCl_2$	Merck
Magnesium Phosphate, $MgSO_4$	Sigma
Peqlab	Peqlab
Polyethylene glycol, PEG_{1450}	Aldrich
SeaKem® LE Agarose	Lonza
Sodium Acetate, $C_2H_3NaO_2$	Sigma-Aldrich
Sodium Chloride, NaCl	Merck
Sodium hydroxide, NaOH	Sigma
Super Optimal broth with Catabolite repression (S. O. C.)	Invitrogen
Trichloracetic acid (TCA), $C_2HCl_3O_2$	Sigma
Tris-base, $C4H_{11}NO_3$	Sigma
Tween-20	Sigma-Aldrich

β-mercaptoethanol	Sigma-Aldrich
Bacteria protect	Qiagen
Droplet generation Oil for EvaGreen	Bio-Rad

2.3 Proteins and enzymes

Protein/Enzyme	Supplier
Antibodies	
Anti-Rabbit IgG-FITC	Sigma
Anti-Mouse IgG-FITC	Sigma
HRP-Rabbit Anti-Mouse IgG	Invitrogen
HRP-Goat Anti-Rabbit IgG	Invitrogen
Anti Mycobacterium tuberculosis Ag85 ABIN361295	Antibodies-online
ESAT6 Mouse mcAb (ab26246)	Abcam
The BenchMark™ Protein Ladder	Invitrogen
Bovine Serum Albumin (BSA)	Sigma
FastDigest® Green Buffer	Thermo Scientific
FastDigest® Restriction enzymes	Thermo Scientific
Acc65I	
AgeI	
BglII	
Bsu15I	
DpnI	
EcoRI	
EcoRI31	
HindIII	
NcoI	
NdeI	
NotI	
SalI	
XhoI	

Inducer peptide SppIP	CASLO
Lysozyme	Sigma
Mutanolysin	Sigma
MagicMark® XP Western Protein Standard	Invitrogen
RED Taq DNA Polymerase Master Mix	VWR
ElectroLigase®	NEB
ElectroLigase® Reaction Buffer	NEB

2.4 DNA

DNA	Supplier
DNA-standards	
GeneRuler™ 1 kb DNA ladder	Fermentas
Quick-Load® Purple 1 kb DNA Ladder	NEB
100 bp DNA ladder	NEB

2.5 Primers

In this study, several primers were used for different approaches. The names and sequence of all primers used in this study are presented in table 2.1. The purpose of each primer is described in table 2.2.

Table 2.1 – Primers and their sequence used in this study

Name	Sequence*	Restriction site
SekF	GGCTTTTATAATATGAGATAATGCCGAC	
SekR	CCTTATGGGATTTATCTTCCTTATTCTC	
Tb10.4F	CGATTGCGGCGGTCGACTTTAGTCGTCC	
Tb10.4R	TCGAACCCGGGGTACCGAATTCTTATGGCC	
SeqAg85_R	CCCATTGATGGACTTGGAAC	
SekFBsaI_F	ACGTTAATCCGAAAAAAACTAACGTT	
Cm1F	GGAGAGATTACATGAACTTTAATAAAATTGATTTAGA CAATT	

pCasR	ACCGAATTCCTCGAGTCAGTCACCTCCTAGCT	
Cas9NcoI_F	AGTATGATTCCCATGGATAAGAAATACTCAATAGGCT T	NcoI
Lp_2645_F	ATTCTGGAAAGTGGTTGGGG	
Lp_2645_R	ACTTCCGAAAAGCGTCTTGA	
Lp_1247_F	CACGATTACGAGTGTGACGA	
Lp_1247_R	CTAGAAATCGTGTCGCCCAT	
Lp_2217_F	CCATGGATGTTGGTCCAAGT	
Lp_2217_R	CAAGATCGCATAGCCTGGAA	
Phospho-SgRNA_R	TATAGTTATTATACCAGGGGGACAGTGC	
ThyA_SgRNA_F	TGTATGTTCCCGTGCCGGTAGTTTAAGAGCTATGCTG GAAACAG	
SgRNA-HL2_F	CGAACCCGGGGTACCGTATTGGCTATTAAAGAAGAA AAATGT	Acc65I
HL-NucA2_R	AGTTGACAATGGCATTCCAATTTTCAATTTTAAAATCC CCAAACTT	
HL-NucA2_F	AAATTGAAAATTGGAATGCCATTGTCAACTAAAAAAT TACATA	
NucA-HH2_R	ACAACTAATATGCCTATTGACCTGAATCAGCGTTG	
NucA-HH2_F	CTGATTCAGGTCAATAGGCATATTAGTTGTTCCGGC	
SgRNA-HH2_R	CTCCAGTAACTCGAGTCGGGACTGTTAGCGCCT	XhoI

* Restriction sites in the sequences are underlined.

Table 2.2 – Description of the primers used in this study

Name	Description
SekF	Forward primer for sequencing of all pSIP derivatives
SekR	Reverse primer for sequencing of all pSIP derivates
Tb10.4F	Forward In-Fusion primer for insertion of the Lp1261_Ag85B_TB10.4 into pLp1261_InvS
Tb10.4R	Reverse In-Fusion primer for insertion of the Lp1261_Ag85B_TB10.4 into pLp1261_InvS
SeqAg85_R	Reverse primer for sequencing of the antigen Ag85

SekFBsaI_F	Forward primer for sequencing of all pSIP derivates from the BsaI restriction site
Cm1F	Binds to the chloramphenicol resistance gene
pCasR	In-Fusion reverse primer for insertion of Cas-genes into pSIP_403 vector
Cas9NcoI_03_F	In-Fusion forward primer for insertion of Cas-genes into pSIP_403 vector
Lp_2645_F	Forward primer that binds to the gene *lp_2645*. Used in ddPCR
Lp_2645_R	Reverse primer that binds to the gene *lp_2645*. Used in ddPCR
Lp_1247_F	Forward primer that binds to the gene *lp_1247*. Used in ddPCR
Lp_1247_R	Reverse primer that binds to the gene *lp_1247*. Used in ddPCR
Lp_2217_F	Forward primer that binds to the gene *lp_2217*. Used in ddPCR
Lp_2217_R	Reverse primer that binds to the gene *lp_2217*. Used in ddPCR
Phospho-sgRNA_promoter_R	Phosphorylated primer that binds to the SgRNA-plasmid. Used for insertion of new base-pairing sequences
ThyA_SgRNA_F	Primer that binds to the SgRNA-plasmid and inserts a base-pairing sequence targeting the gene *ThyA*
SgRNA-HL_F	In-Fusion forward primer for insertion of the left homology arm into the SgRNA-plasmid
HL-NucA_R	Reverse primer with specificity to the left homology arm. Tail is homologous to *NucA*
HL-NucA_F	Forward primer with specificity to *NucA*. Tail is homologous with the left homology arm
NucA-HR_R	Reverse primer with specificity to *NucA*. Tail is homologous with the right homology arm
NucA-HR_F	Forward primer with specificity to the right homology arm. Tail is homologous to *NucA*
SgRNA-HR_R	In-Fusion reverse primer for insertion of the right homology arm into the SgRNA-plasmid

2.6 Bacterial strains and plasmids

All bacterial strains and plasmids used in this study is presented in tables 2.3 and 2.4 respectively.

Table 2.3 – Bacterial strains

Strain	Source
Escherichia coli TOP10	Invitrogen
Lactobacillus plantarum WCFS1	(Kleerebezem et al., 2003)
Lactobacillus plantarum WCFS1 ΔLp_2645 K10 (NZ3557)	(Fredriksen et al., 2012)
Lactococcus lactis MG1363	(Wegmann et al., 2007)

Table 2.4 – Plasmids used in this study

Plasmid name (abbreviation)*	Description	Source
EPI300_P5_1261_Ag85B_TB10.4_DC	The EPI300 plasmid containing the constitutive promoter P_5, the lipoanchor Lp_1261, the synthetic gene *Ag85B-TB10.4* and a dendritic cellbinding peptid (DC)	GenScript, USA
pJET1.2_P11_1261	The pJET1.2 plasmid containing the constitutive promoter P_{11} and the lipoanchor Lp_1261	GenScript, USA
pLp1261_InvS	pSIP401 derivative with the lipo-anchor Lp_1261 attached to the gene *inv*	(Fredriksen et al., 2012)
pLp_3050_Nuc	pSIP401 derivative with signal sequence for secretion (Lp_3050) attached to the reporter protein NucA.	(Mathiesen et al., 2009)
pLP_1261-Ag85B-ESAT6 (pAgE6)	pSIP401 derivative for production of Ag85B-ESAT6 with the Lp_1261 lipo-anchor signal sequence	(Øverland, 2013)
pELS100	Derivative of pLPV111 shuttle vector	(Sørvig et al., 2005b)
pCas	A vector that contains the gene Cas9, encoding the double-	https://www.addgene.org/62225/

	strand digesting endonuclease Cas9	(Song, X. et al., 2017)
pLCNICK	A vector that contains the gene $Cas9^{D10A}$, encoding the single-strand digesting nickase $Cas9^{D10A}$	https://www.addgene.org/84653/ (Song, X. et al., 2017)
pLp_1261-Ag85B-TB10.4 (p1261AgTB)	pSIP401 derivative for production of Ag85B-Tb10.4 with the lipo- anchor Lp_1261 signal sequence	This study
pAg85B-TB10.4 (pCytAgTB)	pSIP401 derivative for intracellular production of Ag85B-Tb10.4	This study
P5*_Lp1261_Ag85_TB10.4 (pP5*AgTB)	pSIP401 derivative for production of Ag85B-Tb10.4 with the lipo- anchor Lp_1261 signal sequence and the constitutive (mutated) promoter P5	This study
pEV	Empty vector. pSIP401 derivative lacking any target genes	(Fredriksen et al., 2010)
pSIP_403	pSIP401 derivative with a 256 replicon	(Sørvig et al., 2003)
pSIP_411	pSIP401 derivative with a Sh71 replicon	(Sørvig et al., 2005a)
pSIP_411_dCas9_Sh71 (pdCas9Sh71)	pSIP401 derivative with the Sh71 replicon, and the catalytically inactive Cas gene *dCas9*	Constructed by G. Mathiesen
pSgRNA_2645 (pSg2645)	SgRNA-plasmid with a base-pairing sequence that targets the *lp_2645* gene in *L. plantarum*	Constructed by G. Mathiesen
pSgRNA_ThyA (pSgThyA)	SgRNA-plasmid with a base-pairing sequence that targets the *lp_ThyA* gene in *L. plantarum*	This study

pSIP_403_Cas9	pSIP401 derivative with an inducible expression of the *Cas9*-gene	This study
pSIP_403_Cas9^{D10A}	pSIP401 derivative with an inducible expression of the *Cas^{D10A}*-gene	This study
pSIP_411_Cas9_Sh71 (pCas9Sh71)	pSIP401 derivative with an inducible expression of the *Cas9*-gene and a Sh71 replicon	This study
pSIP_411_Cas9^{D10A} _Sh71 (pCas9^{D10A}Sh71)	pSIP401 derivative with the *Cas^{D10A}*-gene and a Sh71 replicon	This study
pSgRNA_2645_HL_NucA_HH (pSg2645Ha)	SgRNA-plasmid with a base-pairing sequence that targets the *lp_2645* gene. *NucA*-gene inserted between sequences homologous upstream and downstream of *lp_2645* to the genome of *L. plantarum*	This study

*Abbreviations will be used in the text

2.7 Kits

Kit	Supplier
GenElute® HP Plasmid Midiprep Kit	Sigma-Aldrich
GenElute® HP MIdiprep Filter Syringes	
GenElute® HP Midiprep Binding Columns	
Collection tubes, 15 mL conical	
Column Preparation solution	
RNase A Solution	
Resuspension solution	
Lysis Solution	
Neutralization Solution	
Binding Solution	

Wash Solution 1	
Wash Solution 2	
Elution Buffer (10 mM Tris-HCL, pH 8,5)	
iBlot® Dry Blotting System	Invitrogen
iBlot® Gel Transfer Device	
Blotting roller	
iBlot® Gel Transfer Stack, Regular	
iBlot® Cathode stack, Top	
iBlot® Anode stack, bottom	
iBlot® Disposable sponge	
iBlot® Filter Paper	
In-Fusion® HD Cloning kit	Clontech
5X In-Fusion® HD Enzyme Premix	
Novex® NuPAGE® SDS-PAGE Gel system	Invitrogen
NuPAGE® Novex Bis-Tris gels 8 cm x 8 cm x 1 mm, 10 and 15 wells	
NuPAGE® LDS Sample Buffer (4X)	
NuPAGE® Reducing agent (10X)	
The NucleoSpin® Gel and PCR Clean-up	Macherey-Nagel
The NucleoSpin® Gel and PCR Clean-up columns	
Collections Tubes, 2 mL	
Binding Buffer NTI	
Wash Buffer NT3	
Elution Buffer NE	
NucleoSpin® Plasmid	Macherey-Nagel
Buffer A1	
Buffer A2	
Buffer A3	
Buffer A4	

Elution Buffer AE	
NucleoSpin® Plasmid/Plasmid (NoLid) column	
Collection Tubes, 2 mL	
Quick Ligation® kit	NEB
Quick T4 DNA Ligase	
2X Quick Ligation Reaction Buffer	
SNAP i.d. ® Protein Detection System	Millipore
SNAP i.d. ® Single Well Blot Holder	
SNAP i.d. ® Spacer	
SNAP i.d. ® Blot roller	
Filter paper	
SuperSignal® West Pico Chemiluminescent Substrate	Thermo Scientific
Luminol/Enhancer	
Stable Peroxide Buffer	
RNeasy Mini Kit	Qiagen
RNeasy Mini Spin Columns (pink)	
Collection Tubes (1.5 ml)	
Collection Tubes (2 ml)	
Buffer RLT	
Buffer RW1	
Buffer RPE	
RNase-Free Water	
NucleoSpin® Microbial DNA	Macherey-Nagel
Lysis Buffer MG	
Wash Buffer BW	
Wash Buffer B5	
Elution Buffer BE	
Liquid Proteinase K	

NucleoSpin® Bead Tubes Type B NucleoSpin® Microbial DNA Columns (light green rings) Collection Tubes (2 mL)	
Q5® Hot Start High-Fidelity 2X Master Mix	NEB
Heat&Run gDNA removal kit 10X reaction Buffer HL-dsDNase	ArcticZymes
iScript™ Reverse Transcription Supermix	Bio-Rad
2x QX200 ddPCR EvaGreen Supermix	Bio-Rad

2.8 Agars and media

All components and suppliers are listed in section 2.2.

Brain-Heart-Infusion (BHI)

Medium:

37 g BHI dissolved in 1 L dH2O.

Sterilized in a CertoClav at 115 °C for 15 minutes.

Agar:

BHI broth supplemented with 1.5 % (w/v) agar.

After sterilization in a Certoclav, the medium was allowed to cool down to ~60 °C, before the addition of the appropriate antibiotic. The medium was poured into petri dishes, and allowed to solidify, before storage at 4°C.

De Man, Rogosa, Sharpe (MRS)

Medium:

52 g MRS broth in 1 L dH2O.

Sterilized in a CertoClav at 115 °C for 15 minutes.

Agar:

MRS broth supplemented with 1.5 % (w/v) agar.

After sterilization in a Certoclav, the medium was allowed to cool down to ~60 °C, before the addition of appropriate antibiotic. The medium was poured into petri dishes, and allowed to solidify, before storing them at 4°C

MRSSM medium

5.2 g MRS

17.1 g Sucrose (0.5 M)

2.0 g MgCl2 (0.1 M)

in 100 mL dH_2O

Sterile filtrated using a 0.2 μm pore size filter.

GM17

Medium:

37.25 g M17

dH_2O to 1 Litre

Sterilized in a CertoClav at 115 °C for 15 minutes.

After sterilization, the medium was cooled to ~60°C before adding 0.5% sterile filtered glucose.

Agar:

M17 medium with 1.5% (w/v) agar

After sterilization, the medium was cooled to ~60°C before adding appropriate antibiotics. The medium was poured into petri dishes, and allowed to solidify, before storing them at 4°C

SGM17 medium

GM17 medium

0.5 M Sucrose (sterile filtered using 0.2 µM pore sized filter)

Super Optimal broth with Catabolite repression (S. O. C.)

Pre-made by the manufacturer of competent cells.

2.9 Buffers and solutions

Phosphate Buffered Saline (PBS)

8 g/l NaCl

0.2 g/l KCl

1.44 g/l Na_2HPO_4

0.24 g/l KH_2PO_4

Tris Buffered Saline (TBS)

150 mM NaCl

10 mM Tris-HCl, pH 8

TTBS

TBS

0.1 % (w/v) Tween-20

Tris-acetate/EDTA (TAE) 50X

242 g Tris base

57.1 mL Acetic acid

100 mL 0.5 M EDTA, pH 8

dH_2O to 1 L

Tris-Glycine-SDS (TGS) 10X

From manufacturer

3 Methods

3.1 Cultivation of bacteria

Bacteria was cultured in liquid medium or on agar plates and enriched with appropriate antibiotics for selection.

Escherichia coli was cultured overnight at 37°C in BHI for both liquid medium and agar plates. Liquid medium was incubated with vigorously shaking. *L. plantarum* was cultured overnight in liquid or solid MRS at either 30°C or 37°C without shaking. *L. lactis* was cultured overnight in liquid or solid GM17 at 30°C without shaking.

Table 3.1 – The type of antibiotics to be added depended on the plasmid, and the amount of antibiotics to be added based on type of media.

Antibiotics	**Solid medium– *E. coli* (µg/ml)**	**Liquid medium – *E. coli* (µg/ml)**	**Solid medium – Lactic acid bacteria (µg/ml)**	**Liquid medium – Lactic acid bacteria (µg/ml)**
Erythromycin	200-300	200	5-10	5-10
Chloramphenikol	34	34	5-10	5-10
Ampicillin	100	200	-	-
Kanamycin	50-100	100	-	-

3.2 Storage of bacteria

For long-term storage of bacteria, glycerol stocks were made and kept at -80°C. The glycerol prevents disruption of the cells when stored at low temperatures.

Materials

Cultured bacteria in suitable medium

87% (w/v) Glycerol

1.5 mL Cryovial

Procedure

Bacteria was cultured overnight in 10 mL growth medium. 1 mL of the culture was transferred to a 1.5 mL cryovial. Then 300 µL 87% (w/v) sterile glycerol was added, the tube was inverted a few times for mixing and kept in a -80°C freezer.

To later cultivate bacteria from a glycerol stock, a toothpick was used to pluck a small amount of frozen glycerol stock and transferred to a tube containing appropriate growth medium.

3.3 Plasmid isolation from bacteria

For plasmid isolation from bacteria, the NucleoSpin® Plasmid Kit (MACHEREY-NAGEL, Düren, Germany) were used. Depending on whether the replicon of the plasmid was high- or low-copy, either the NucleoSpin® Plasmid Kit protocol 5.1 or 5.2 was followed.

Isolation of *L. lactis* required some additional lysis steps. In the first step of cell lysis, the bacterial pellet was resuspended in 220 µL buffer A1(from NucleoSpin® Plasmid Kit), 25 µL of 100 mg/mL lysozyme and 5 µL of 5000 U/mL mutanolysin. The suspension was incubated at 37°C for 30 minutes, before continuing as described in NucleoSpin® Plasmid Kit protocol.

For a larger volume of plasmid eluate, the GeneJET Plasmid Midiprep Kit (ThermoFisher Scientific) was used, following the manufacture's protocol.

3.4 Isolation of microbial DNA

Genomic DNA was isolated from bacterial cultures by using the NucleoSpin® Microbial DNA Kit (MACHEREY-NAGEL). Isolation was performed by following the manufacturer's Standard protocol for gram-positive and gram-negative bacteria.

The cells were lyzed using a FastPrep-24 instrument (MP Biomedicals) at 6.5 m/s^2 for 30 seconds. The agitation was repeated three times, with one-minute pause between each run.

3.5 Digestion of DNA with restriction enzymes

Restriction enzymes cleaves double stranded DNA at or near sites of the genome containing a specific sequence. The restriction enzymes can either cut the two DNA strands at the same position on each strand, creating blunt ends, or at slightly different positions on each strand to create overhangs. Digestion of DNA by restriction enzymes is a commonly used method for

preparing DNA fragments for ligation. Each DNA fragment is then double digested, meaning that two different restriction enzymes are used for excision of the fragment. This creates compatible ends between the fragments to be ligated. After incubation, the digestion mixtures are loaded onto an agarose gel for separation using agarose gel electrophoresis of the digested fragments and further isolation (See 3.7).

Materials

dH_2O

10X FastDigest Green Buffer

DNA

FastDigest Enzyme

Procedure

1. The reaction was combined at room temperature in the order indicated as shown in Table 3.2.

Table 3.2 - Restriction enzyme digestion(setup) using FastDigest Restriction enzymes

Component	Volume (µL)
dH_2O up to	50
10X FastDigest Green Buffer	5
DNA	x
RE Enzyme	5

2. The mixture was gently mixed and spun down
3. The reaction was incubated at 37°C for 45 minutes.
4. The mixture was directly loaded into a gel.

3.6 Ligation

Ligation of DNA fragments is normally done using a DNA ligase. The ligase facilitates the formation of phosphodiester bonds between the 5'- phosphate and 3' hydroxyl- ends of adjacent DNA bases. The enzymatic reaction uses ATP and the cofactor Mg^{+}, these components are supplied in the ligation buffer.

3.6.1 In-Fusion Cloning

In-Fusion HD Cloning Kit was used for cloning of genes into a linearized vector. The enzymes in this kit recognizes a 15 base pair overhang at each end of the DNA-fragment to be inserted (Figure 3.1). These 15 base pairs are homolog to the ends of the linearized vector. The overhangs are inserted by PCR using primers which are specific to the DNA-fragment target sequence and have a 15 base pair tail. In the first round of PCR, only the gene specific part of the primer binds (section 3.13).

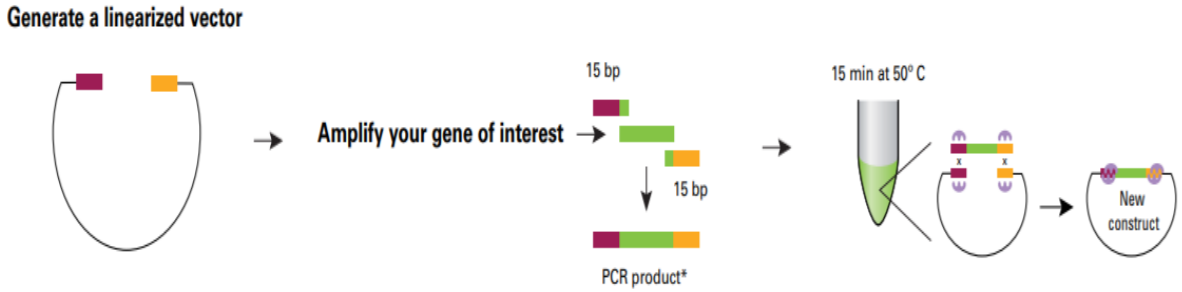

Figure 3.1. A simplified illustration of the In-Fusion cloning procedure. A linearized vector is generated, and gene specific primers with a 15 bp overhang with homology to the vector (red and yellow blocks) are designed. The insert is PCR-amplified with the In-Fusion primers. The reaction mix containing a linearized vector and the amplified insert is incubated at 50°C for 15 minutes, before being transformed. The illustration is a modified version from the original taken from the In-Fusion® HD Cloning Kit User Manual.

Materials

5X In-Fusion HD Enzyme Premix

Linearized vector

Purified PCR fragment

dH_2O

Procedure

1. The In-Fusion® Molar Calculator (http://bioinfo.clontech.com/infusion/molarRatio.do) was used to determine the amount of purified PCR product and linearized vector needed for each reaction. The insert was added in a 2-fold excess to the vector.
2. The components shown in table 3.3 was added to an Eppendorf tube

Table 3.3 – Components used for In-Fusion cloning.

Component	Volume (µL)
5X In-Fusion HD Enzyme Premix	2
Linearized vector	X
Purified PCR fragment	X
dH_2O as needed	X
Total volume	10

3. The reaction was incubated at 50°C for 15 minutes, and subsequently placed on ice for 2 min.
4. The mixture was either transformed into competent cells or stored at -20°C.

3.6.2 Quick Ligation

The Quick T4 DNA Ligase is an enzyme that can ligate both sticky- and blunt-ends, in 5 minutes.

Materials

dH_2O

Vector

Insert

2X Quick Ligation Reaction Buffer

Quick T4 DNA Ligase

Procedure

1. In a 1.5 mL Eppendorf tube, 50 ng of the vector and a 3-fold molar excess of insert was mixed. The volume was adjusted to 10 µL with dH_2O.
2. 10 µL 2X Quick Ligation Reaction Buffer was added and mixed.
3. 1 µL Quick T4 DNA Ligase was added and mixed thoroughly.
4. The tube was briefly centrifugated and incubated at room temperature for 5 minutes.
5. After incubation, the ligation mixture was chilled on ice and transformed within a few hours, or stored at -20°C.

3.6.3 Ligation with ElectroLigase

For constructs that was transformed directly into an electrocompetent bacteria, the ligation was performed using ElectroLigase to minimize the concentration of salt.

Materials

dH_2O

Insert

Vector

ElectroLigase Reaction Buffer

ElectroLigase

Procedure

1. 20-100 ng of vector was combined with a 3-fold molar excess of insert and the volume was adjusted with dH_2O to 5 µL.

2. 5 µL of ElectroLigase Reaction Buffer and 1 µL of ElectroLigase was added to the reaction and mixed by pipetting up and down 7-10 times.
3. The ligation reaction was incubated at room temperature (25°C) for 30-60 minutes.
4. Inactivation of the ligase was done by incubating the reaction at 65°C for 15 minutes.
5. The ligation mix was then chilled on ice if transformed within a few hours, or stored at -20°C.

3.7 Agarose gel electrophoresis

Agarose gel electrophoresis is a method used for separation of DNA fragments based on their size. Fragments are separated using an electric current that moves the negatively charged DNA fragments through the agarose gel towards the positive pole. Because the agarose gel contains pores, smaller fragments will move faster than bigger fragments. Fragments >200 bp was separated by a 1.2% agarose gel, while fragments <200 bp was separated by a 2% agarose gel. The fragments were then compared to a DNA ladder with known sizes to determine the size of the fragments.

Materials

SeaKem® LE Agarose

1 x TAE Buffer

peqGREEN

Loading dye

DNA ladder

Procedure

1. 12 g of SeaKem® LE Agarose was dissolved in 1 L of 1 x TAE buffer to make a 1.2% Agarose gel.

2. The solution was sterilized in a CertoClav for 15 minutes at 115°C. The 1L stock solution of 1.2% Agarose gel was kept at 60°C until use.
3. One gel was prepared by taking 60 mL from the 1 L stock solution and adding 2.5 µL peqGREEN. The mix was poured into a moulding tray with combs.
4. After about 20 minutes the gel had harden, and the combs was removed.
5. The gel was transferred to an electrophoresis chamber and covered with 1 x TAE buffer.
6. Loading dye was added to the samples to be run, and the samples was loaded into wells in the gel. A ladder was also added in one well.
7. The gel was run at 90V for up to 60 minutes, depending on the fragment sizes.

3.8 Purification of DNA and extraction of DNA fragments from agarose gels

The NucleoSpin® Gel and PCR Clean-up from MACHEREY-NAGEL was used to purify DNA amplified with PCR and for DNA extraction from agarose gels. The purification and extraction steps were carried out according to the relevant protocol supplied by the manufacturer.

3.9 Determination of RNA and DNA concentration

The DNA concentration of eluates were determined with a spectrophotometer and a 1 mm cuvette. 2 µL of the eluate was placed on the cuvette and placed in the BioPhotometer D30. The spectrophotometer measures absorbance at 260 nm for DNA. RNA concentrations were determined by using a NanoDrop Spectrophotometer. 1 µL of the RNA sample was placed on the NanoDrop, and the concentration was measured. The NanoDrop spectrophotometer measured the absorbance at 230 nm for RNA.

3.10 DNA sequencing of plasmids and PCR fragments

Plasmids or amplified PCR fragments was sequenced by GATC biotech for verification of relevant sequences. Sequencing of a plasmid required 400 ng template, while sequencing of a PCR fragment required 100-400 ng template. This was added in an Eppendorf tube and combined with 25 pmol primer and dH_2O to a total volume of 11 µL. Each tube was labelled

with a unique barcode and sent to Eurofins for Sanger sequencing. The returned sequences were analysed using CLC DNA Main Workbench 7.

3.11 Preparation of electrocompetent *Lactobacillus plantarum* WCFS1

Bacteria must have the ability to take up free, extracellular genetic material to be able to undergo transformation. Such a bacterial cell is called competent. Bacterial cells are made artificially competent either chemically or by electrical pulses. The electrical pulse makes the cell wall permeable.

Electrocompetent *Lactobacillus plantarum* cells were grown in MRS medium containing glycine. The glycine replaces the L-alanine in the cell wall, which makes it more permeable for uptake of plasmids. The procedure was done in accordance to the protocol described in (Aukrust et al., 1995).

Materials

L. plantarum

MRS medium

MRS + 1% glycine

30% w/v PEG_{1450}

MRS + 0.5 M Sucrose + 0.1 M $MgCl_2$

Procedure

1. *L. plantarum* from glycerol stock was cultured overnight in 10 mL MRS at 37°C.
2. 1 mL of the overnight culture was used to make a serial dilution (10^{-1}-10^{-10}) in MRS + 1 % glycine. The cultures were incubated overnight at 37°C.
3. 1 mL of the culture with an OD_{600} of 2.5 ± 0.5 was further diluted in 20 mL MRS + 1% glycine. The culture was then grown until it reached the logarithmic phase (OD_{600} of 0.7 ± 0.07) and placed on ice for 10 minutes.

4. The culture was centrifuged at 5000x g for 5-10 minutes at 4°C and the supernatant discarded.
5. The pellet was resuspended in 5 mL ice cold 30% w/v PEG_{1450} (freshly made), additional 20 mL of the PEG_{1450} was added, before the tube was inverted gently and placed on ice for 10 minutes.
6. The cells were collected by centrifugation at 5000x g for 5-10 minutes at 4°C.
7. The pellet was resuspended in 400 µL 30% w/v PEG_{1450} and portions of 40 µL were pipetted into Eppendorf tubed and immediately frozen at -80°C.

3.12 Transformation

3.12.1 Transformation of Chemically Competent *E. coli*

Materials

OneShot TOP10 chemically competent cells

Ligation mix

S.O.C media

BHI agar plates with appropriate antibiotic

Procedure

1. One vial for each transformation of OneShot TOP10 chemically competent cells was thawed on ice.
2. 1-5 µL of the DNA was added into a vial of OneShot TOP10 cells, and gently mixed.
3. The vials were then incubated on ice for 30 minutes.
4. The cells were heat-shocked for 30 seconds at 42°C without shaking.
5. After the heat shock, the cells were placed on ice for 2 minutes.
6. Aseptically, 250 µL pre-warmed S.O.C. medium was added to each of the vials and placed in 225 rpm shaking-incubator at 37°C for 1 hour.

7. 100 µL of the incubated transformation mix was spread out on BHI agar plates with appropriate antibiotics and incubated at 37°C overnight.

3.12.2 Transformation of Electrocompetent Competent Cells

Materials

Electrocompetent cells

Plasmid/ligation mix

Appropriate media

GenePulser® Electroporation cuvette 0.2 cm on ice

Bio-Rad GenePulser® II

Bio-Rad Pulse controller plus

Agar plates

Table 3.4 – Settings on the GenePulser, media and incubation conditions vary between different bacterial strains.

Strain	Cuvette (cm)	Capacitance (µF)	Volt (kV)	Resistance (Ω)	Media	Incubation
L. plantarum	0.2	25	1.5	400	950 µL MRSSM	37°C, 2-4 hours
L. lactis	0.2	25	2.0	200	700 µL SGM17MC	30°C, 2-4 hours

Procedure

1. Electrocompetent cells was thawed on ice.
2. 5 µL of the plasmid was transferred to each tube with electrocompetent cells.
3. The mixture was transferred to the electroporation cuvette

4. The cuvette was placed in the electroporator and subjected to optimal current (Table 3.4).
5. Immediately after, the appropriate media (Table 3.4) was added to the cuvette, and the transformed cells were transferred to a sterile Eppendorf tube.
6. The cells were incubated at the appropriate temperature without shaking for 2-4 hours
7. After incubation, 100 µL of the cells were spread out on either MRS or GM17 agar plate with appropriate antibiotics and incubated overnight.

3.13 Polymerase Chain Reaction

The polymerase chain reaction (PCR) is a method used for *in vitro* amplification of a specific DNA fragment. PCR relies on thermocycling. Double stranded DNA is heated to 94-98°C, which causes the strands to separate. When the strands are separated, they can be used as template for synthesis of a new strand. When the temperature is lowered, specific oligonucleotides (primers) bind to the single stranded target DNA sequence and serve as primers for the DNA polymerase which extends the strands by incorporating deoxynucleotides (dNTPs) from the solution. This cycle of heating, annealing and extension is repeated in a thermal cycling device, leading to an exponential increase in the number of synthesized fragments.

3.13.1 PCR using Q5® Hot Start High-Fidelity 2x Master Mix

1. The PCR reactions was carried out as suggested by the manufacturer of the Q5® Hot Start High-Fidelity 2x Master Mix. The Master Mix contains dNTPs, Mg^{++} and proprietary broad use buffer. In the order indicated by table 3.5, the reactants were mixed in a sterile 0.2 mL PCR tube

Table 3.5 – Q5 PCR components

Components	Volume (µL)	Final concentration
dH_2O	Up to 50	-
10 µM Forward primer	2.5	0.5 µM
10 µM Reverse primer	2.5	0.5 µM
Template	variable	<1 µg
Q5® Hot Start High-Fidelity 2x Master Mix	25	1X

2. The reactions were placed in a thermal cycler, and the cycling program showed in table 3.6 was applied

Table 3.6 – Q5 Cycling program

Step	Temperature (°C)	Time	Cycles
Initial denaturation	98	30 seconds	1
Denaturing	98	10 seconds	25-35
Annealing	50-72*	30 seconds	25-35
Elongation	72	20-30 sec/kb	25-35
Fina elongation	72	2 minutes	1

*The annealing temperature is dependent on the primers.

3.13.2 PCR with VWR Red Taq Polymerase Master Mix

The Red Taq DNA polymerase was normally used to check if colonies harboured the desired plasmids. Colonies were transferred directly from agar plates to a PCR tube with a toothpick. Colonies of gram-positive bacteria was microwaved for 1 minute on full effect to ensure lysis, before adding the other components.

1. The PCR reactions was carried out as suggested by the manufacturer of the Red Taq DNA Polymerase 2x Master Mix (VWR). In the order indicated by table 3.7, the reactants were mixed in a sterile 0.2 mL PCR tube

Table 3.7 – Taq PCR components

Components	Volume (µL)	Final concentration
dH_2O	Up to 50	-
10 µM Forward primer	1	0.2 µM
10 µM Reverse primer	1	0.2 µM
Template	variable	<1000 ng
Red Taq DNA Polymerase 2x Master Mix	25	1X

2. The reactions were placed in a thermal cycler, and the cycling program showed in table 3.8 was applied

Table 3.8 – Red Taq Polymerase Cycling program

Step	Temperature (°C)	Time	Cycles
Initial denaturation	95	2 minutes	1
Denaturing	95	10 seconds	25-35
Annealing	50-65*	30 seconds	25-35
Elongation	72	30 sec/kb	25-35
Fina elongation	72	5 minutes	1

*The annealing temperature is dependent on the primers.

3.14 Preparation of samples for analysis of gene products in *L. plantarum*

Genes expressed by the inducible system pSIP are under the control of SppIP promoter, which requires the presence of an inducer peptide, SppIP to initiate expression. To analyse the production of the target genes in *L. plantarum* harbouring different plasmids, the expression was induced by addition of the inducer peptide. Induced bacteria were harvested, and the products were investigated through Western blot analysis. Flow cytometry and confocal laser scanning microscopy was used to determine the localization of the target proteins. Droplet digital PCR was used to perform transcriptional analysis. Bacteria harbouring non-pSIP vectors was harvested equally to bacteria harbouring pSIP vectors.

3.14.1 Cultivation and harvesting of bacteria

Materials

MRS medium

Inducing peptide SppIP

Antibiotics

Procedure

1. *L. plantarum* strains were grown at 37°C overnight in MRS medium containing appropriate antibiotics.

2. The overnight cultures were diluted in 10 mL prewarmed MRS medium to an OD_{600} of 0.13-0.15.
3. The culture was incubated at 37°C until it reached an OD_{600} of 0.3. and the gene expression was induced with SppIP (25 ng/mL).
4. The induced cells were further incubated for 2 hours, and harvested by centrifugation at 5000x g for 10 minutes at 4°C.

3.14.2 Harvesting of bacterial cells for transcriptional analysis with ddPCR and

Bacterial cells were harvested for isolation of RNA in a similar way as described in section 3.14.1 However, From the overnight culture, only 50 µL was transferred to 10 mL prewarmed MRS, to achieve an OD_{600} ~0.01, and immediately induced. The bacteria were harvested at OD_{600} = 0.4.

3.15 Gel electrophoresis of proteins

The technique Sodium dodecyl sulphate-polyacrylamide gel electrophoresis (SDS-page) separates denatured proteins according to mass. Due to the availability of precast gels and automated gel imaging, the SDS-page is a rapid and safe method for visualization and analysis of protein samples.

Addition of the anionic detergent lithium dodecyl sulphate (LDS) leads to breakage of non-covalent bindings, while addition of the reducing agent dithiothreitol (DTT) causes disulphide bridges to break. The denaturation of the proteins gives the proteins a uniform negative charge which is used to separate the proteins in a stain-free polyacrylamide gel, according to molecular weight.

By applying an electric current to the gel, the negatively charged proteins will migrate towards the anode, analogue to DNA gel electrophoresis. The pore structure of the SDS-page gel leads to more rapid migration of proteins with lower molecular weight (kDa) than heavier proteins, allowing effective separation of proteins. The molecular weight of the proteins is determined using a protein standard.

Materials

Mini-PROTEAN® TGX Stain-Free™ Precast Gels

NuPAGE® LDS Sample Buffer (4X)

NuPAGE® Reducing agent (10X)

TGS Buffer (Section 2.9)

Benchmark™ Protein Ladder

MagicMark™ XP Western Protein Standard

Procedure

1. A 2X working solution was prepared by mixing NuPAGE® LDS Sample Buffer (4X) and NuPAGE® Reducing agent (10X)
2. Protein solution and working solution were mixed 1:1 and boiled for 10 minutes.
3. The Mini-PROTEAN® TGX Stain-Free™ Precast Gel was assembled in the electrophoresis chamber, and TGS buffer was added.
4. The boiled samples and ladders were applied to the gel, and the gel was run at 280 V for 18 minutes.
5. After electrophoresis, the gel was placed briefly in dH2O before further analysis.

3.16 Western blotting analysis

Western blot analysis is a method for detection of proteins using antibody hybridisation. Proteins are first separated by SDS-PAGE gel electrophorese (section 3.15), before the proteins in the gel are blotted to a nitrocellulose membrane using electroblotting. Prior to the antibody hybridisation, the membrane is treated with a blocking solution, containing bovine serum albumin (BSA) which binds and block potential sites for nonspecific interactions of the antibody. The primary antibody binds specifically to epitopes on the protein of interest. After incubation, excess of primary antibody is washed away, before a new incubation with the secondary antibody. The secondary antibody binds to the primary antibody. The secondary antibody is conjugated with a reporter enzyme that gives a detectable fluorescent signal when appropriate substrate is added. The secondary antibody is conjugated with the enzyme horse radish peroxidase (HRP) which oxidizes luminol. The oxidation releases a detectable light, which leads to visualisation of the protein of interest, if present.

3.16.1 Blotting with the iBlot™ Dry Blot System

Proteins were blotted from the SDS-page gel to the nitrocellulosemembrane using the iBlot™ Dry Blot System. The components necessary for performing the transfer was arranged as shown in figure 3.2.

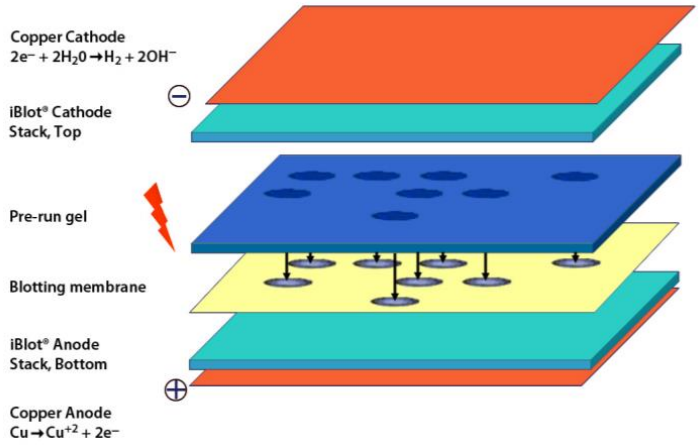

Figure 3.2. Assembly of the components of the iBlot™ Dry Blot System. The bottom part consists of a copper anode, one layer of the buffer gel and the nitrocellulose membrane. On top of the nitrocellulose membrane is the polyacrylamide gel with the proteins covered with a wet filter paper (not shown). The top part consists of another layer of the buffer gel and a copper cathode. The figure is taken from the iBlot® Dry Blotting system manual.

Materials

iBlot™ Dry Blotting system (section 2.7)

TBS, pH 7.4

Procedure

1. The SDS-page gel was washed for 5 minutes in dH_2O.
2. The anode stack (Figure 3.2), containing the nitrocellulose membrane, was placed in the gel transfer device and the gel was placed on top of the membrane. Air bubbles trapped between the gel and membrane was removed by using a blotting roller.
3. A filter paper wetted in dH_2O was placed on top of the gel.
4. The cathode stack (Figure 3.2) was placed on top of the filter paper, with the copper electrode side facing up.
5. A disposable sponge was placed in the lid of the transfer device before closing the lid.

6. The blotting was carried out at 20 V for 7 minutes.
7. After the blotting, the membrane was placed in TBS before antibody hybridisation.

3.16.2 SNAP i.d.® immunodetection

The SNAP i.d.® immunodetection system is a fast and easy method for hybridization of antibodies to proteins on a membrane. The membrane is placed in a blot holder, that is placed on top of the SNAP i.d.® immunodetection device, which utilizes vacuum to pull the reagents through the membrane, which is faster than more traditional hybridization methods.

Materials

SNAP i.d.® Protein detection system (section 2.7)

TTBS

TTBS/ 0.5% BSA (blocking solution)

Primary antibody Ag85 (1 mg/mL)

Secondary antibody HRP-Goat Anti-Rabbit IgG (1 mg/mL)

Procedure

1. The blot holder was wetted with dH_2O before the blotted membrane was placed in the middle of the blot holder with the protein side facing down.
2. A wetted filter paper was placed on top of the membrane and the blot holder was closed. In case of air bubbles, a blotting roller was used to remove them.
3. The blot holder was placed in the SNAP i.d.® Protein detection system device.
4. 30 mL of the blocking solution was poured on to blot holder, and the vacuum was turned on until all the solution had moved through the membrane.
5. 3 mL of TTBS/ 0.5% BSA with 2 µg/mL primary antibody was added to the membrane and incubated for 10 minutes.
6. The membrane was washed three times with TTBS, with the vacuum continuously running. The vacuum was turned off after the last wash.

7. 3 mL of TTBS/0.5 % BSA with 0.4 µg/mL secondary antibody was added and incubated for 10 minutes.
8. Step 6 was repeated.
9. The membrane was removed from the blot holder for incubation with an appropriate detection agent.

3.16.3 Chemiluminescent detection of proteins

Materials

SuperSignal® West Pico PLUS Chemiluminescent Substrate

Luminol/Ehancer

Stable peroxide buffer

Procedure

1. The substrate working solution was made by mixing 10 mL Luminol/Enhancer with 10 mL Stable Peroxide Buffer.
2. The membrane was incubated with the substrate working solution for 5 minutes in the dark.
3. Azure c400 was used for visualisation of the membrane. Pictures of the membrane was also captured with the same instrument.

3.17 Detection of antigens localized on the surface of *L. plantarum*

One commonly used method for detection of surface localized proteins is the use of antibodies conjugated with different fluorochromes. In this kind of method, the primary antibody binds to a specific protein, while the secondary antibody binds to the primary antibody. In this study the secondary antibody is attached to the fluorochrome Fluorescein Isothiocyanate (FITC). The fluorochrome FITC emits light when excited by a laser beam. Through analysing FITC-stained bacterial cells with flow cytometry or confocal laser scanning microscopy, surface localized proteins can be visualised.

3.17.1 Flow cytometry

In flow cytometry, cells are detected by passing a laser beam one by one. Detectors register forward scatter (FSC) and side scatter (SSC) as respectively cell size and the granularity of the cell. Cells with antigens localized on the surface will be detected when the laser beam hits the FITC conjugated molecule, which causes excitation of light, and registration of a fluorescent signal. Based on these data, cell populations can be compared. Detection of antigens localized on the surface a bacterial cell by confocal laser scanning microscopy follows the same principles as flow cytometry.

3.17.2 Cell staining with FITC for flow cytometry and confocal laser scanning microscopy

Materials

PBS

PBS + 2% BSA

Primary antibody (Anti Ag85)

Secondary antibody Anti-Rabbit IgG-FITC

Procedure

1. Recombinant *L. plantarum* was cultivated and induced as described in section 3.14.1
2. The cells were harvested three hours after induction and centrifuged at 5000x g at 4°C for 5 minutes. The supernatant was discarded.
3. The cells were resuspended in 1 mL cold PBS, and centrifuged at 5000x g at 4°C. The supernatant was discarded, and the washing step was repeated one more time.
4. The cells were then resuspended in 50 µL PBS + 2 % BSA with 5 µL of the primary antibody. The suspension was incubated at room temperature for 30 minutes.
5. After incubation, excess antibody was removed by centrifugation at 5000x g for 1 minute.

6. The cells were washed with 600 µL PBS + 2 % BSA and centrifuged at 5000x g for 2 minutes. This step was repeated three times. The supernatant was discarded.
7. An extra centrifugation at 5000x g for 1 minute was performed after the last wash to remove all the supernatant.
8. The cells were the resuspended in 50 µL PBS + 2 % BSA with 0.8 µL secondary antibody. The sample was incubated for 30 minutes at room temperature in the dark.
9. Steps 5-7 was repeated. Step 6 was repeated four times.
10. The cells were resuspended in 100 µL PBS and immediately analysed by MacsQuant® Analyser and MacsQuantify™ software.

3.18 Confocal laser scanning microscopy

All microscopy analyses were performed on a Zeiss LSM 700 Confocal Microscope by using Zen software.

3.18.1 Cell staining with DAPI and Nile-Red

To do morphological analyses of *L. plantarum* strains, bacterial cultures were stained with DAPI and Nile-Red. The fluorescent stain DAPI (4,6-diamidino-2-phenylindole) can penetrate the cell membrane and bind strongly to thymidine-adenine rich regions in the DNA. Nile-Red is a lipophilic stain, which binds to the cell membrane. Nile-Red is highly fluorescent in lipid-rich environments.

Materials

0.1 mg/mL Nile-Red

0.1 mg/mL DAPI

Bacterial culture

Procedure

1. In an Eppendorf tube, 80 µL of the bacterial culture with an OD_{600} = 0.4 was combined with 0.5 µL DAPI and 0.5 µL Nile-Red, and gently mixed.
2. The solution was kept in the dark until analysis.

3.19 Preparation of samples for transcriptional analyses

To perform transcriptional analyses on samples harvested as described in section 3.14.2, the total RNA from the samples had to be isolated. To further purify the isolated RNA, the RNA-samples were treated with DNase to remove residual genomic DNA (gDNA), as the transcriptional analyses would be affected by gDNA in the samples. Due to the highly unstable nature of RNA, it is often reverse transcribed into complementary DNA (cDNA) by reverse transcriptase before further analyses.

3.19.1 Isolation of RNA

Before harvesting, 5 mL of RNAprotect Bacteria was added in a 50 mL, to ensure immediate stabilization of RNA in the bacterial samples. 5 mL of the bacterial culture was combined with the 5 mL of RNAprotect Bacteria. The solution was vortexed for 5 s and incubated for 5 minutes at room temperature. The cells were then harvested by centrifugation at 5000x g for 10 minutes at room temperature.

RNA was isolated from the harvested cultures using the RNeasy Mini Kit following the manufacturer's protocols for "Mechanical Disruption of Bacteria" and "Purification of Total RNA from Bacterial Lysate Using the RNeasy Mini Kit".

3.19.2 Treatment with DNase for removal of genomic DNA

Residual genomic DNA (gDNA) of the isolated RNA samples affects quantification of RNA in downstream analyses. To further purify the RNA-samples, the Heat&Run gDNA (section 2.7) removal kit were utilized.

Materials

10x Rxn Buffer

HL-dsDNase

RNA

Procedure

1. 8-50 µL of the RNA sample was transferred to an empty Eppendorf tube on ice.
2. 1 µL of 10x Rxn Buffer was added for each 10 µL of RNA-sample added.

3. Subsequently, 1 µL HL-dsDNase was added. The suspension was gently mixed.
4. The mixture was then incubated at 37°C for 10 minutes, then at 58°C for 5 minutes for deactivation of the enzyme.

The RNA concentration of the samples was measured after this step, as described in section 3.9, before proceeding to reverse transcription.

3.19.3 Reverse transcription

Reverse transcription was performed with the iScript™ Reverse Transcription Supermix for RT-qPCR. The Supermix contains all necessary components (RNase H+ Moloney murine leukemia virus reverse transcriptase, RNase inhibitor, dNTPs, oligo(dT), random primers, buffer, $MgCl_2$ and stabilizers), except the template RNA. To control gDNA levels in the RNA-samples, negative controls were made by adding the iScript No-RT Control Supermix instead of the iScript RT Supermix.

Table 3.9 – Reaction set up for reverse transcription of RNA to cDNA

Component	Volume per Reaction (µL)
iScript RT Supermix	4
RNA template	Variable
Nuclease free water	To 20

Components were assembled in a 0.2 mL PCR tube on ice, mixed and placed in a thermal cycler.

Table 3.10 – Reaction protocol for synthesis of RNA to cDNA

Step	Temperature (°C)	Time (min)
Priming	25	5
Reverse transcription	46	20
RT inactivation	95	1

The resulting cDNA samples was either used right away in downstream analyses, or stored at -20°C until further use.

3.20 Droplet digital PCR

Droplet digital PCR (ddPCR) is a method for calculation of absolute concentration of RNA, by using gene specific primers. ddPCR is a digital PCR method using end-point analysis to calculate the absolute concentration of a given sample. In ddPCR, the target molecules of a sample are randomly fractioned into 20,000 droplets, resulting in some droplets containing the template and other droplets lacking the template. In a droplet generator device, the original sample containing target molecules, primers and PCR reaction mix is mixed with droplet generator oil. The droplet generator vacuums both the sample and the oil through a tube. Due to the hydrophobic properties of oil, the sample will disperse when mixed with the sample, resulting in equally nanolitre-sized droplets. Subsequently, the template in the droplets are amplified by qualitative PCR containing a DNA dye, such as the non-specific dsDNA-binding dye EvaGreen. Following amplification, droplets containing a template molecule binds to the dsDNA-binding dye in the PCR reaction mix and each sample is analysed by a droplet reader. The total number of droplets in the sample are counted, as well as the number of droplets containing template based on fluorophore readings (positive droplets).

Unlike other quantitative PCR methods, such as Real-Time PCR (RT PCR), ddPCR does not require a standard curve to calculate the concentrations of the samples. In ddPCR, the concentration is calculated by the statistical Poission model. The Poission model utilizes the number of positive droplets containing one or more template fragments and calculates the absolute concentration of the fragments in the sample.

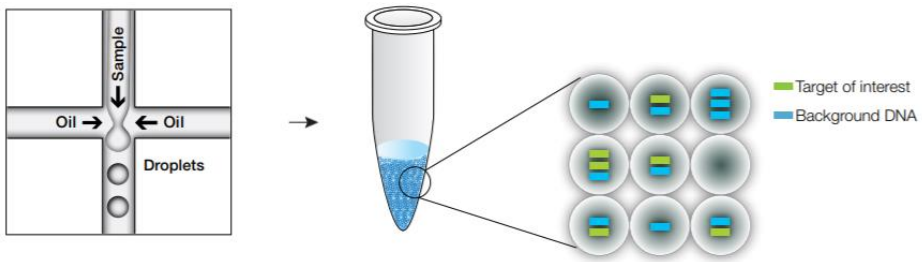

Figure 3.3. Droplet digital PCR is a method based on water-oil emulsion droplet technology. In the droplet generator, the sample is divided into 20,000 equally small droplets by exploiting water-in-oil traits. This leads to a random partitioning of target DNA in the droplets. Instead of one PCR-reaction, there will be as many individual PCR-reactions as there are droplets.

Materials

2x QX200 ddPCR EvaGreen Supermix

Droplet generation Oil for EvaGreen

Primers

Nuclease-free water

Template

DG8 Cartridges

QX200 Droplet Generator

Thermal cycler

QX200 Droplet Reader

QuantaSoft Software

Procedure

1. Before setting up an assay, a test run should be performed with dilutions of the cDNA samples ranging from 10x to 100,000x to determine the dilution returning the most accurate analysis (ratio between positive and total amount of droplets, see https://www.bio-rad.com/en-no/applications-technologies/absolute-quantification-pcr-targets-with-droplet-digital-pcr-system?ID=MDV359ESH#Poisson for more details). In this study, all samples were made into an 100x dilution.
2. The cDNA samples generated through reverse transcription were diluted to the appropriate dilution
3. The EvaGreen ddPCR reaction mix was prepared as shown in table 3.11 and dispensed into 8-strip tubes. When assembling the reaction mix, it is important to avoid making bubbles because this inhibits the droplet generation in the droplet generator.

Table 3.11 – Preparation of the EvaGreen ddPCR reaction mix

Component	Volume per reaction (µL)	Final concentration
2x QX200 ddPCR EvaGreen Supermix	11	1x

2 µM Forward primer	1	100 nM
2 µM Reverse primer	1	100 nM
RNase/DNase-free water	7	-
cDNA template	2	Up to 100 ng

4. To the 20 µL reaction mix, 2 µL of the cDNA template was added.
5. 20 µL of each reaction was loaded into a sample well of the DG8™ Cartridge, followed by 70 µL of QX200 Droplet generation Oil for EvaGreen into the oil wells.
6. When the DG8™ Cartridge was placed into the QX200 Droplet Generator, and the instrument was closed, the droplet generation started.
7. After completion of droplet generation, 40 µL of the droplet-suspension was transferred to a 96-well PCR plate.
8. The all samples were transferred to the PCR plate, it was sealed with foil by the PX1 plate sealer.
9. The sealed 96-well plate was loaded into a standard thermocycler, and the PCR was carried out by the program shown in table 3.12.

Table 3.12 – Cycling program for 2x QX200 ddPCR EvaGreen Supermix

Step	Temperature (°C)	Time	Cycles
Enzyme activation	95	5 min	1
Denaturation	95	30 sec	40
Annealing/extension	60	1 min	40
Signal stabilization	4	5 min	1
	90	5 min	1
Hold	4	Infinite	1

10. Upon completion of the PCR, the 96-well plate was loaded into the QX200 Droplet Reader for analysis of the droplets.
11. Results were analysed using the QuantaSoft Software.
12. The QuantaSoft Software reports the concentration as Copies/ 20 µL well. Copies refers to the target molecule. In the present study, 2 µL were used as template for the PCR reaction. The Copies/ 20 µL value is therefore divided by two obtain Copies/µL. Copies/µL is then multiplied by the dilution factor, which in the present study was 100x.

As 100 ng RNA was revers transcribed into cDNA, the template of this analysis, the final formula for calculating Copies/ng RNA is:

$$\frac{(Copies{*}\mu L^{-1}){*}dilution\ factor}{Amount\ of\ RNA\ in\ revers\ transcription\ (ng)} = \frac{(Copies{*}\mu L^{-1}){*}100}{100} = \text{Copies/ng RNA}$$

4 Results

The antigen used in the present study is Ag85B_TB10.4_DC, a fusion protein of the two *Mycobacterium tuberculosis* derived antigens Ag85B and TB10.4. As described in section 1.6, the antigens, both individually and fused together, have shown promising immune response. Vectors have previously been constructed for production and anchoring of another hybrid antigen, Ag85B_ESAT-6, which have shown to induce antigen specific immune responses in mice after nasal and oral immunization (Kuczkowska et al., 2016). The novel antigen combination Ag85B_TB10.4_DC (AgTB) has not previously been expressed in *L. plantarum*. Therefore, the first step in developing a new recombinant strain was to construct vectors for production of AgTB analogous to the Ag85B_ESAT-6 vectors, to have the ability to compare the production of AgTB with the already characterized AgESAT-6.

The present study is a part of a project where the long-term goal is to develop a new vaccine against *M. tuberculosis*, hence potential safety issues must be addressed. Plasmid-based production of tuberculosis antigens in *L. plantarum* have been successful. However, plasmids carry other heterologous genes in addition to the antigen is disadvantageous in regard to horizontal gene transfer. It is therefore desirable that the bacteria as delivery vectors contains as few heterologous genes as possible. By moving onward from plasmid-based production of antigens, to integration of only the antigen expression system in the bacteria's genome, the number of heterologous genes would decrease. Current plasmid-based antigen production is controlled by the pSIP expression system. As the pSIP expression system is dependent on two regulatory genes (see section 1.3.1), integration of the system would be complicated. An alternative to overcome this issue is the utilization of a constitutive expression system for antigen production, as it is not dependent on neither helper genes nor additives for activation (see section 1.3.2). To mediate integration of antigen production into the genome of *L. plantarum*, a gene editing tool such as the CRISPR/Cas9 system can be exploited.

Initially, the goal of the present study was to construct a total of four vectors for expression of AgTB. To obtain the four new vectors, the pSIP-vector pLp1261_InvS (Fredriksen et al., 2012) was utilized as the backbone starting point. Construction of the two constitutive vectors were meant to be performed by replacing the original inducible promoter P_{SppA} in the pSIP-vector by the constitutive promoters P_5 and P_{11}, respectively. The last two vectors expressed AgTB through the inducible system of the pSIP vector, where one vector surface displayed the

antigens through the lipoprotein anchor derived from the *L. plantarum* gene; *Lp_1261*, and the second with intracellular localization of the antigen.

The AgTB gene was codon optimized for expression in *L. plantarum* to facilitate efficient gene expression and ordered from GenScript, as the full-length sequence of P5_Lp1261_Ag85B_TB10.4_DC (Table 2.4), that consist of the P_5 promotor upstream of the lipo-anchor Lp_1261, which was translationally fused to the Ag85B_TB10.4_DC sequence. GenScript cloned the fragment into a plasmid called EPI300. EPI300 is a low copy vector, that was utilized because GenScript had problems cloning the sequence in the normally used high copy pUC57 plasmid. In addition, the promoter P_{11} was ordered from GenScript translationally fused to the lipoprotein Lp_1261. The P11_Lp1261 sequence was delivered in the cloning vector pJET1.2 (Table 2.4).

4.1 Construction of the inducible vectors

The first step in construction of the inducible vectors were to isolate the EPI300 plasmid containing the P5_Lp1261_Ag85B_TB10.4 sequence from the *E. coli* culture. The concentration of the plasmid after isolation was low, because the EPI300 was a low copy plasmid. Therefore, the fragment P5_Lp1261_Ag85B_TB10.4 was amplified using PCR, to achieve a high concentration of the target sequence Ag85B_TB10.4. For construction of p1261AgTB (Table 2.4), primers TB10.4F and TB10.4R (Table 2.1) were used to amplify the P5_Lp1261_Ag85B_TB10.4. The PCR reaction was run on agarose gel and the PCR product was cut out from the gel and purified. The PCR amplified P5_Lp1261_Ag85B_TB10.4 fragment was digested with SalI and Acc65I to remove the P_5 promoter and the lipo-anchor, and the remaining AgTB fragment was ligated into SalI/Acc65I digested pLp1261_InvS (Tab 2.4), yielding p1261AgTB (Figure 4.1).

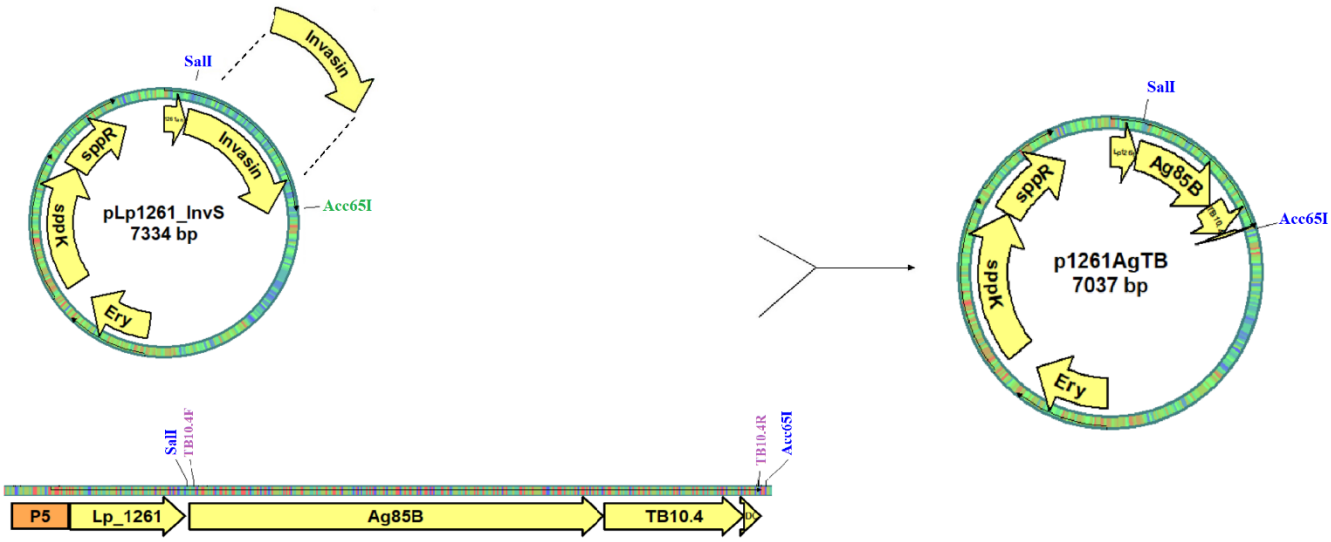

Figure 4.1. Strategy for construction of the vector p1261AgTB. The antigen was first amplified by PCR with primers TB10.4F and TB10.4R. Subesquently, the purified PCR product and the pLp1261_InvS vector were both digested with the restriction enzymes SalI and Acc65I. The digested fragments were then ligated, yielding the vector p1261AgTB.

To construct the plasmid for inducible cytoplasmic expression of AgTB, the sequence P5_Lp1261_Ag85B_TB10.4 from the EPI300 plasmid served as a template for amplification of Ag85B_TB10.4 with In-Fusion primers NdeISIP_F and TB10.4R (Table 2.1). The vector pLp1261_InvS was digested with the restriction enzymes NdeI and Acc65I. In-Fusion cloning (see section 3.6.1 for details) was utilized to insert the PCR-fragment into the digested pLp1261_InvS vector to obtain the vector pCytAgTB (Figure 4.2).

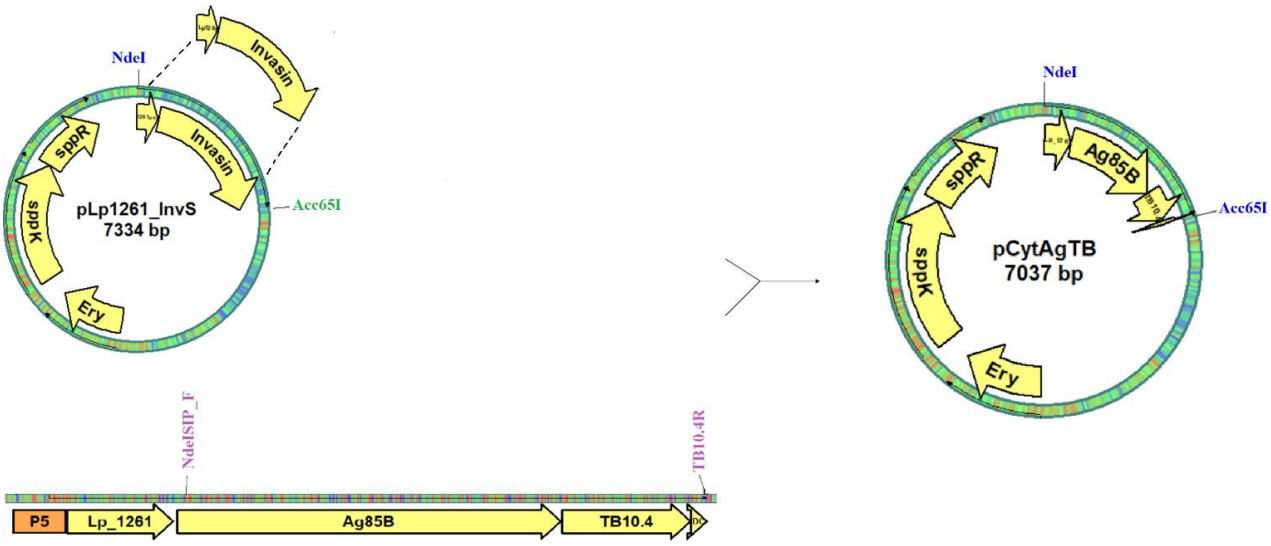

Figure 4.2. Strategy for construction of the vector pCytAgTB. The antigen was first amplified by PCR with primers NdeISIP_F and TB10.4R. Then, the pLp1261_InvS vector was digested with the restriction enzymes NdeI and Acc65I. The inducible vector pCytAgTB was obtained through In-Fusion ligation of the fragments.

Subsequently, the constructed p1261AgTB and pCytAgTB were transformed into OneShot® TOP10 chemically competent *E. coli* cells. Correct clones were first verified by colony PCR, and subsequently all PCR amplified parts of the constructed plasmids were verified by DNA sequencing (data not shown), before transformation into *L. plantarum*. The inducible antigen vectors p1261AgTB and pCytAgTB were both successfully constructed at the first attempt.

4.2 Construction of the constitutive vectors

As one of the goals of this study was to constitutively express the fusion protein AgTB, two promoters from the synthetic constitutive promoter library constructed by Rud et al. (2006) was chosen. One weak and one strong promoter, P_5 and P_{11}, respectively.

Several strategies were attempted for constructing the vectors with constitutive production of AgTB. An overview of the strategies that were tested are given in table 4.1 and 4.2. The plasmid map of pP5AgTB and pP11AgTB can be seen in figure A-1 of the Appendix.

Table 4.1 – Different cloning strategies utilized for construction of the constitutive vector pP11AgTB.

5' Cut	EcoRI31	Bsu15I	BglII	EcoRI31	Bsu15I	Bsu15I
3' Cut	SalI	SalI	SalI	SalI	SalI	SalI

Ligation method	T4 quick ligase	T4 quick ligase	T4 ligase - overnight	T4 ligase - overnight	T4 ligase - overnight	T4 quick ligase
Incubation temperature	Room temperature	Room temperature	16°C	16°C	16°C	Room temperature

None of the strategies attempted for the P_{11} constructs resulted in successful cloning, although colonies always appeared on the agar plates after transformation to *E. coli*. Although fewer than on the positive plates, colonies did also appear on the negative control plates, indicating some relegation of the vector backbone, which was confirmed by colony PCR.

Table 4.2 – Different cloning strategies utilized for construction of the constitutive vector pP5AgTB.

5' Cut	SalI	Bsu15I	Bsu15I	Bsu15I	BglII	Eco31I*
3' Cut	Acc65I	Acc65I	Acc65I	Acc65I	SalI	EcoRI*
Ligation method	T4 quick ligase	In-Fusion	T4 ligase – overnight	ElectroLigase	T4 ligase – overnight	T4 ligase – overnight*
Incubation temperature	Room temperature	50°C	16°C	Room temperature	16°C	16°C*

*One colony gave correct size

As for the P_{11} constructs, the P_5 constructs some colonies appeared on the agar plates, but most of them showed to be relegated vector. However, after several attempts with different strategies, finally when using Eco31I and EcoRI for digestion and overnight ligation with T4 ligase, 1 colony out of 15 tested on a plate gave correct fragment size after colony PCR.

After verification by colony PCR, the colony was sent for sequencing. The results from sequencing revealed that the colony had a mutation in the -35 box of the promoter. The mutant colony had substituted a Guanine with an Adenine compared to the original sequence of the P_5 promoter and the consensus sequence that was compiled for the synthetic library (Figure 4.3).

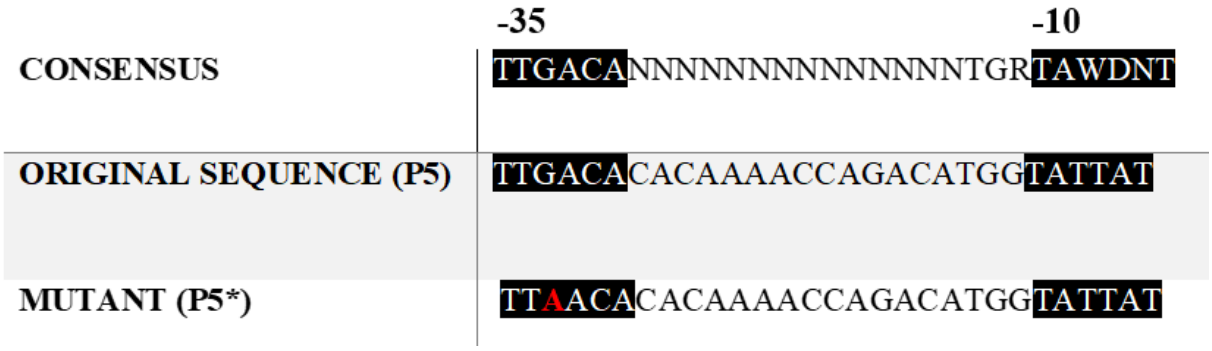

Figure 4.3. Mutation of the P_5 promoter in the colony-PCR verified colony. As illustrated by the figure, there is a deviation in the -35 box of the mutant promoter compared to the original P_5 and consensus sequence from the synthetic promoter library constructed by Rud et al. (2006). R= A or G, W= A or T, D= A, G or T, N= A, G, C or T.

4.2.1 Trouble shooting of construction of the constitutive expression

Due to a promoter mutation in the only correct colony after several attempts to construct a constitutive vector, some measures were taken to overcome the putatively toxicity of constitutive expression of AgTB in *E. coli*. It could be that the constitutive promoter is functional in *E. coli* and AgTB is produced, this might explain the toxicity.

The number of low copy plasmids in a cell is usually around 1-10 copies (Baldridge et al., 2010), while the number of high copy plasmids can be over 1000 copies (Jones et al., 2000). If the constitutive promoters P_5 and P_{11} are functional in *E. coli*, and the antigen is toxic to the cell, a reduced copy number of plasmids might decrease the toxicity in *E. coli*. Therefore, one strategy was to replace the high copy pSIP-vector with the low copy pELS100-vector (Sørvig et al., 2005b) (Table 2.4) (Figure 4.4). In an attempt to insert the P5_Lp1261_Ag85B_TB10.4 fragment into pELS100, the restriction site of NotI was implemented to the insert through PCR. The insert and low copy vector were both digested with NotI and HindIII and ligated with T4 Quick ligase.

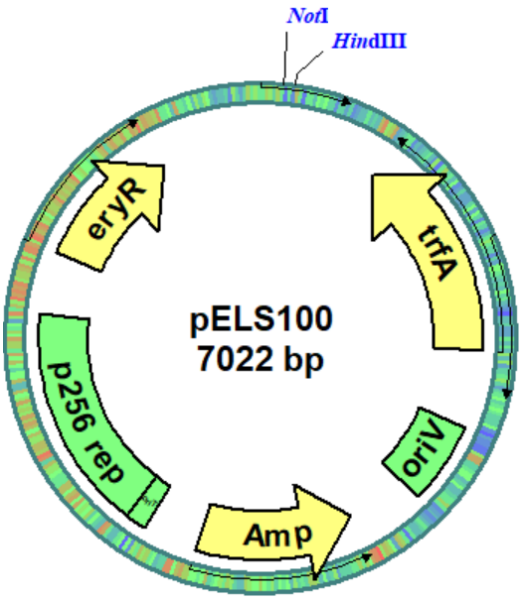

Figure 4.4. The low copy vector pELS100. pELS100 contains both Erythromycin and Ampicillin resistance genes, as well as multiple cloning sites which contain the indicated NotI and Hind III sites.

In the first attempt with the new cloning strategy using the pELS100 vector, interestingly, seven out of nine colonies clearly gave the correct band on agarose gel after colony PCR (figure 4.5)

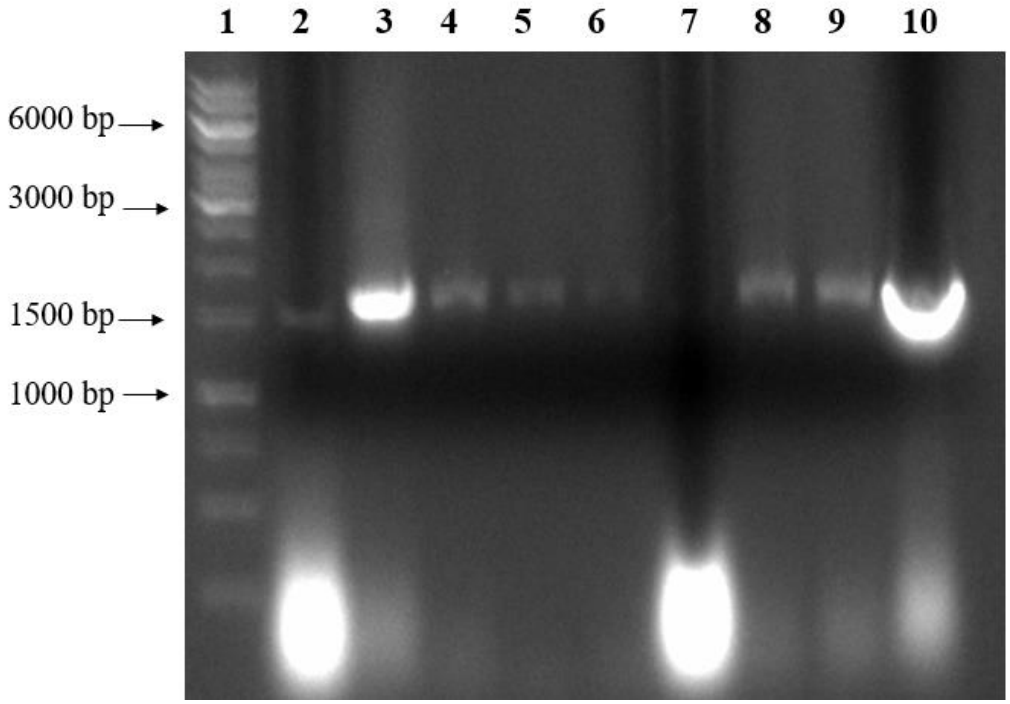

Figure 4.5. Colony PCR of pELS100P5AgTB. Seven out nine analysed colonies gave the correct size of 1600 bp as indicated by an arrow. Well number 1) GeneRuler™ 1 kb DNA ladder, wells 2-10 colonies of pELS100P5AgTB.

The correct colonies were grown overnight in BHI medium containing Erythromycin (Table 3.1) for low copy plasmid isolation. Surprisingly, after isolation of the pELS100P5AgTB plasmid from TOP10 cells, the antigen-insert of the plasmid was no longer detected by PCR. Concomitantly, sequencing confirmed that the antigen-insert was in fact no longer present on the plasmid. The purification process was repeated several times, always resulting in the disappearance of the insert.

As the low copy pELS100-vector appeared to be unstable, all further experiments were carried out with the pSIP-vector. To check whether the constitutive promoter, the antigen or possibly the combination of the two were the reason for the problems, the antigen was replaced by a gene encoding the small reporter protein NucA (Table 2.4). This protein has successfully been used in the inducible pSIP vectors previously (Mathiesen et al., 2009). Construction of three vectors attempted, containing the P_5 promoter upstream of the *NucA* gene: intracellular expression, secretion with the signal sequence Lp_3050 and surface localization by the lipoprotein Lp_1261. The plasmid maps are shown in figure A-2 of the Appendix. However, the replacement of the antigen with *NucA* did not solve any problems.

4.3 Growth curve analysis on *L. plantarum* harbouring different plasmids

Several studies have shown that production of heterologous proteins may reduce the bacterial growth (Fredriksen et al., 2010; Kuczkowska et al., 2015; Lulko et al., 2007). Overnight cultures of *L. plantarum* harbouring different plasmids for AgTB production was grown overnight. The overnight cultures were diluted to an OD_{600} of 0.15 in pre-warmed MRS, and 200 µL of the diluted culture was transferred to a 96-well microtiter plate. The absorbance of the cultures was measured for one hour, before induction of the cultures with 25 ng/mL SppIP. After induction, the OD_{595} was measured every fifth minute for 20 hours by MultiSkan FC microplate reader. *L. plantarum* carrying the pEV plasmid was used as a control, as it lacks P_{sppA} expressed genes.

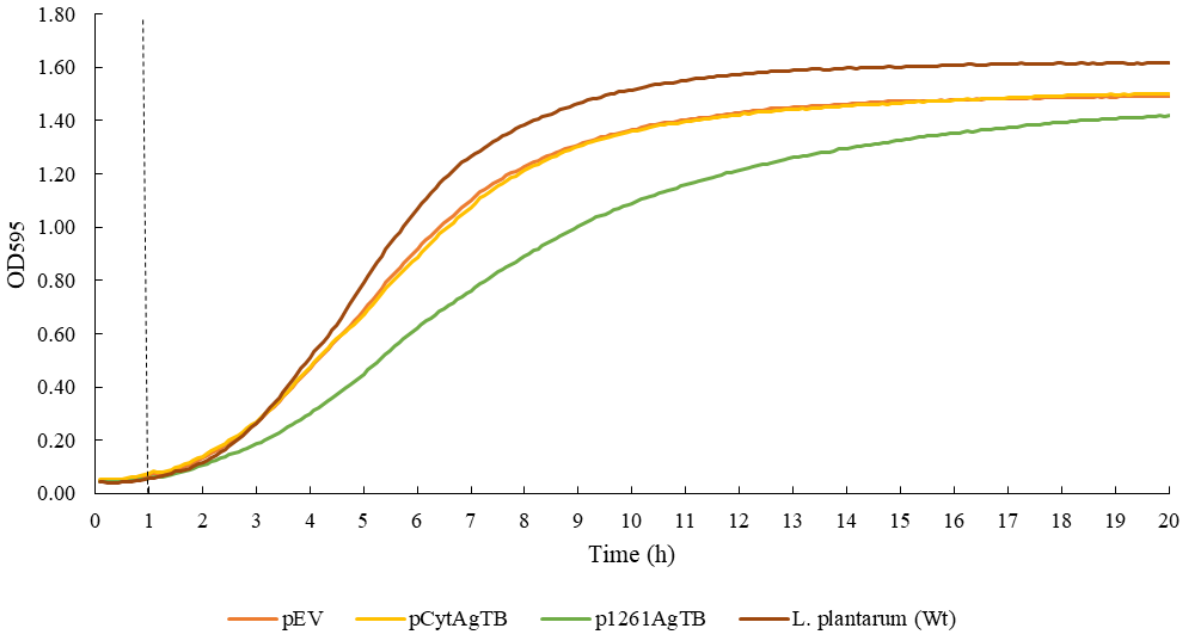

Figure 4.6. Growth curves of recombinant *L. plantarum* harbouring plasmids for antigen production. The bacterial cultures were induced with 25 ng/mL SppIP one hour after start (approx. ~OD_{600}=0.3), indicated by the stapled line. The presented results are an average of three independent experiments.

Figure 4.6 shows the growth of the recombinant *L. plantarum* harbouring either pCytAgTB, p1261AgTB or the control pEV. The wild-type *L. plantarum* were also included in the analysis. *L. plantarum* harbouring the pEV and the pCytAgTB showed similar growth rates, while the wild type bacteria grew slightly faster. However, *L. plantarum* harbouring the p1261AgTB plasmid showed clearly reduced growth after induction compared to pEV and pCytAgTB.

4.4 Western blot analysis of antigen production

Western blot analysis was utilized to investigate antigen production in bacteria harbouring p1261AgTB and pP5*AgTB, using Ag85B specific antibodies for detection (section 3.16). The wild type strain of *L. plantarum* was included as a negative control, while protein extract from *L. plantarum* harbouring pAgESAT6 (Table 2.4) served as the positive control (Figure 4.7). The bacterial cultures were cultivated and harvested as described in sections 3.14.1 and mechanically disrupted as described in section 3.4. The OD_{600} of the cultures were measured and based on this, the volume taken from each culture were adjusted to ensure an equal number of cells was used in the experiment.

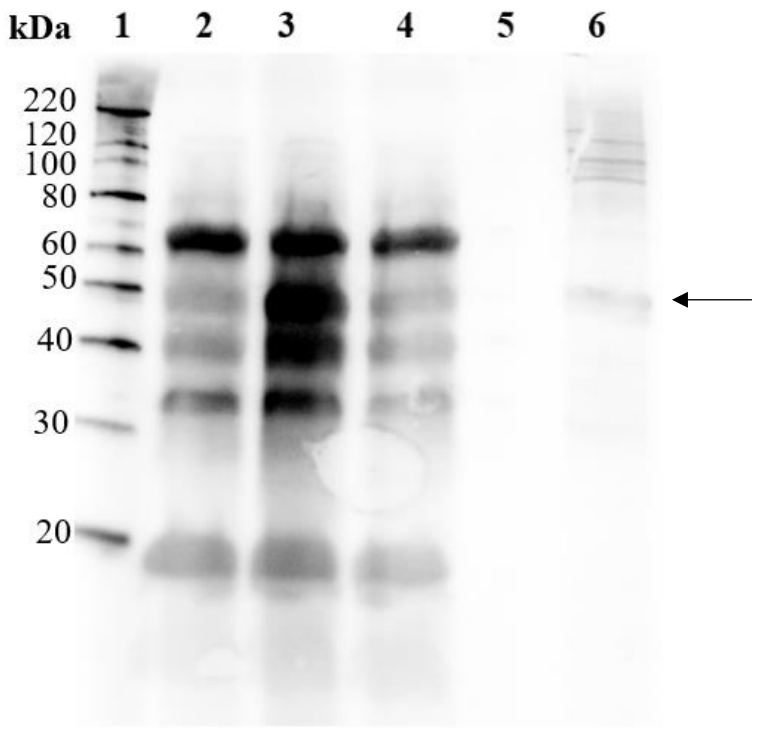

Figure 4.7. Western blot of cell-free protein extracts from *L. plantarum* harbouring p1261AgTB and pP5*AgTB. Well number 1) MagicMark® XP Western Protein Standard, 2) pP5*AgTB 3) wild type strain of *L. plantarum (*negative control), 4) p1261AgTB 5) empty 6) Protein extract from *L. plantarum* harbouring pAgESAT6. A band at about 52 kDa is indicated in the positive control by an arrow.

The size of the fusion protein AgTB is 52 kDa, and a weak band at this size is visible in well 6 for the positive control in figure 4.7. In well 2-4 however, probably due to unspecific binding of the secondary antibody, more than one band is visible in the crude protein extracts.

The experiment was repeated, using the same protein extracts with some adjustments. Figure 4.7 shows strong protein bands on the membrane. Therefore, to reduce the amount of protein applied to the gel, the volume of protein extract was halved. In addition, the concentration of the primary antibody was increased, from 2 to 4 µg/mL. The concentration of the secondary antibody was decreased from 0.4 to 0.2 µg/mL, to potentially reduce the unspecific binding of the secondary antibody. However, the adjustments did not affect the unspecific binding (data not shown).

4.5 Detection of antigen on the surface of *L. plantarum* using flow cytometry

Flow cytometry of the bacterial cells was performed to investigate whether the antigen was successfully localized and exposed at the surface of the bacteria. The data generated from the flow cytometry analysis may be presented in a histogram where the y-axis represents the number of bacterial cells sampled and the x-axis represents the relative fluorescence of FITC as measured by the flow cytometer. Therefore, a higher intensity of fluorescent signal is indicated by a shift along the x-axis to the right.

Bacterial cultures of *L. plantarum* carrying the inducible constructs p1261AgTB and pCytAgTB, as well as the constitutive plasmid pP5*AgTB were cultivated and harvested according to section 3.14.1. The bacterial cells were stained as described in section 3.17.2 and analysed by Flow cytometry (Figure 4.8).

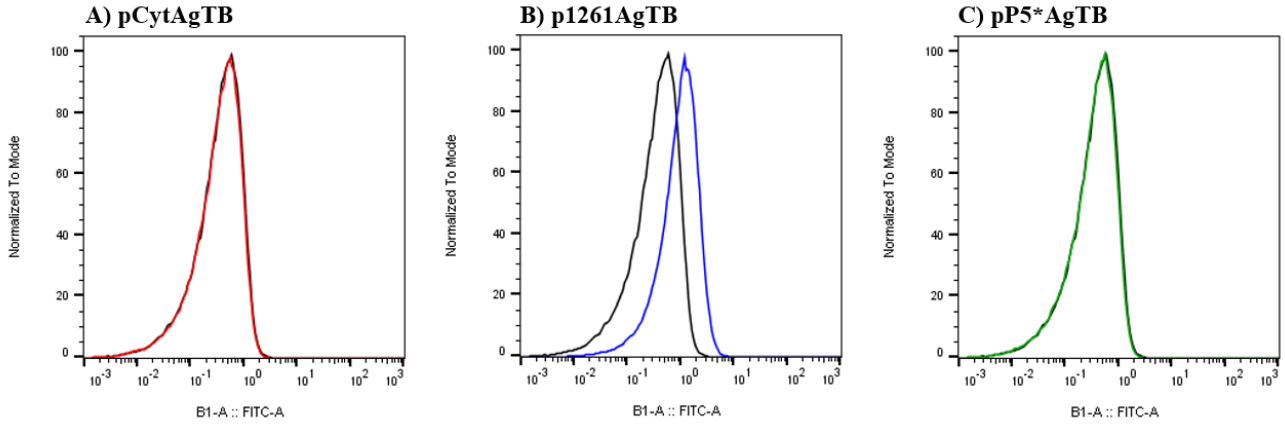

Figure 4.8. Flow Cytometry analysis of FITC stained recombinant *L. plantarum*. Histogram A-C shows *L. plantarum* harbouring plasmids producing **A)** intracellular pCytAgTB, **B)** lipo-anchored p1261AgTB, **C)** lipo-anchored pP5*AgTB. Bacteria harbouring pEV are indicated as a black line in the histograms A-C, and serves as a negative control with no fluorescent signal. The results are shown as histograms with the relative fluorescence (x-axis) plotted against number of events (y-axis). The y-axis was normalized and smoothed by the MacsQuantify™ Software.

As expected, no fluorescent signal was detected for the negative control pEV (Figure 4.8A-C). Neither was a signal detected for the bacteria harbouring pCytAgTB (Figure 4.8A). However, for the bacteria harbouring p1261AgTB a slight shift to the right were detected (Figure 4.8B). Some optimisation of the procedure had to be done to obtain this result, by adding more of the primary antibody and increase the incubation times of the antibodies. No shift was detected for the bacteria harbouring pP5*AgTB (Figure 4.8C).

Figure 4.9 shows the flow cytometry analysis of *L. plantarum* harbouring lipo-anchored pAgESAT6 (2.4) stained with both primary antibody Anti Ag85 (A) and Anti ESAT-6 (B). This analysis was performed to compare the fluorescent signal emitted from hybridizing with primary antibodies Ag85 and ESAT-6, because the fluorescent signal detected from Anti Ag85B- hybridized p1261AgTB was weak (Figure 4.8B).

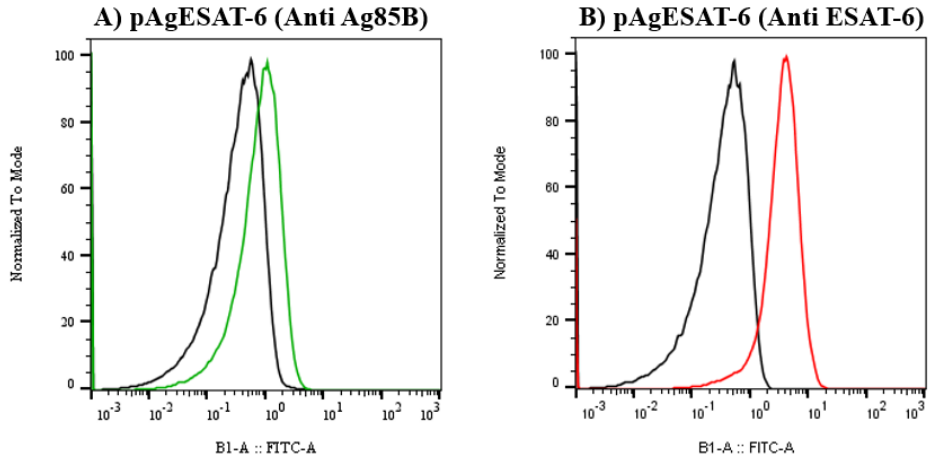

Figure 4.9. Flow Cytometry analysis of recombinant *L. plantarum* harbouring AgESAT-6 stained with different antibodies. A) *L. plantarum* harbouring pAgESAT6 hybridized with primary antibody anti Ag85. B) *L. plantarum* harbouring pAgESAT6 hybridized with primary antibody anti ESAT-6. Bacteria harbouring pEV are shown as a black line in histogram A and B, and serves as a negative control. The results are shown as histograms with the relative fluorescence (x-axis) plotted against number of events (y-axis). The y-axis was normalized and smoothed by the MacsQuantify™ Software.

L. plantarum harbouring pAgESAT6 stained with the primary antibody anti ESAT-6, shown in figure 4.9B, is clearly more shifted compared to the bacteria stained with primary antibody anti Ag85 shown in figure 4.9A. A possible explanation for the difference in emitted fluorescent signal might be that the Ag85B part of the fusion protein Ag85B_ESAT-6 is more embedded in the membrane compared to the ESAT-6 part of the fusion protein, making it more unavailable for interactions with the antibody.

4.6 Detection of Antigen on the Surface of *L. plantarum* with Immunofluorescent Microscopy

To further confirm the presence of antigen on the surface of *L. plantarum* harbouring p1261AgTB, Immunofluorescent microscopy was utilized. The immunofluorescent analysis

was performed on bacterial cells stained as described for Flow cytometry. The results of the microscopy analysis are shown in Figure 4.10.

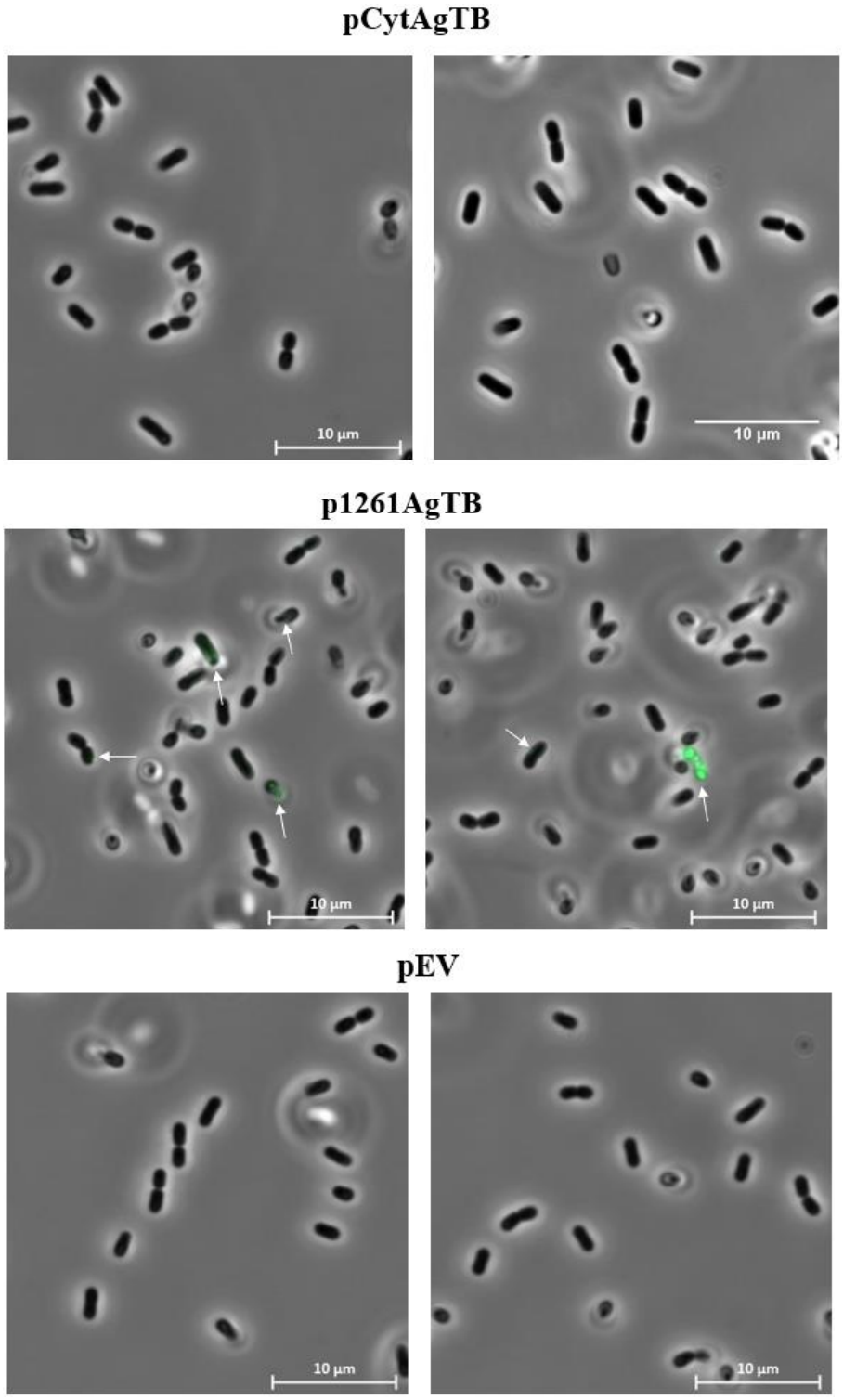

Figure 4.10. Immunofluorescent microscopy of FITC stained recombinant *L. plantarum*. Only a few green fluorescent bacteria (indicated by white arrows) are detected in the two bottom rows, showing *L. plantarum* harbouring p1261AgTB. No fluorescent bacteria are detected in the top and middle row windows showing *L.*

plantarum harbouring pCytAgTB or pEV. Bacteria harbouring the mutated constitutive construct were not included in this analysis.

No fluorescent signal was detected in bacteria harbouring either the pEV or pCytAgTB (Figure 4.10). For p1261AgTB, only a few fluorescent bacteria were seen with the immunofluorescence analysis (Figure 4.10). However, although the Flow cytometry results (Figure 4.8A-B) were weak, the number of green fluorescent bacteria observed with immunofluorescence analysis was fewer than expected.

4.7 Adaption of the CRISPR/Cas system for use in *L. plantarum*

In the present study, the CRISPR/Cas system was developed as a two-plasmid system to exploit the system for genomic modification. One plasmid contained the Cas-coding gene under the control of an inducible promoter P_{sppA}, a selection marker (Ery) and the *L. lactis* derived, broad-host-range Sh71 replicon (Figure 4.12). *L. lactis* was utilized as a subcloning host for the Cas-plasmids. The second plasmid contained the Cas-handle and the 20 nucleotide (nt) base pairing region (SgRNA) under the control of the constitutive promoter P_3 and a resistance gene (Cat) (Figure 4.13). The SgRNA-transcribing vector also contains an *E. coli* replicon (pUC ori) in addition to the *L. plantarum* 256 replicon (see Figure 1.1).

The system was developed to mediate integration of genes of interest, as well as depletion and editing of *L. plantarum* native genes. Table 4.3 shows the combinations of plasmids that were used in this study. The abbreviations will be used in the text.

Table 4.3 – *L. plantarum* harbouring the two-plasmid CRISPR/Cas9 system

Plasmids	Abbreviation	Description
pSgRNA_luc+ psIP_411_dCas9_Sh71	pSgluc-dCas9	Empty vector plasmid. Contains the complete CRISPR/dCas9 system, but the target gene, *luc*, is not present on the *L. plantarum* genome.
pSgRNA_2645+ pSIP_411_dCas9_Sh71	pSg2645-dCas9	Two-plasmid system for depletion of *lp_2645* using inducible dCas9

pSgRNA_1247+ pSIP_411_dCas9_Sh71	pSg1247-dCas9	Two-plasmid system for depletion of *lp_1247* with dCas9
pSgRNA_2217+ pSIP_411_dCas9_Sh71	pSg2217-dCas9	Two-plasmid system for depletion of *lp_2217* with dCas9
pSgRNA_1247_2217+ pSIP_411_dCas9_Sh71	pSg1247_2217-dCas9	Two-plasmid system for depletion of *lp_1247* and *lp_2217* with dCas9
pSgRNA_2645+ pSIP_411_Cas9_Sh71	pSg2645-Cas9	Two-plasmid system for editing of *lp_2645* mediated by double strand cleavage with Cas9.
pSgRNA_2645+ pSIP_411_Cas9^{D10A}_Sh71	pSg2645-Cas9^{D10A}	Two-plasmid system for editing of *lp_2645* mediated by single strand cleavage with Cas9^{D10A}
pSgRNA_2645_HLNucAHH+ pSIP_411_Cas9_Sh71	pSg2645Ha-Cas9	Two-plasmid system for exchange of native *lp_2645* in *L. plantarum* with *NucA* mediated by double strand cleavage with Cas9.
pSgRNA_2645_HLNucAHH+ pSIP_411_Cas9^{D10A}_Sh71	pSg2645Ha-Cas9^{D10A}	Two-plasmid system for exchange of native *lp_2645* in *L. plantarum* with *NucA* mediated by single strand cleavage with Cas9^{D10A}.

4.7.1 The CRISPR/Cas-system developed as a two-plasmid system in *L. plantarum*

The construction, and primers used for construction, of the Cas-plasmid was similar for all three variants of the Cas-genes utilized in this study: Cas9, Cas9^{D10A} and dCas9. The plasmids containing the *Cas9* (pCas) and *Cas9^{D10A}* (pLCNICK) genes were ordered from Addgene (Table 2.4). *Cas9* was amplified from pCas and *Cas9^{D10A}* was amplified from pLCNICK, using the In-Fusion primers CasNcoF and pCasR (Table 2.1). The construction process is only showed for

construction of pCas9Sh71 (Figure 4.11 & 4.12), although the same construction was performed to obtain pCas9^{D10A}Sh71 (Table 2.4). Firstly, the inducible vector pSIP_403 (Table 2.4) were digested with NcoI and XhoI. Subsequently, an In-Fusion cloning between the *Cas9* fragment, amplified using the primer pair CasNcoF/pCasR, and the digested pSIP403 vector were performed to obtain pSIP403_Cas9 (Figure 4.11).

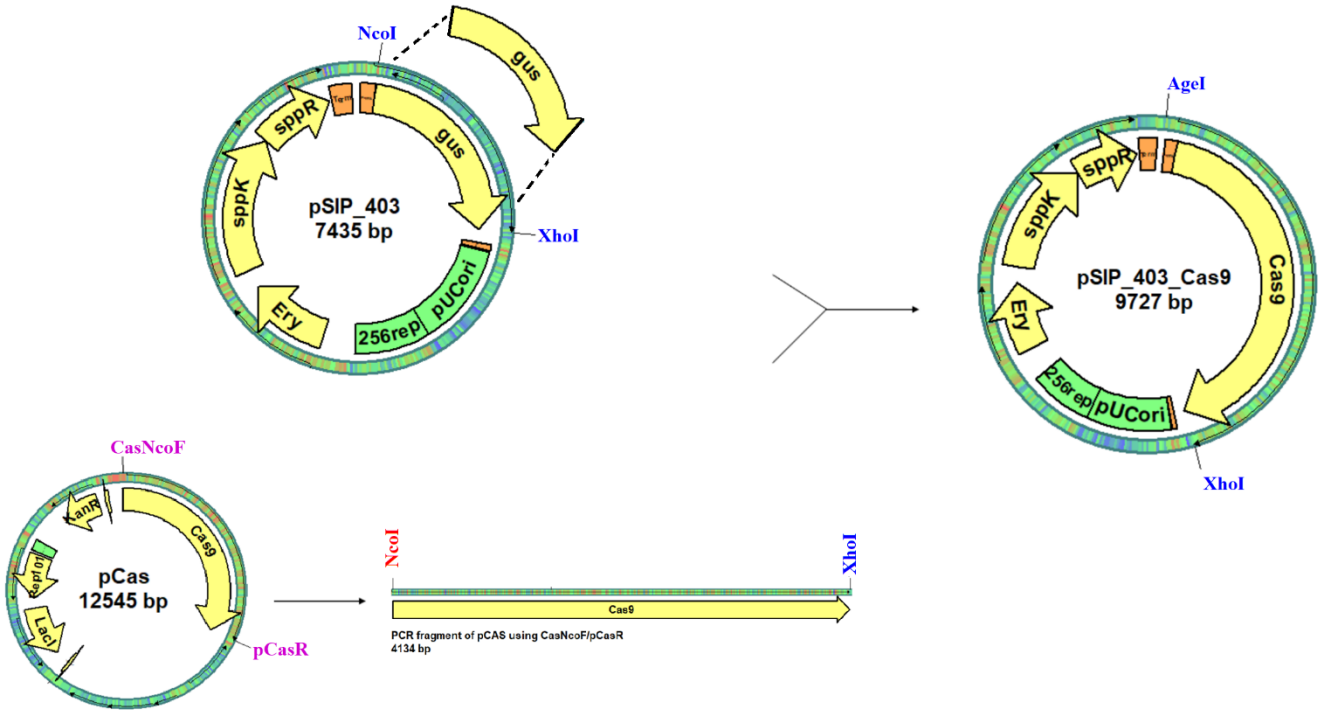

Figure 4.11. The first step in construction of the Cas-plasmid with an inducible promoter. The Cas-gene was amplified with the primer pair CasNcoF/pCasR with pCas as the template (Table 2.1 and 2.4). At the same time, the inducible vector pSIP403 was digested with NcoI and XhoI. The digested vector and PCR-amplified fragment were cloned through In-Fusion cloning to obtain the plasmid on the right: pSIP403_Cas9. pSIP403_Cas9 was transformed into *E. coli*.

Next step in the construction was to replace the 256-replicon in pSIP_403_Cas9 (Figure 4.11) with the Sh71 replicon. Both pSIP403_Cas9 and pSIP411 were digested with AgeI and XhoI, the fragments were then ligated using ElectroLigase as described in figure 4.12 and transformed into electrocompetent *L. lactis* to obtain pCas9Sh71 (Figure 4.12).

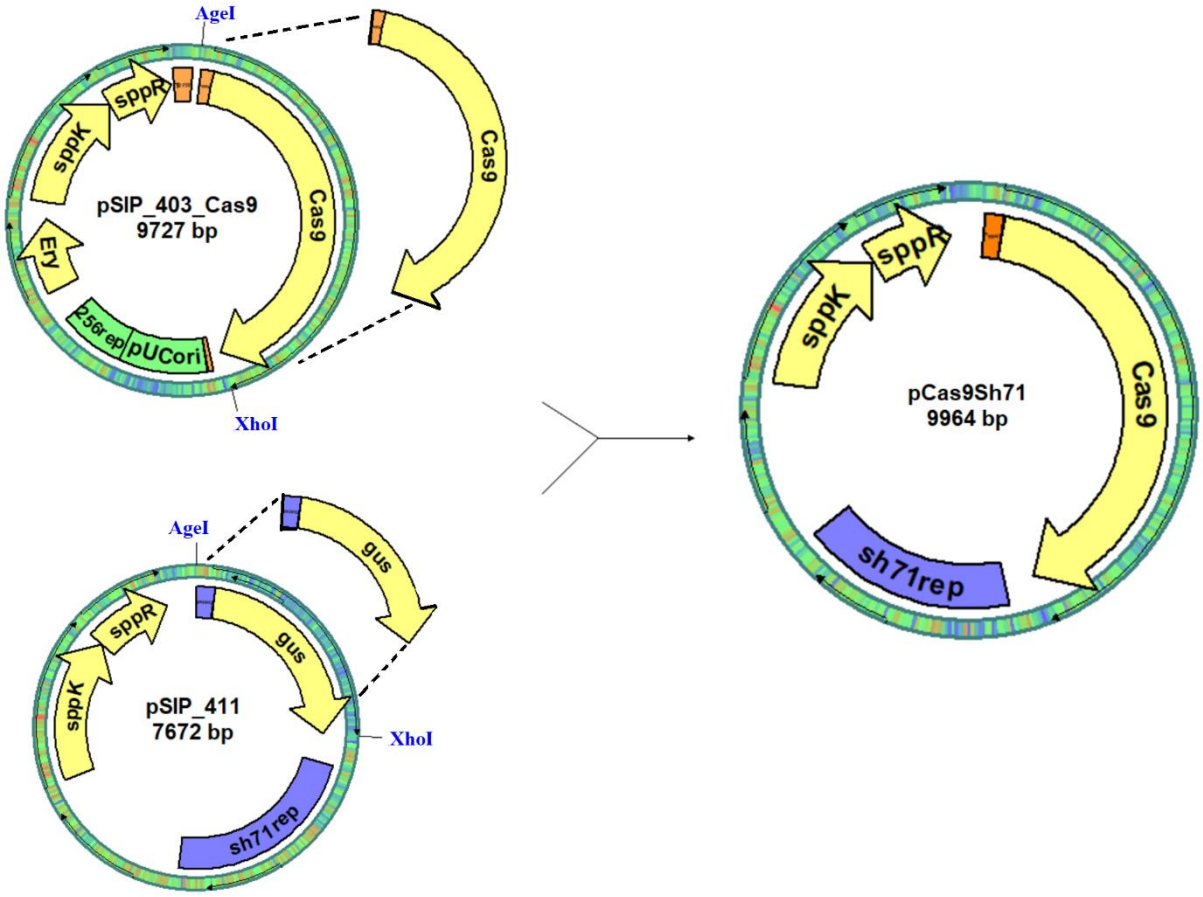

Figure 4.12: Change of replicon to obtain the pCas9Sh71 vector. The pSIP403_Cas9 plasmid from figure 4.11 are digested with AgeI and XhoI. pSIP411, containing the Sh71-replicon, are digested with the same restriction enzymes. The digested fragments are ligated with ElectroLigase and transformed into electrocompetent *L. lactis* to obtain the pCas9Sh71 vector.

The construction of pCas9Sh71 and pCas9^{D10A}Sh71 was both successfully performed at the first attempt. The two constructed Cas-plasmids with the Sh71-replicon were subsequently isolated from *L. lactis* and transformed into *L. plantarum.*

4.7.2 Construction of a new SgRNA-plasmid

The software CRISPR primer designer (section 2.1) was utilized to construct 20 nucleotide (nt) SgRNA sequence with target gene specificity. The open reading frame of the target gene or region served as input into the designer software, which created a list of potential 20 nt SgRNA-sequences adjacent PAM sequences. CRISPR primer designer also provides information about whether the sequence is located on the positive or negative strand, and its position on the gene. For SgRNA used in combination with catalytically inactive dCas9, sequences from the negative strand are most effective (Rossi et al., 2015). To avoid off target binding with suggested SgRNA

sequences, a BLAST search using the 20 nt SgRNA sequences against the *L. plantarum* genome was performed. The 12 nucleotides closest to the PAM sequence, called the seed region, was used as the query.

The plasmid expressing the SgRNA is a relatively small plasmid of about 3 kb (Figure 4.13). Because of its small size, the base pairing region can easily be exchanged through inverse-PCR. The primers utilized for inverse-PCR was the Phospho-SgRNA_R and a SgRNA-primer containing the base pairing region (Figure 4.13) (Table 2.1). The PCR reaction was performed as describe in section 3.6.2.

Table 4.4 – The base pairing region is inserted through inverse-PCR, using a primer containing the 20 nt SgRNA sequence (shown in blue), as well as a region that is complementary to the plasmid (black). The sequences in blue and black are ordered as one primer.

	SgRNA (N_{20})	Complementary region (plasmid)	
5'-	NNNNNNNNNNNNNNNNNNNN	GTTTAAGAGCTATGCTGGAAACAG	-3'

Figure 4.13 shows how the Phospho-sgRNA_promoter_R and the SgRNA_F primer binds to the SgRNA template plasmid. Following the PCR reaction and gel purification (Section 3.8), the PCR amplified plasmid was digested with DpnI to remove the template plasmid and ligated with T4 Quick ligase.

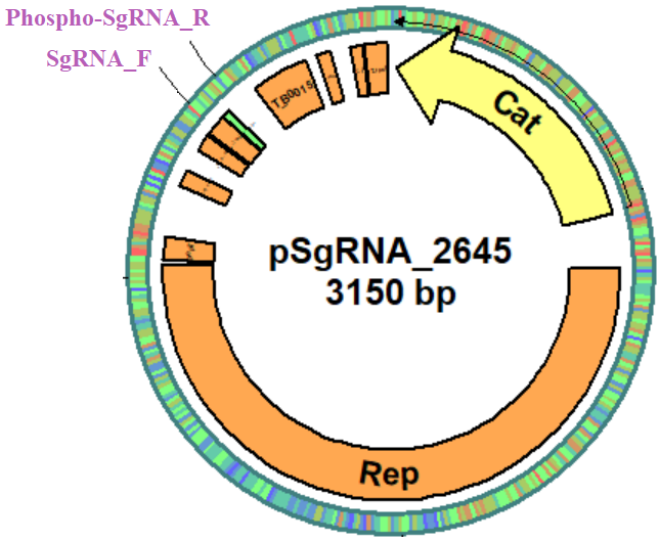

Figure 4.13: Insertion of a new base pairing region using inverse-PCR. The SgRNA_F primer contains the 20-nt base pairing region as well as a complementary region to the plasmid. The Phospho-SgRNA_R primer is

complementary to the plasmid and is phosphorylated. The primers bind to the plasmid on each side of the base pairing region (green region) to replace or insert a new 20 nt base pairing region.

All constructed SgRNA plasmids (Table 2.4) was transformed into electrocompetent *L. plantarum* which already harboured a *Cas9* expressing plasmid. *L. plantarum* with both plasmids contain a complete CRISPR/Cas-system. As the Cas-gene is under the control of an inducible promoter, the bacteria must be induced for the system to be activated.

4.7.3 Construction of a SgRNA with homologous arms for CRISPR/Cas9 mediated gene exchange

CRISPR/Cas9-mediated gene exchange between native *lp_2645* and the reporter protein NucA was attempted as a proof-of-concept experiment, due to problems with constructing vectors for constitutive production of AgTB. When Cas9 introduces double stranded break in the DNA, the damage can be repaired either through nonhomologous end joining (NHEJ) or homology directed repair (HDR) mechanisms (see section 1.7.1). HDR can be utilized for gene editing by delivery of the desired sequence into the cell as a repair template together with a SgRNA and a Cas9 protein. The repair template must contain the edit or gene, as well as additional homologous sequences immediately upstream and downstream of the target on the genome.

In this study, to replace the native *L. plantarum* gene *lp_2645*, *NucA* was flanked by 1000 bp on each side homologous to the sequence upstream and downstream of *lp_2645*, and co-localized on the plasmid expressing the SgRNA (Figure 4.14 and 4.15).

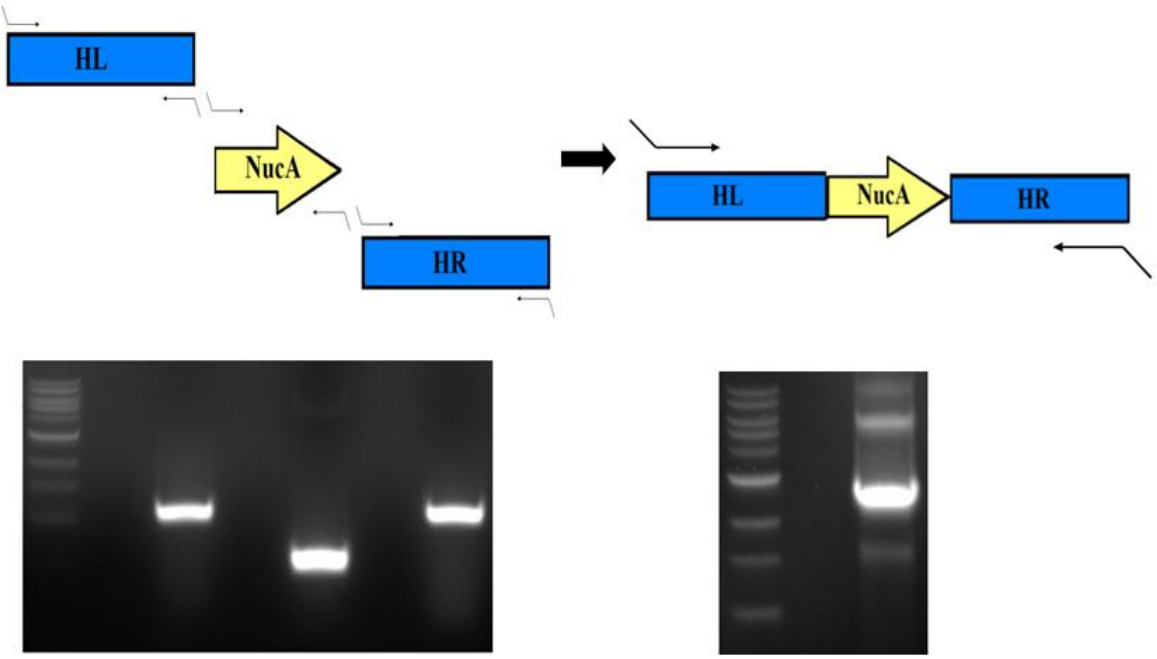

Figure 4.14. Construction of the fragment HL_NucA_HR through PCR. Primers with 15 bp overhangs complementary to the adjacent fragment where designed for each of the three fragments, the individual fragments were fused together in a second PCR reaction (right). The figure shows both a schematic overview of the process, as well as pictures taken of the agarose gel after running the PCR-reactions. The size of the homologous arms- and the NucA- fragments are ~1000 and ~500 bp respectively. The size of the constructed HL_NucA_HR fragment are ~2500 bp.

Primers SgRNA-HL_F, HL-NucA_R, NucA-HH_F and SgRNA-HH_R (Table 2.1) were designed to amplify the Left and Right homologous arm from the *L. plantarum* genome, with a 15 bp overhang complementary to the *NucA* gene on one end, and to the pSgRNA_2645 plasmid on the other end. Primers HL-NucA_F and NucA-HH_R (Table 2.1) were also made to amplify the *NucA* gene with 15 bp overhangs on each side, complementary to the left and right homologous arm respectively. The three fragments were amplified by their respective primer pair, in individual PCR reactions (Figure 4.14). After purification of the PCR-fragments, the three fragments, with complementary overhangs, were combined in a PCR-tube with only the outer primers. The outer primers were made as In-Fusion primers between the homologous arms and the pSgRNA_2645 plasmid. This PCR-reaction were performed to obtain one full-length fragment of the left homologous arm (HL), the NucA-gene and the right homologous arm (HR) (Figure 4.14). Subsequently, the pSgRNA_2645 plasmid was digested with Acc65I and XhoI. The PCR-fragment HL_NucA_HR were ligated with the digested pSgRNA_2645 obtaining pSg2645Ha (Table 2.4) (Figure 4.15).

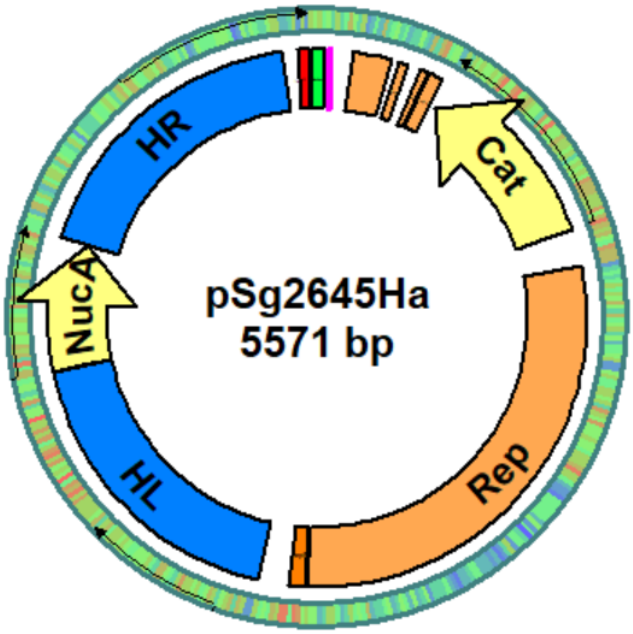

Figure 4.15: Plasmid map of pSg2645Ha. The red region marks the *S. pyogenes* constitutive promoter (P_3), the green region marks the Cas-handle and the short pink region marks the 20 nucleotides. In addition, it contains the *NucA* gene flanked by homologous arms, a Chloramphenicol resistance gene (Cat) and a 256 replicon (Rep).

4.7.4 Growth curve analysis of *L. plantarum* harbouring the two-plasmid system

As per usual for recombinant strains, the growth of the individual strains was characterized. The growth curves were constructed to investigate whether production of the heterologous dCas9 protein and the SgRNA affected the growth rate of the bacteria.

Overnight cultures of the samples were diluted to an OD_{600} ~0.15 and induced directly. The samples were measured every fifth minute for 20 hours.

Included in the analysis were the wild type *L. plantarum*, *L. plantarum* harbouring the individual dCas9- and SgRNA_2645 plasmids and *L. plantarum* containing pSg2645-dCas9, as well as the *lp_2645* knock out (Δ2645) (Figure 4.16).

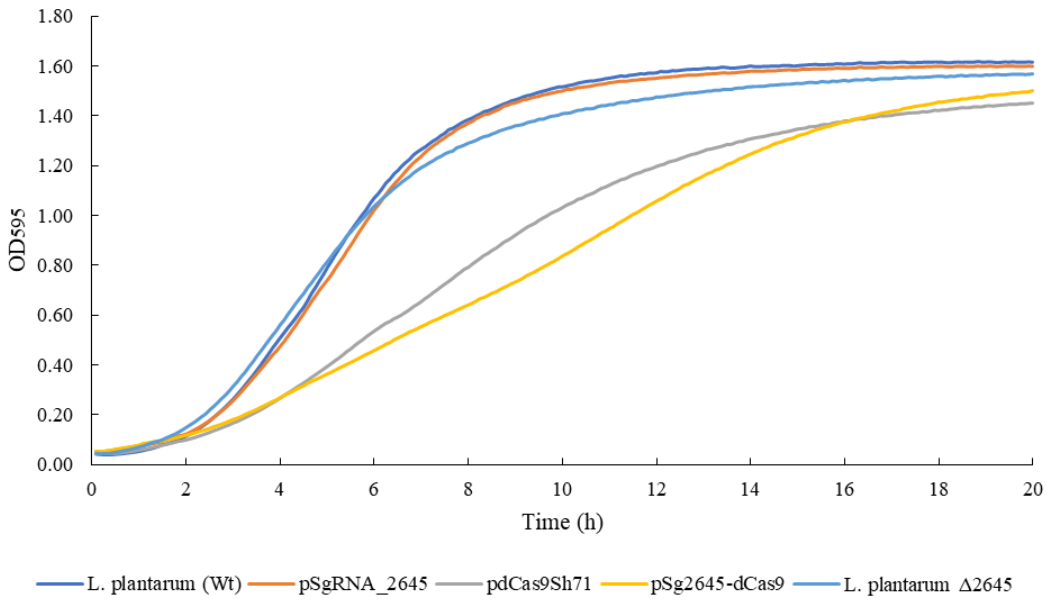

Figure 4.16. Growth curves of recombinant *L. plantarum* harbouring plasmids CRISPR-plasmids. All bacterial cultures were induced with 25 ng/mL SppIP at start (OD600=0.15). The growth of the cultures was measured by MultiSkan FC every fifth minute for 20 hours. The absorbance values at each time point is the average of three biological replicates

Figure 4.16 shows inhibited growth for the *L. plantarum* strain harbouring the inducible pdCas9Sh71 plasmid and the two-plasmid system pSg2645-dCas9. The *L. plantarum* strain harbouring only the pSgRNA_2645 plasmid or the *L. plantarum* Δ2645 (knock out) strain, did not show considerable inhibited growth rate compared to the wild type strain.

4.8 Microscopy analysis of *L. plantarum* harbouring CRISPR/Cas-plasmids

Microscopy analysis of *L. plantarum* harbouring the CRISPR/dCas9 system was performed to assess the functionality of the system. It was expected that successful depletion of *lp_2645* with the CRISPR/dCas9 system would lead to drastic morphological changes based on pervious analyses of the *lp_2645* knock out Δ2645 (Fredriksen et al., 2012). Therefore, *L. plantarum* harbouring Sg2645-dCas9 (Table 4.3) was the first to be analysed (Figure 4.17).

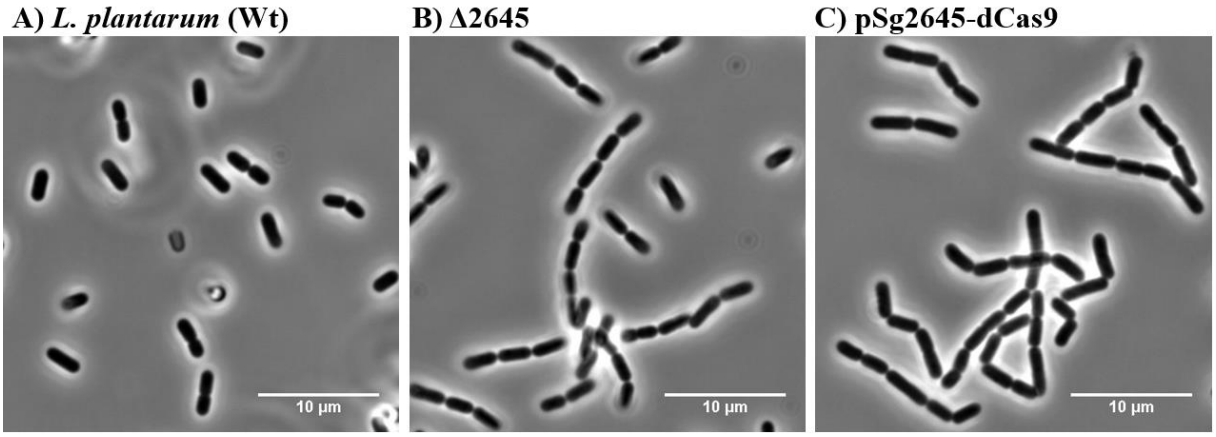

Figure 4.17. Microscopy analysis of *lp_2645* depleted *L. plantarum*. A) wild type *L. plantarum*, B) *L. plantarum* Δ*lp_2645* (knock-out), C) *lp_2645* depleted *L. plantarum* harbouring pSg2645-dCas9.

Figure 4.17 shows a clear morphological difference between wild type *L. plantarum* and the Δ2645 strain. The Δ2645 strain seems to consist of longer chains of cells compared to the wild type cells. There is a resemblance between the phenotype of the Δ2645 strain and *L. plantarum* harbouring pSg2645-dCas9, which indicates that the two-plasmid CRISPR/dCas9 system successfully knocked down the gene expression of *lp_2645*.

As mentioned in section 1.7.2, the genes *cozE* in *Streptococcus pneumoniae* (oval shaped cocci) and its homologs *cozEa* and *cozEb* in *Staphylococcus aureus* (cocci) have been shown to be involved with the cell division and elongation of the bacteria, and depletion of the *cozE* genes affects their morphology (Fenton et al., 2016; Stamsås et al., 2018). In the present study, analyses were performed on the *cozEa* and *cozEb* homologs in *L. plantarum: lp_1247* and *lp_2217*. The genes were depleted by dCas9 to investigate if it affected the morphology in the rod-shaped *L. plantarum* as well. Both phase contrast (PC) and fluorescent microscopy were utilized to investigate the morphology of these genes in *L. plantarum.*

Bacterial overnight cultures were diluted to an OD_{600} of ~0.01 and induced with 25 ng/mL SppIP. Addition of the inducer led to activation of the CRISPR/dCas9-system, and subsequently depletion of the SgRNA-targeting genes (*lp_1247* and *lp_2217*). The cultures were harvested at an OD_{600} of 0.4. Harvested bacterial culture was stained with Nile-Red (membrane staining) and DAPI (DNA staining) as described in section 3.18.1. Three different *L. plantarum* strains harbouring either pSg1247-dCas9, pSg2217-dCas9 or pSg1247_2217-dCas9 was harvested, stained and analysed by microscopy (Figure 4.18). Wild type *L. plantarum* was included as a control.

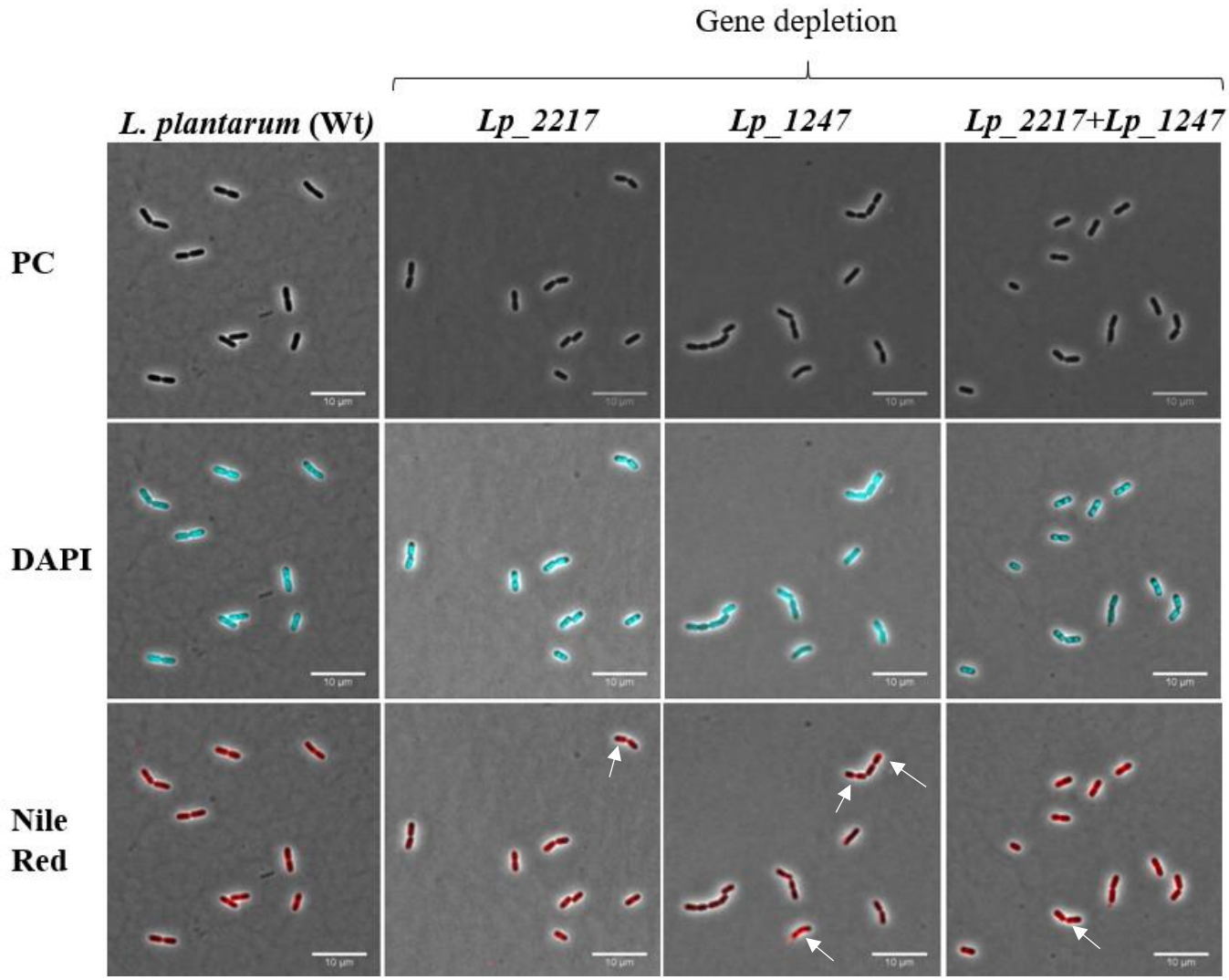

Figure 4.18. Investigation of the functions of the genes *lp_1247* and *lp_2217* in *L. plantarum* through microscopy. The top row shows the phase contrast microscopy pictures of the four strains. The second row shows bacteria stained with DNA-binding DAPI. The third row shows bacteria stained with membrane-binding Nile Red. The arrows indicate bright red spots detected. The scale bar is 10 µM.

The phase contrast microscopy pictures (Figure 4.18, PC) does not indicate a change in morphology when *L. plantarum* is depleted of *lp_1247*, *lp_2217* or when both genes are depleted compared to the wild type. Neither does the DAPI stained cells in Figure 4.18 differ, which indicates that depletion of the genes does not affect the arrangement of DNA in the cells. For the Nile Red stained bacteria (Figure 4.18), a few bright spots at random localizations can be observed for depleted bacteria (indicated by the white arrows), which may indicate that depletion affects arrangement of the membrane.

4.9 Transcription analysis with droplet digital PCR

4.9.1 Transcriptional analysis of *L. plantarum* depleted of the *lp_2217* and *lp_1247* genes

As the microscopy analyses did not reveal a clear morphological change in *L. plantarum* depleted of *lp_1247*, *lp_2217* or both genes, further analyses were performed to determine if the CRISPR/dCas9 system was functional. dCas9 is not catalytically active, but binds to the DNA, and thereby blocking transcription. Therefore, transcription level analysis of depleted genes would indicate if the CRISPR/dCas9 system was functional. Droplet digital PCR was utilized to determine transcript copies per ng RNA of the gene of interest. For a more detailed description of the method, see section 3.20. p-values are calculated using the student t-test.

Overnight cultures of the recombinant strains were grown as described for microscopy in section 3.14.2. In short, the overnight cultures were diluted to an OD_{600} of ~0.01, induction with 25 ng/mL SppIP and harvested at an OD_{600} of 0.4. Harvested samples was prepared for transcription analysis with ddPCR as described in section 3.19.1, 3.19.2 and 3.19.3.

The total RNA from the recombinant strains and the wild type was diluted into stock solutions of 50 ng/µL RNA. To achieve similar concentrations of cDNA in each sample, 2 µL was taken from each stock solution to get a total of 100 ng RNA in the reverse transcription (RT) reactions. As the primers in the downstream PCR reaction would bind to gDNA as well as cDNA if present, negative controls were made for each RNA sample without adding reverse transcriptase, to control the amount of residual gDNA in the samples. These negative control samples (RT-) were treated the exact same way as the positive samples (RT+).

The transcription level of *lp_1247* and *lp_2217* was analysed in *L. plantarum* strains harbouring pSg1247-dCas9, pSg2217-dCas9 and pSg1247_2217-dCas9 (Figure 4.19, 4.20 and 4.21). Wild type *L. plantarum* served as a positive control for RNA isolation and reverse transcription, as well as indicating the baseline transcription level of *lp_1247* and *lp_2217*. *L. plantarum* harbouring pSgluc-dCas9 (Table 4.3) targeting the luciferase gene, a gene that is not present in *L. plantarum*, was to control that the target genes are not depleted simply by the presence of dCas9. Ideally, the transcription levels of the genes in the two control strains would be similar.

As the fluorochrome used in this study, EvaGreen, does not allow multiplexing, each sample was added in two separate wells and analysed with both primer pair Lp_1247_F/Lp_1247_R and Lp_2217_F/Lp_2217_R (Table 2.1).

Figure 4.19 shows the transcription level of *lp_2217* in *L. plantarum* strains harbouring pSg1247-dCas9, pSg2217-dCas9, pSg1247_2217-dCas9 and pSgluc-dCas9 as well as wild type *L. plantarum*.

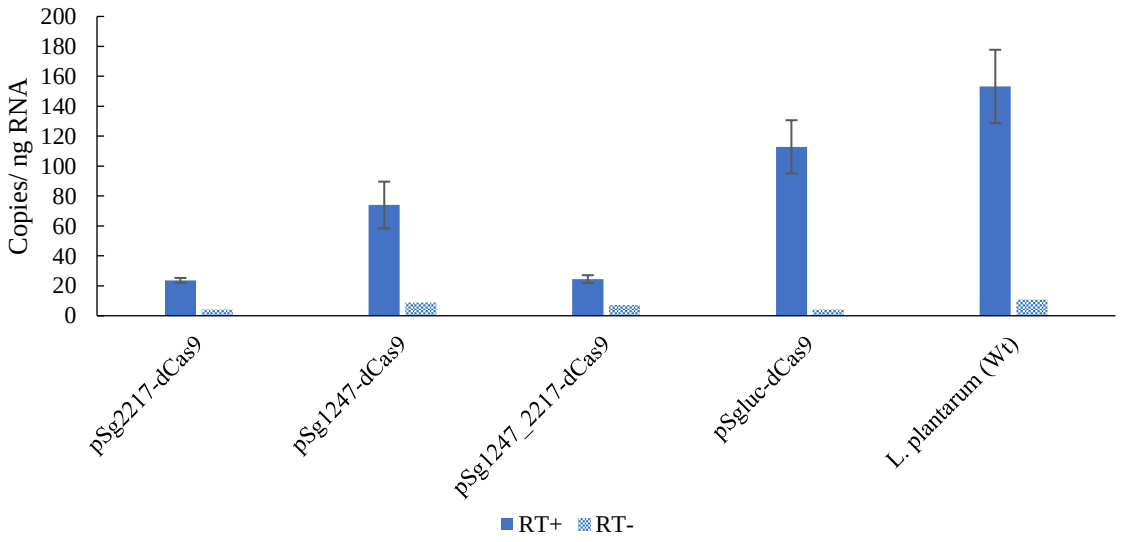

Figure 4.19. Transcriptional levels of *lp_2217* in RT+ samples and negative control RT- samples for *L. plantarum* harbouring the CRISPR/dCas9 system. Each sample in this experiment represents three biological replicates and four technical replicates. The standard deviation is calculated between the biological replicates.

The transcription level of *lp_2217* are much higher in the two control strains pSgluc-dCa9s and wild type *L. plantarum* compared to the strains with targeting SgRNA's (Figure 4.19). However, a slight decrease is observed in pSgluc-dCas9 compared to the wild type, but the difference is not statistically significant (p=0.09). In theory, for *L. plantarum* harbouring pSg1247-dCas9, *lp_2217* should not be depleted compared to the wild type, since pSgRNA_1247 only represses transcription of *lp_1247*. Despite this, there are fewer detected copies/ng RNA in this sample compared to the controls, which indicates a slight depletion.

As expected, the samples containing *L. plantarum* harbouring either pSg2217-dCas9 or pSg1247_2217-dCas9, the transcription level of *lp_2217* are significantly decreased compared to the other three (Figure 4.19), which strongly indicates depletion of the gene. The RT- sample-bars are much lower than the RT+ sample-bars, which indicates minimal residual gDNA from RNA isolation, and does not seem to affect the interpretation of the transcriptional levels.

Figure 4.20 shows the transcription level of *lp_1247* in *L. plantarum* strains harbouring pSg1247-dCas9, pSg2217-dCas9, pSg1247_2217-dCas9 and pSgluc-dCas9 as well as wild type *L. plantarum* without any plasmids.

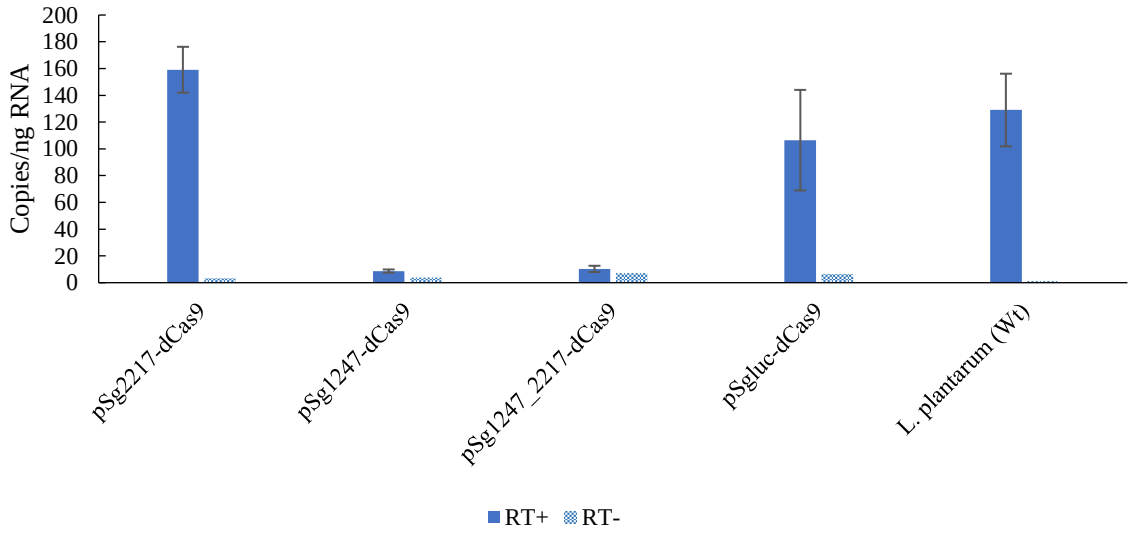

Figure 4.20. Transcriptional levels of *lp_1247* in RT+ samples and negative control RT- samples for *L. plantarum* harbouring the CRISPR/dCas9 system. Each sample in this experiment represents three biological replicates and four technical replicates. The standard deviation is calculated between the biological replicates.

The transcription level of *lp_1247* in the two control strains, pSgluc-dCas9 and wild type *L. plantarum* is not significant different (p=0.45) (Figure 4.20). The transcription level of *lp_1247* in the strain harbouring pSgRNA_2217-dCas9, where only *lp_2217* are depleted, are slightly higher compared to the controls, but not significantly (p=0.19). However, for *L. plantarum* strains harbouring either pSg1247-dCas9 or pSg1247_2217-dCas9 the transcription levels decreased by 93 % compared to the wild type. This strongly indicates that *lp_1247* is indeed depleted in these strains by the CRISPR/dCas9-system. The RT- sample-bars of figure 4.20 are much lower than the RT+ sample-bars and does not seem to affect the interpretation of the transcriptional levels, as in figure 4.19.

Figure 4.21 compares the transcription levels of *lp_2217* (dark blue) and *lp_1247* (light blue) in all five *L. plantarum* strains, harbouring pSg1247-dCas9, pSg2217-dCas9, pSg1247_2217-dCas9 and pSgluc-dCas9 as well as wild type *L. plantarum.*

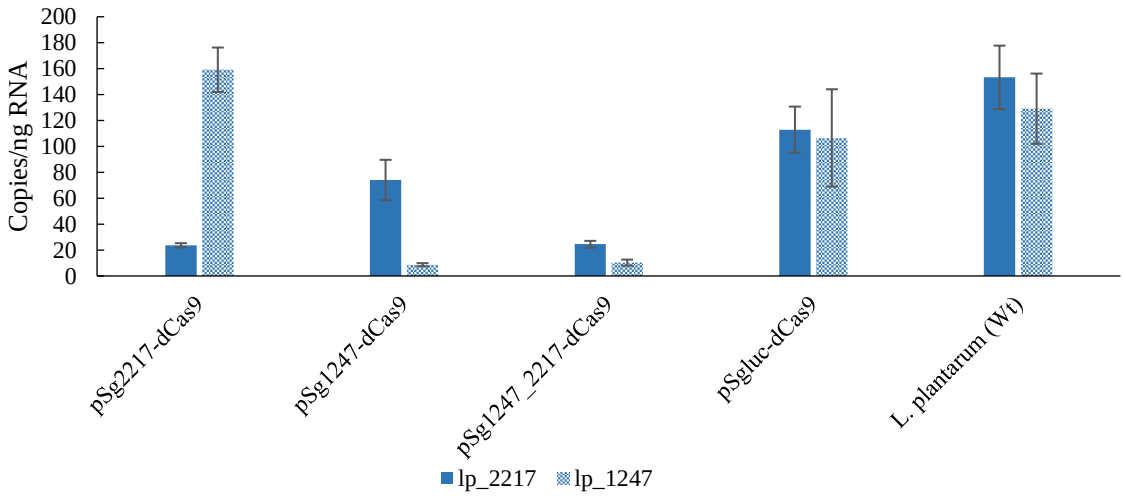

Figure 4.21. Comparison of transcription levels of the genes *lp_1247* and *lp_2217* in the five strains. The transcription level of the two genes *lp_1247* (light blue) and *lp_2217* (dark blue) of the five *L. plantarum* strains harbouring either pSg2217dCas9, pSg1247-dCas9, pSg1247_2217-dCas9, pSgluc-dCas9 or wild type *L. plantarum* are shown.

4.9.2 Dose response analysis using ddPCR

A dose response analysis was carried out to investigate if the depletion of target genes could be regulated by adding different concentrations of the inducer SppIP to the bacteria containing pSg2645-dCas9.

An overnight culture of *L. plantarum* harbouring pSg2645-dCas9 was diluted to an OD_{600} of 0.15 and incubated with different concentrations of the inducer peptide (SppIP): 0, 1, 10 and 25 ng/mL to investigate if it affected transcription of *lp_2645*. The wild type strain of *L. plantarum,* as well as *L. plantarum* harbouring pSgluc-dCas9 were included as controls (Figure 4.22). After induction, the cultures were grown for three hours before harvesting and RNA purification.

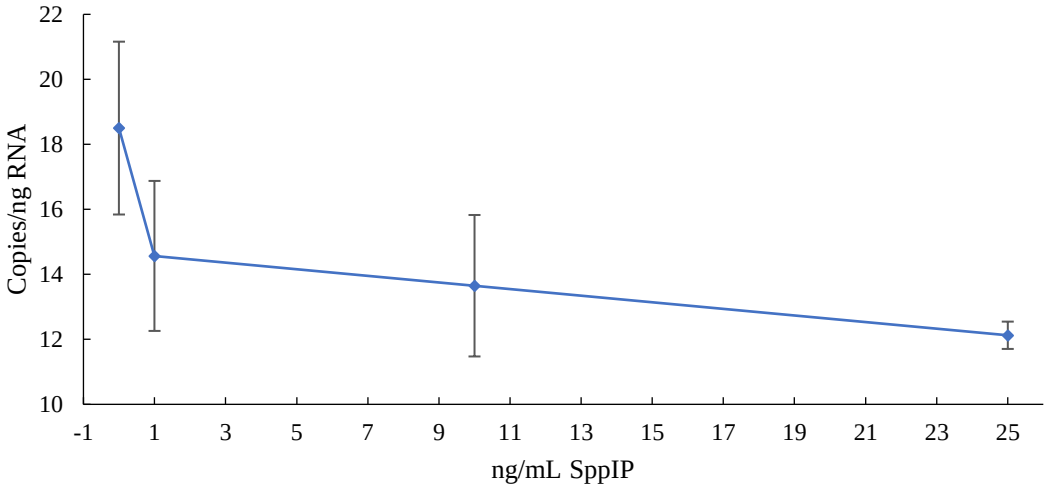

Figure 4.22. SppIP response in *L. plantarum* harbouring pSg2645-dCas9. The graph shows the transcription level of *lp_2645* in cultures induced with different concentrations of SppIP. All samples in the experiment represents three biological replicates and two technical replicates. The standard deviation is calculated from the biological replicates.

Figure 4.22 shows that highest transcription level of *lp_2645* was detected in the uninduced sample of *L. plantarum* harbouring pSg2645-dCas9, as expected. There is not a statistically significant difference of the transcription level of *lp_2645* between the uninduced sample and the sample induced with 25 ng/mL SppIP (p=0.42). The transcription level in the sample induced with 25 ng/mL only decreased by 34 % compared to the uninduced sample.

Figure 4.23 compares the transcription level of *lp_2645* in *L. plantarum* strains harbouring pSg2645-dCas9 induced with concentration 0-25 ng/mL to the wild type *L. plantarum* and *L. plantarum* harbouring pSgluc-dCas9.

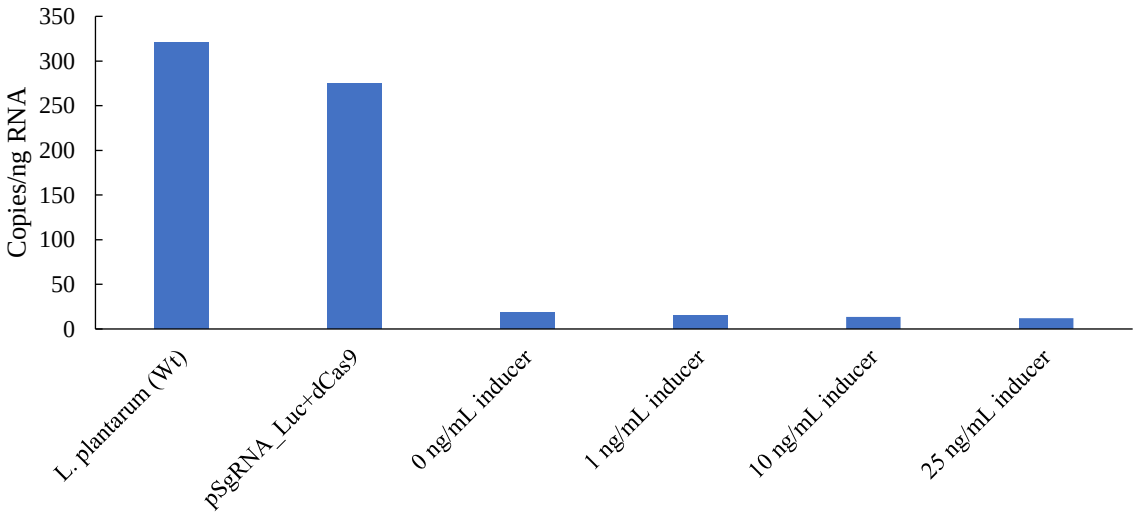

Figure 4.23. Transcription level of *lp_2645* in cultures induced with SppIP to different final concentrations, compared to the controls.

The difference observed between the wild type *L. plantarum* and the uninduced *L. plantarum* harbouring pSg2645-dCas9 in figure 4.23 is 94%. This indicates that the system is poorly regulated and leakage of the promoter P_{sppIP}. Although not significant (p=0.57), *lp_2645* seems to be depleted in *L. plantarum* harbouring pSgluc-dCas9 compared to the wild type, despite not having a *lp_2645* targeting SgRNA.

4.10 CRISPR/Cas9 assisted genome editing in *L. plantarum*

The main purpose of implementing the CRISPR/Cas9 system in *L. plantarum* was to potentially utilize the system to mediate integration of the hybrid antigen into the genome of the bacteria. To perform CRISPR/Cas9 assisted genome editing, electrocompetent *L. plantarum* harbouring either the double-strand breaking Cas9- plasmid or the single-strand breaking $Cas9^{D10A}$-plasmid was utilized. To obtain all necessary components of the CRISPR/Cas9-system in *L. plantarum* a SgRNA plasmid was transformed to competent strains harbouring Cas expression plasmid (Figure 4.13 & 4.12).

To target *lp_2645* and introduce a random mutation, possibly leading to a frameshift of the gene, the pSgRNA_2645 (Figure 4.13) plasmid was utilized. The gene *lp_2645* was selected as the target gene because it was expected that successful editing of the gene was easily detectable by microscopy, as depletion and knock out of *lp_2645* caused a characteristic change in the morphology of *L. plantarum* (Figure 4.17). The SgRNA plasmid that was utilized for the gene exchange, was pSg2645Ha (Figure 4.15), which contained the *NucA* gene flanked by 1000 bp

of homology to the *L. plantarum* genome on each side. The strategy followed for gene exchange and insertion of a random mutation were the same, therefore only the gene exchange method is described in this section. Both Cas9 and Cas9^{D10A} was utilized in independent experiments in the attempts of successfully edit the genome *L. plantarum.* Because *NucA* is a shorter gene than *lp_2645*, a replacement would be easily detectable by PCR. For gene editing without the repair template, where only random mutations were expected to be inserted, colonies were sequenced by GATC Biotech, as possible changes would have been undetectable by PCR.

L. plantarum already harbouring pCas9Sh71 was transformed with pSgRNA_2645 to obtain pSg2645-Cas9 (Table 4.3). Subsequently, the transformed bacteria were induced at different stages in order to successfully perform a gene exchange between *lp_2645* and *NucA* (Figure 4.24). As it was desirable to develop a quick and easy method as possible, the first stage was to induce one aliquot of the transformation mixture with 25 ng/mL SppIP. A second aliquot was spread on agar plates with and without 25 ng/mL SppIP. Colonies from agar plates containing SppIP were screened with PCR, while colonies on plates without inducer were picked with a tooth-pick, induced with 25 ng/mL SppIP and grown overnight in 10 mL MRS with proper antibiotics. The overnight culture was then spread on agar plates, and colonies were screened.

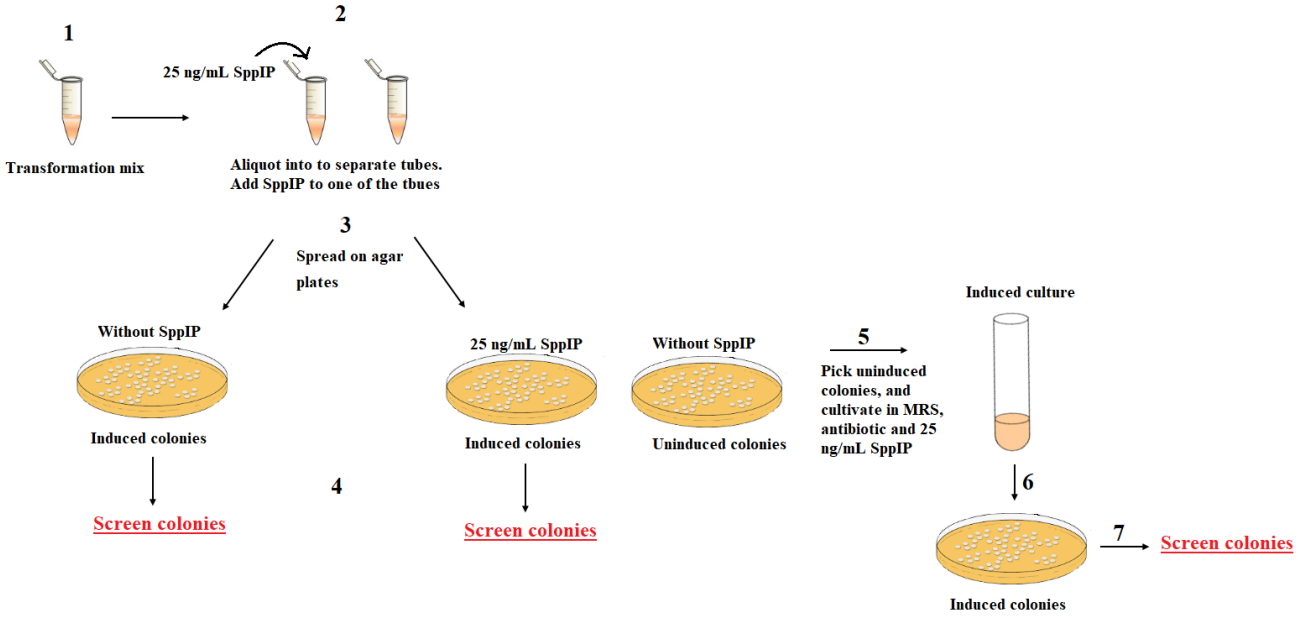

Figure 4.24. Induction of the bacterial culture at different stages. Following transformation, the bacterial culture was induced for activation of the CRISPR/Cas9 system either at step 2, 3 or 5. Colonies were screened in either step 4 or 7. The bacteria were always induced with 25 ng/mL SppIP.

Colonies obtained from all strategies were also investigated by microscope, as the characteristic phenotype of the *lp_2645* -knock out and -dCas9 depletion could easily be observed (Figure 4.17). A distinct phenotypic discrepancy was observed between the wild type *L. plantarum*

(Figure 4.25A) and induced *L. plantarum* harbouring pSg2645-Cas9 (Figure 4.25D). The phenotype observed in figure 4.25D shows clear similarity to the phenotypes observed in figure 4.25B and 4.25C.

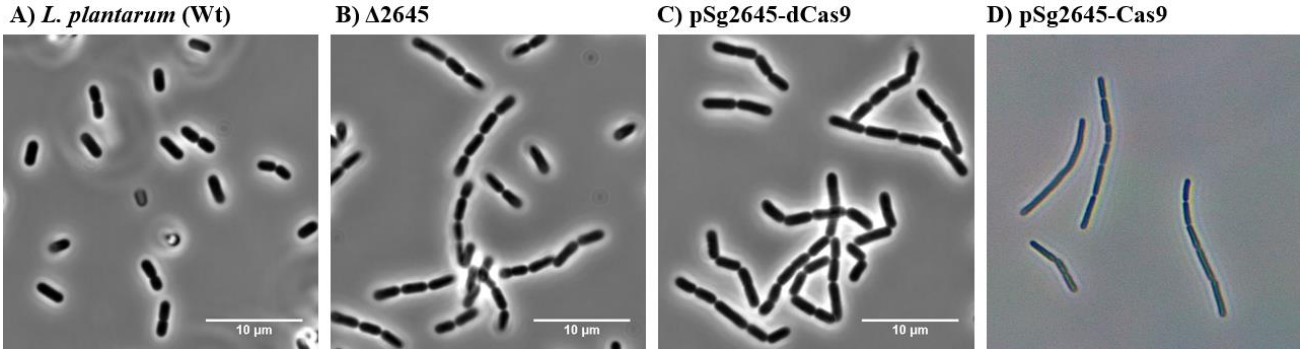

Figure 4.25. Microscopy analysis of *L. plantarum* colonies harbouring pSg2645-Cas9. A) wild type *L. plantarum,* B) *L. plantarum* lacking the *lp_2645* gene. C) *L. plantarum* harbouring pSg2645-dCas9 D) *L. plantarum* harbouring pSg2645-Cas9.

Although most of the colonies showed the characteristic phenotype (Figure 4.25D), the PCR screenings showed that none of the analysed colonies had exchanged *lp_2645* with *NucA* through the CRISPR/Cas9 mediated gene editing experiments. Sequencing revealed that none of the colonies were the characteristic phenotype had been observed had been edited.

On the plates with *L. plantarum* harbouring pSg2645Ha-Cas9^{D10A} (Table 4.3) more than 100 colonies had appeared. On the plates with *L. plantarum* harbouring pSg2645Ha-Cas9 (Table 4.3) only five colonies had appeared. This may indicate that Cas9, inducing double-stranded DNA breaks exerts more strain on the bacteria compared to bacteria harbouring Cas9^{D10A}, which only induces single-stranded break.

Some of the bacteria that showed the phenotype were grown further in MRS medium without antibiotics or SppIP, to see whether the phenotype would be reversed or not. After diluting the culture ten times, three times over three days the phenotype of the bacteria had returned to the wild type phenotype.

5 Discussion

5.1 Construction of AgTB-producing plasmids

The tuberculosis antigens Ag85B and TB10.4 was chosen as they have shown to induce a significant protection against *Mycobacterium tuberculosis*, both individually and in combination as a hybrid antigen (Dietrich et al., 2005; Kou et al., 2018). In the present study, the hybrid antigen Ag85B_TB10.4 (AgTB) was translationally fused to the N-terminal part of the lipoprotein Lp_1261 for production of surface localized antigen in *Lactobacillus plantarum*. A study conducted by Kuczkowska et al. (2016) showed that anchoring of heterologous proteins with the N-terminal lipoprotein Lp_1261 in *L. plantarum* induced a higher immune response compared to other anchors in the study. Although lipo-anchored proteins are sufficiently exposed to the surroundings to induce an immune response, it is also suggested that the anchoring mechanism provides beneficial protection against detrimental conditions in the environment, such as in the gastro intestinal tract (GIT) of humans, compared to other anchoring mechanisms (Michon et al., 2016).

To compare AgTB with previously constructed and tested inducible plasmids producing Ag85B_ESAT-6 in *L. plantarum*, inducible vectors producing AgTB was constructed and characterized in the present study. The inducible vectors pLp_1261-Ag85B-TB10.4_DC (p1261AgTB) (Figure 4.1) and pAg85B-TB10.4_DC (pCytAgTB) (Figure 4.2) were successfully constructed for production of surface and cytoplasmic localization of AgTB, respectively.

Attempts were made to exchange the inducible P_{sppA} promoter with constitutive promoters P_5 and P_{11} to obtain constitutive expression of AgTB. The colonies obtained from these attempts mostly contained religated vectors. After several trials, one colony contained a vector with P5*_Lp1261_Ag85B_TB10.4 (P5*AgTB). However, sequencing revealed a single mutation in the -35 box of promoter (Figure 4.3). The -35 box is important for proper binding between the promoter and polymerase (Watson et al., 2014). As the single colony with the correct insert contains a mutation in the promoter indicates that the constitutive promoter is also active in *E. coli* and that production of AgTB is stressful and toxic to the cell. Stress on the bacteria is known to be able to increase mutation rates (Tenaillon et al., 2004). One way to reduce expression is to replace the high copy pSIP vector with the low copy vector pELS100, because this will lower the gene dose of the target gene. Figure 4.5 showed that seven out of nine colonies clearly contained the plasmid with the constitutive antigen insert. Surprisingly, the

AgTB-insert could not be detected in the pELS100 vector following overnight growth and plasmid isolation. The isolated plasmid was sent to sequencing, and it was confirmed that the pELS100 vector had been isolated, but the constitutive AgTB insert was absent. Construction of constitutive secretion of the antigen Ag85B_ESAT-6 has been attempted previously. Similar to the present study, the author concluded that the constitutive secretion of the antigen was toxic to *E. coli*, as the promoter sequence of the constitutive promoters P_{11} and P_{27} was removed by the bacteria following transformation (Tjåland, 2011). Direct transformations to *L. plantarum* was also attempted, but unsuccessful.

All the promoter sequences from the synthetic promoter library constructed by Rud et al. (2006), including P_5 and P_{11} utilized in the present study, is based on the sequences of 10 rRNA promoters from *L. plantarum* WCFS1. A BLAST search using the promoter sequence as the query was performed to investigate potential homology between the P_5 promoter and native *E. coli* promoters. However, the only hits generated was sequences originated from lactobacilli and lactococci. To further investigate whether the constitutive promoter was active in *E. coli*, western blot analysis could have been performed on the plasmid in *E. coli*. Another strategy that should be explored is to utilize a *L. plantarum* homolog constitutive promoter, such as the lactate dehydrogenase promoter P_{ldhL}, which has formerly been employed (Bron et al., 2004; Sasikumar et al., 2014). Utilization of *Lactococcus lactis* as a subcloning host rather than *E. coli* could also be an option to solve the toxicity problem. An advantage of the gram-positive *L. lactis* over the gram-negative *E. coli* is that it is monoderm, which might reduce potential toxicity linked to secretion of AgTB.

5.2 Growth of *L. plantarum* harbouring antigen plasmids

Reduced growth rates are commonly detected in Lactobacilli and other Gram-positive bacteria producing and secreting heterologous proteins (Antelmann et al., 2003; Bolhuis et al., 1999; Karlskås et al., 2014; Kuczkowska et al., 2015). *L. plantarum* harbouring p1261AgTB is no exception (Figure 4.6). About one hour following induction with SppIP, the growth of *L. plantarum* harbouring pCytAgTB and pEV diverged from the growth of the strain harbouring p1261AgTB. The growth of pEV and pCytAgTB plateaued after approximately 15 hours of measuring, while the growth of p1261AgTB was still slightly increasing after 20 hours (Figure 4.6). The growth of pCytAgTB did not show any reduction in growth compared to pEV. Both p1261AgTB and pCytAgTB produces AgTB, and the only difference between the two plasmids

is the Lp_1261 signal sequence of p1261AgTB. The Lp_1261 signal sequence is therefore the most likely explanation for the reduction in growth observed for p1261AgTB compared to pCytAgTB. A reason for the reduction in growth can be linked to secretion stress. Secretion of a protein can lead to an overload on the translocation machinery and consequently impaired growth (Mathiesen et al., 2009). However, although growth rate reduction is observed in figure 4.6 for p1261AgTB, previous studies have shown that compared to several other anchors, the Lp_1261 anchored constructs had the lowest reduction in growth (Fredriksen et al., 2012; Kuczkowska et al., 2015; Øverland, 2013).

A discrepancy is observed between the positive controls pEV and the wild type *L. plantarum* (Figure 4.6) about three hours after induction. From this point, the growth of *L. plantarum* harbouring pEV was slightly reduced compared to the wild type. In the pEV plasmid, no gene is expressed downstream of the promoter P_{sppA}, unlike in pCytAgTB and p1261AgTB. Since a discrepancy is observed despite this, it might indicate that the presence of an inducible system alone is enough to inhibit the growth of *L. plantarum.*

5.3 Characterization of AgTB production and localization

To confirm production of AgTB by *L. plantarum* harbouring p1261AgTB and pP5*AgTB, cell free protein extracts of the strains were analysed by Western blot. Figure 4.7 shows unspecific binding of the secondary antibody, which binds specifically to Ag85B, leading to difficulties in confirming AgTB production by p1261AgTB and pP5*AgTB. Attempts at optimisation was performed without affecting the results (data not shown). In further optimisation steps, the BSA concentration of the blocking solution could have been increased, to prevent unspecific binding. However, previous testing of the primary and secondary antibody has shown weak signals (personal communication Lise Øverland (2018)), therefore no further optimisation of the Western blot analysis was performed.

To ensure that AgTB produced by p1261AgTB and potentially pP5*AgTB was localized on the surface of *L. plantarum*, the constructs were analysed by flow cytometry (Figure 4.8). As no shift were detected between the negative control and the pP5*AgTB histograms from flow cytometry, it appeared that the -35 box of the P_5 promoter was a missense mutation, resulting in a non-functional promoter. However, although a slight shift was observed between pEV and p1261AgTB histograms, thereby confirming production and surface localization of AgTB, the fluorescent signal was weak. The promoter controlling p1261AgTB, the pSIP promoter P_{sppA},

is considered a strong promoter unlike the weak constitutive promoter P_5. The P_5 promoter originates from a synthetic promoter library, constructed by Rud et al. (2006). In the article, they state that for the weakest promoters, a higher concentrated aliquot was utilized in a downstream assay to investigate promoter activity. Out of the 35 constructed promoters in the synthetic promoter library, P_5 was the 15th weakest. In the present study, the same number of cells were harvested from cultures of both pP5*AgTB and p1261AgTB for downstream analyses. Based on this, it is possible that no fluorescent signal was detected for pP5*AgTB because the mutation of the P_5 promoter led to an undetectable production of AgTB. Perhaps if the culture of *L. plantarum* harbouring P5*AgTB was allowed to grow for a longer period of time, a fluorescent signal would have been detected from flow cytometry. In the P_{5*} promoter, one nucleotide of the -35 box is substituted, however for the weakest promoter of the synthetic promoter library, P_{15}, the -35 box was completely absent. This indicates that the P_{5*} promoter should not be unfunctional due to only one mutation.

Previous studies have speculated that anchoring of proteins by the lipoprotein Lp_1261 leads to a less exposed protein, and thereby reducing its ability to be recognized and interact with the antibody (Michon et al., 2016; Nguyen et al., 2016). The primary antibody utilized in the present study for antibody hybridization interacts with Ag85B, which is immediately downstream from the N-terminal lipoprotein anchor. There is reason to assume that Ag85B of the hybrid antigen AgTB is more embedded in the membrane compared to TB10.4, which might explain the weak shift presented in Figure 4.8B. The results from Figure 4.9, showing *L. plantarum* harbouring AgESAT-6 stained with both Anti Ag85B and anti ESAT-6 primary antibodies, further substantiated that the position and exposure of the targeted antigen strongly affects emitted fluorescent signal.

The results from immunofluorescent microscopy analysis of the cells showed only a few green fluorescent bacteria for *L. plantarum* harbouring p1261AgTB (Figure 4.10). Although the fluorescent signal from flow cytometry was weak, the result from the microscopy analysis was weaker than expected. No fluorescent bacteria were observed for strains harbouring either pEV or pCytAgTB, which indicates low degree of unspecific binding during the antibody hybridization.

No conclusions can be made as to whether the P_{5*} promoter is unfunctional or only made weaker by the mutation. Characterizations of *L. plantarum* harbouring p1261AgTB confirmed that the vector produced secreted surface anchored antigen, although the fluorescent signal emitted from flow cytometry analysis was weak (Figure 4.8). Performing the antibody hybridization with a

primary antibody with specificity to the probably more exposed TB10.4, might enhance the results from flow cytometry and immunofluorescent microscopy analyses, as was seen for AgESAT-6 stained with an antibody specific to ESAT-6 (Figure 4.9).

5.4 Development of the two-plasmid CRISPR/Cas9 system

In previous studies implementing the CRISPR/Cas9 system into various lactobacilli, such as *Lactobacillus casei*, *Lactobacillus reuteri*, and also very recently *L. plantarum*, the gene encoding the Cas9 protein and the SgRNA has been delivered into the cell on one plasmid (Leenay et al., 2018; Oh & van Pijkeren, 2014; Song, X. et al., 2017). In the present study, the Cas9-gene and the SgRNA was expressed on separate plasmids, controlled by an inducible and a constitutive promoter respectively (Figure 4.12 & 4.13). By expressing the SgRNA on a separate plasmid, exchange of the 20 nt base pairing region could easily be performed by inverse-PCR, providing a simple and fast way of changing the target of SgRNA. Production of Cas9 through the pSIP inducible system allowed for regulated activation of the system. In the present study, experiments were performed with three genes encoding different versions of the *Streptococcus pyogenes* derived Cas9 protein: original double-strand breaking Cas9, single-strand breaking $Cas9^{D10A}$ and catalytically inactive dCas9.

Initial experiments conducted in the present study on *L. plantarum* harbouring the CRISPR/Cas9 system, targeted genes known to affect the phenotype upon depletion either in *L. plantarum* or other LAB. However, as the long-term goal of the project which this study is a part of is to develop mucosal vaccines, the targets selected in this study is not necessarily the most advantageous regarding *L. plantarum* as a delivery vector. An important factor to consider is to limit the release of the recombinant bacteria. The Thymidylate synthase gene (*thyA*) is essential for growth of *L. plantarum*, and disruption of the gene would lead to dependence on external thymidine for growth and survival (Paul et al., 2018), and could therefore limit the release of recombinant *L. plantarum*. A study by Steidler et al. (2003) replaced the essential *thyA* of *L. lactis* with a synthetic human interleukin 10 gene (*IL10*), in an effort to prevent release of genetically modified organisms. The *thyA* gene was successfully replaced with the synthetic *IL10*, a therapeutic protein against inflammatory bowel disease, through homologous recombination. *L. lactis* lacking *thyA* was incubated in thymidine free medium. After 72 hours, no viable cells could be detected. Based on these findings, the *thyA* gene can be an advantageous gene to target for integration of tuberculosis antigens into the genome of *L. plantarum*. A

SgRNA plasmid was constructed to target *thyA* (Table 2.4), but experiments utilizing this plasmid was not executed due to limited amount of time.

5.5 Growth curves of *L. plantarum* harbouring CRISPR/Cas9 plasmids

Growth rates of *L. plantarum* harbouring the CRISPR/dCas9 plasmids are shown in figure 4.16, and clearly illustrates that only strains harbouring pdCas9Sh71 shows reduced growth compared to the wild type strain of *L. plantarum*. The dCas9 protein, produced from the plasmid pdCas9Sh71, is a large protein of ~159 kDa. Due to its large size, the production of dCas9 might exert additional stress on the bacteria. Figure 4.6 also indicated that solely the presence of the pSIP inducible expression system led to reduction in growth of the bacteria. A possible explanation can be because the bacteria have to express two additional genes, the histidine kinase and response regulator gene, to produce proteins regulated by the pSIP system. Growth curves comparing inducible and constitutive expression of cytoplasmic Ag85B-ESAT6 made by Tjåland (2011), showed that *L. plantarum* harbouring the constitutive vectors had a slightly higher growth rate compared to the inducible plasmid. In the present study, *L. plantarum* constitutively expressing the SgRNA_2645, did not show reduced growth compared to the growth of the wild type. Whereas SgRNA only has to be transcribed, the mRNA encoding dCas9 also has to be translated and folded to become a mature, functional protein. Consequently, it might be much easier for bacteria to produce SgRNA than dCas9, consequently affecting the growth rates. Importantly, although the growth of *L. plantarum* harbouring pdCas9Sh71 showed reduced growth, production of dCas9 does not seem to be toxic to cell.

5.6 Microscopy analysis of *L. plantarum* harbouring the CRISPR/dCas9 system

Microscopy analysis was utilized to evaluate the ability of the CRISPR/dCas9 system to repress selected genes of *L. plantarum*, by investigating whether a change in morphology followed depletion of the genes.

L. plantarum harbouring pSg2645-dCas9 was utilized to deplete *lp_2645*. This gene has previously been knocked out by the *loxP*/Cre system and showed that the knock out affected the phenotype of *L. plantarum* (Fredriksen et al., 2012). Figure 4.17 shows that depletion of

lp_2645 by the CRISPR/dCas9 system successfully resulted in a phenotype similar to the knock out (Δ2645), which strongly suggests that the designed SgRNA manages to guide dCas9 to the target site, and that dCas9 successfully binds to the DNA.

After confirming that the CRISPR/dCas9 successfully affected the morphology of *L. plantarum* by depletion of *lp_2645*, two new genes were investigated (Figure 4.18). The function of these two genes, *lp_1247* and *lp_2217*, is unknown in *L. plantarum*. Proteins encoded by *lp_1247* and *lp_2217* are homologous to CozEa and CozEb in *Staphylococcus aureus* and CozE in *Streptococcus pneumoniae*. These proteins are known to be involved in cell elongation and division in *S. pneumoniae* and *S. aureus* (Fenton et al., 2016; Stamsås et al., 2018). Based on BLAST searches, the identity between the amino acid sequences of Lp_1247 and Lp_2217 compared to CozE, CozEa and CozEb was found to be ~33% on average. Lp_1247 has the highest percentage of identity to CozE and CozEa (35 and 34%, respectively), while Lp_2217 has the highest percentage of identity to CozEb (35%). Previously, it was found that depletion of *cozE* in the oval shaped cocci *S. pneumoniae,* led to less elongated cells, resulting in a morphology more similar to round cocci such as *S. aureus* (Fenton et al., 2016). Although elongation is not performed to the same extent in the round cocci *S. aureus* as it is in ovococcal or rod-shaped bacteria, two *S. aureus* proteins were found to be homologous to the CozE protein: CozEa and CozEb (Stamsås et al., 2018). Depletion of CozEa and CozEb utilizing the CRISPR/dCas9 was performed to unravel the function of the proteins in *S. aureus*. Analyses suggested that depletion of *cozEa* and *cozEb* affected the cells ability to position and correctly time cell division. The cell division in *S. aureus* follows an intricate pattern, where the cell divides in three consecutive planes and each round of division is orthogonal to the previous plane (Pinho et al., 2013). Depletion of *cozEa* and *cozEb* resulted in deformed cells, as they were no longer able to divide in perpendicular planes. Figure 4.18 shows that depletion of *lp_1247* and *lp_2217* in *L. plantarum*, by the CRISPR/dCas9 system, did not drastically change the morphology of the rod-shaped *L. plantarum*, which were seen following depletion of *cozE* in *S. pneumoniae*. Neither the DNA-staining with DAPI gave any indications to the function of the two genes. Stamsås et al. (2018) revealed by DAPI staining of *S. aureus* that depletion of *cozEa* or *cozEb* resulted in uneven distribution of DNA, and that some cells did not contain any DNA due to random division of the cell. Depletion of *lp_1247* and/or *lp_2217* did not seem to have any effect on the distribution of DNA in *L. plantarum*, based on the observations from the DAPI stained bacteria (Figure 4.18). The most abnormalities seen for *lp_1247* and *lp_2217* depleted bacteria, was for the Nile Red, membrane stained bacteria (Figure 4.18). Brighter spots

of fluorescence can be observed, as indicated by white arrows in figure 4.18. No such bright spots are observed for the wild type bacteria. The bright spots might indicate a thicker membrane at that point. It can also indicate the formation of new septums, observed as a dividing line in the bacteria. These results might indicate that the function of Lp_1247 and Lp_2217 is more involved in cell division as the CozEa and CozEb proteins in *S. aureus*, rather than cell elongation as CozE in *S. pneumoniae*, although no conclusions can be made. An important distinction between *cozEa* and *cozEb* in *S. aureus* compared to *lp_1247* and *lp_2217* in *L. plantarum* is the apparent essentiality of the genes. When Stamsås and co-workers tried to deplete both *cozEa* and *cozEb* simultaneously, the bacteria were not able to survive. However, in *L. plantarum*, depletion of both *lp_1247* and *lp_2217* did not appear to be lethal to the bacteria. This might indicate that despite homology, the function of the *L. plantarum* and *S. aureus* proteins are not equal. Another possibility is that there are more genes involved in cell division in *L. plantarum*, and thereby reducing the effects following depletion of *lp_1247* and *lp_2217*. A third possibility, that was investigated by transcriptional analysis, was that the genes were not effectively depleted by the CRISPR/dCas9 system.

5.7 Transcription analysis with ddPCR

To show that the CRISPR/dCas9 system functioned, transcription analyses was conducted using droplet digital PCR (ddPCR). The ddPCR method are a highly precise, absolute nucleic quantification method compared to methods such as real-time PCR (Hindson et al., 2013).

Figure 4.19 and 4.20 showed the transcription levels of *lp_2217* and *lp_1247* in five strains, both in RT+ and RT- samples. Ideally the concentration of the RT- samples should have been zero, which would indicate that no residual genomic DNA (gDNA) after RNAase treatment. However, there were some trace of gDNA in the RT- samples, and therefore probably also in the RT+ samples. However, the RT- bars are much lower than the RT+ bars for all samples where no genes are depleted. As the RT+ bars of samples depleted of *lp_1247* or *lp_2217* (or both) are so low, the RT- bars cannot be much lower. Despite this, there is no doubt that transcription of the *lp_1247* or *lp_2217* are repressed by dCas9 in these samples. Consequently, the amount of residual gDNA amount does not affect the interpretation of the results.

Both Figure 4.19 and 4.20 shows that the transcription level of the genes is slightly reduced in the pSgluc-dCas9 samples, compared to the wild type. However, the difference in copies/ng RNA between the two control samples are not significant ($p=0.09$, $p=0.45$). As the

pSgRNA_luc does not contain a 20 nt sequence complementary to the genome of *L. plantarum*, it was expected that the transcription level of the targeted genes would be equal in the two control strains. However, a discrepancy is observed, and it might be linked to growth. As observed in Figure 4.16, there is a reduction in the growth rate for strains harbouring the inducible dCas9-encoding plasmid, compared to the wild type strain. The genes investigated in the transcription analysis are assumed to be involved with cell division. It is not unreasonable to believe that the expression of cell division genes needs to be higher in bacteria rapidly dividing, than in stressed, slower dividing bacteria. Similarly, the transcription level of *lp_2217* in the strain depleted only of *lp_1247*, is significantly lower than in the wild type sample ($p=0.01$) (Figure 4.19). Accordingly, this might be due to the slow growth of the strain (data not shown), affecting the expression of genes encoding cell division proteins. An additional possibility is that the genes play overlapping roles, as Stamsås et al. (2018) concluded was true for the *S. aureus* proteins CozEa and CozEb. If they play overlapping roles, it is possible that the expression of each gene is affected by the other, consequently leading to a higher or lower expression of one gene when the other is depleted, to compensate. The transcription level of *lp_1247* of the strain only depleted of *lp_2217*, is significantly higher than of the wild type ($p=0.02$). In samples depleted of either both genes or none of the genes, the expression of *lp_2217* appears to be moderately upregulated compared to the expression of *lp_1247*. This dynamic, and the apparent high transcription of *lp_1247* in the *lp_2217* depleted strain, might further imply that the two genes in some way are expressed dependently.

In the present study, dCas9 is controlled by the inducible promoter P_{sppA} through the pSIP expression system. It has previously been investigated how the amount of a reporter protein produced correlated with different amounts of the peptide pheromone SppIP added to the culture (Mathiesen et al., 2004). It was found that the protein activity increased almost linearly when SppIP was added to a final concentration of 0.5-15 ng/mL. The maximum production of the reporter protein was achieved at 25 ng/mL. Based on these results, the standard for induction of cultures have become addition of SppIP to a concentration of 25 ng/mL. However, investigating the effect of different concentrations of SppIP on the transcription level, instead of the translation level, might provide more information about the regulatory possibilities of the pSIP expression system. Hence, a dose response analysis was performed on *L. plantarum* harbouring pSg2645-dCas9 (Figure 4.22). Cultures were induced with SppIP to concentrations ranging from 0-25 ng/mL. As expected, the uninduced culture (0 ng/mL SppIP) showed the highest transcription level of *lp_2645*. Copies/ng RNA detected in the induced cultures

decreased concomitantly to increased concentration of SppIP. However, the difference in copies/ng RNA did not decrease significantly from 1 ng/mL to the culture induced with 25 ng/mL ($p=0.63$).

Sørvig et al. (2005a) concluded that the pSIP system is suitable for overexpression of heterologous proteins. This is an advantageous property when expressing the dCas9 protein, however, it has also been shown that the pSIP-regulatory promoter P_{sppIP} displays some activity under non-inducing conditions (Nguyen et al., 2011; Risøen et al., 2000). The leakiness of the pSIP system is clearly displayed in Figure 4.23, comparing the *L. plantarum* strains harbouring pSg2645-dCas9 with the wild type strain and the strain harbouring pSgluc-dCas9. The number of copies/ng RNA decreases by 94% from the wild type to the uninduced sample of *L. plantarum* harbouring pSg2645-dCas9. In assays measuring the ability of the expression system to overexpress heterologous proteins, as was performed by Sørvig et al. (2005a), the activity of the P_{sppIP} promoter in non-inducing conditions is not an issue, as it only leads to higher expression of the protein. In the present study however, it was desirable to utilize the pSIP system as a control switch of the CRISPR/dCas9 system. Therefore, the leakiness of the system poses a problem. The results from transcriptional analysis of *lp_2645* by ddPCR indicate that it is difficult to regulate the CRISPR/dCas9 system in respect to number of transcripts of the target gene.

5.8 CRISPR/Cas9 assisted genome modification of *L. plantarum*

After developing the CRISPR/dCas9 system, attempts were made to develop the CRISPR/Cas9 and CRISPR/$Cas9^{D10A}$ systems. Both gene editing and gene exchange was attempted with both double-strand breaking Cas9 and single-strand breaking $Cas9^{D10A}$. Analogous to *dCas9*, the genes encoding these proteins were under the control of the pSIP system. Ultimately, the gene exchange method was meant to mediate genome integration of constitutively expressed antigens. As the construction of the constitutive vectors were unsuccessful, proof-of-concept experiments were conducted with *NucA*.

Double- or single-stranded DNA break are normally repaired through the nonhomologous end joining pathway (NHEJ). This repair pathway is an error-prone mechanism, resulting in insertions or deletions of nucleotides of variable size. The mutations can cause a frameshift, which results in disruption of the gene. In the present study, the target gene *lp_2645* was selected to test the ability of Cas9 and $Cas9^{D10A}$ to mediate genomic modifications in *L.*

plantarum. The *lp_2645* gene is an ideal target since it is not an essential gene, but at the same time will an out of frame mutation result in a characteristic phenotype. *L. plantarum* had to undergo two consecutive transformations in order to obtain a complete CRISPR/Cas9 system, containing both Cas9 protein and the SgRNA. The survival of the bacteria following the second transformation, of the SgRNA plasmid, was poor. Only five colonies combined appeared on several plates. The survival of the bacteria harbouring the CRISPR/Cas9^{D10A} system was good, as >100 colonies appeared on the plates. In both colonies containing CRISPR/Cas9 and CRIPSR/Cas9^{D10A} the observed phenotype was similar to that observed when using dCas9 for depletion of the gene (Figure 4.25D). All colonies sent for DNA sequencing still exhibited the wild type *lp_2645* sequence. Poor transformation and editing efficiency for strains harbouring the double-strand breaking Cas9 has previously been detected in experiments performed on other lactobacilli. A study performed in *Lactobacillus casei* by Song, X. et al. (2017) increased the mutation efficiency from no mutants with Cas9 to an efficiency of 65% with Cas9^{D10A}, following promoter optimisations. In the present study, neither of the Cas9 or Cas9^{D10A} introduced mutations in the genome. Song and co-workers suggested that Cas9 breaks the DNA, but that bacteria fails to repair it, which might be true for double-stranded break in *L. plantarum* as well. Perhaps is a single-stranded break more rapidly detected by the repair system compared to double-stranded breaks, although double-stranded breaks might be more lethal to the bacteria, allowing bacteria harbouring CRISPR/Cas9^{D10A} to grow faster than those harbouring CRISPR/Cas9. Assuming that is true, the breaks are most likely repaired through another repairing mechanism than NHEJ, as no mutations were detected. The error-prone NHEJ is probably only utilized in the absent of a homologous DNA template (Yeeles & Dillingham, 2010).

As the NHEJ activity can be poor in some bacteria (van Pijkeren & Britton, 2014), a new SgRNA plasmid was constructed for exploitation of the homology directed repair (HDR) mechanism. The SgRNA plasmid contained regions with homology to the genome of *L. plantarum* (Figure 4.15), and can therefore be utilized by the bacteria as a repair template following double- or single-stranded breaks. Unlike the error-prone NHEJ, HDR utilize precise repair of the DNA. As a proof-of-concept experiment, *lp_2645* was attempted replaced with a gene encoding the reporter protein NucA, without a promoter. The experiment was performed in order to establish a method for integration of heterologous genes, and eventually it is desirable to perform integration of the tuberculosis antigens into to genome of *L. plantarum.* A fragment was constructed through PCR, consisting of the *NucA* gene flanked by 1000 bp on

each side with homology to the up- and downstream sequence of *lp_2645* (homologous arms, HA) (Figure 4.14). This fragment was ligated into the pSgRNA_2645 plasmid, obtaining pSg2645Ha (Figure 4.15). A similar experiment was performed in *L. casei* by Song, X. et al. (2017), replacing the native gene *LC2W1628* with the reporter gene *eGFP*, where 6 out of 24 transformants was mutants. In the present study, however, the >50 colonies screened were all wild type *L. plantarum*. As for the colonies obtained from editing experiments, the Δ2645 and pSg2645-dCas9 characteristic phenotype was observed in the screened colonies.

The results obtained from attempts at gene editing and gene exchange with both Cas9 and $Cas9^{D10A}$ was very similar. Fewer colonies appeared for *L. plantarum* harbouring CRISPR/Cas9 than those harbouring CRISPR/$Cas9^{D10A}$, regardless of gene editing/exchange. Sequencing and colony PCR revealed that all colonies contained the wild type sequence of *lp_2645*. However, colonies from all experiments showed the Δ2645 characteristic phenotype. In a study conducted by Sternberg et al. (2014) experiments with wild type Cas9 yielded identical results to those obtained using dCas9, without cleaving the DNA, analogous to the results of the present study. Sternberg and co-workers concluded that the Cas9:SgRNA complex only remained tightly bound to the target DNA. The study also found that Cas9:SgRNA may remain bound to the cleaved DNA site *in vivo*, and that the complex are dependent on other cellular factors for dissociation. A study by Gong et al. (2018) showed that Cas9 had the ability to bind reversible to the DNA, without cleaving. Another important finding of the study was that the unwinding of the DNA is the time dependent step when DNA is cleaved by Cas9. The findings of both Sternberg et al. (2014) and Gong et al. (2018) provides a possible explanation to how *L. plantarum* harbouring the CRISPR/Cas9 system in this study could show a phenotype, as observed in *lp_2645* knock out and depleted bacteria, although the sequence had not been edited. Sternberg and co-workers performed an assay to determine the optimal concentrations of Cas9:SgRNA and target DNA, respectively, and to investigate the effect it had on the amount of cleaved DNA. A maximum of 90% cleaved DNA was detected at a concentration of 50 nM for Cas9:SgRNA, and 25 nM for target DNA. The percentage of cleaved DNA increased as the concentration of Cas9:SgRNA increased. Song, X. et al. (2017) enhanced the number of mutants obtained through promoter tuning. The *S. pyogenes*-derived promoter P_{Cas} expressing $Cas9^{D10A}$ was exchanged with the stronger promoter P_{23}. Following the promoter tuning, the percentage of recombinant bacteria harbouring the desired mutant increased from 5% to 35%. This indicates that sufficient expression of the Cas gene is important for efficient editing. All Cas genes in the present study are expressed by the pSIP promoter P_{sppA}, which should provide

high expression of the protein. However, the promoter expressing the SgRNA is the P_3 promoter, a strong constitutive promoter originally constructed for expression in *L. lactis* (Sorg et al., 2015) and might have reduced strength in *L. plantarum*. A possibility is to exchange P_3 with a promoter specifically constructed for high expression in *L. plantarum*, such as P_{23} utilized by Song and co-workers or the P_{11} promoter, to obtain higher expression of the SgRNA.

In a very recently published article, the CRISPR/Cas9 system and an exogenous recombinase machinery was successfully utilized to perform genomic modifications in three strains of *L. plantarum:* WCFS1, NIZO2877, and WJL (Leenay et al., 2018). They compared the differences between two approaches for genome editing with Cas9. The two methods utilized were distinguished based on how the recombination machinery was delivered to the bacteria. While the endogenous recombination machinery was utilized in one of the approaches, the recombinase was delivered as a single-stranded DNA recombinase in the other. In one experiment, a point mutation was introduced into the essential *rpoB* gene, with 100% efficiency for *L. plantarum* WCFS1 by providing the recombinase as a single-stranded DNA recombinase. In the present study however, no exogenous recombinases were provided in order to mediate genomic modifications, because it was desirable to keep the CRISPR/Cas9 system as simple as possible. For the strain exploited in the present study, *L. plantarum* WCFS1, an endogenous recombination machinery has previously been identified (Yang et al., 2015). To confirm the functionality of the endogenous recombination machinery, it was exploited by Yang and co-workers to perform homologous recombination between a heterologous double-stranded DNA substrate and *L. plantarum* genomic DNA, mediated by the *loxP*/Cre system.

In the present study, attempts were made at replacing the ~2.3 kb gene *lp_2645* with the smaller ~0.5 kb *NucA*. Yang et al. (2015) points out that for the endogenous *L. plantarum* recombination system, recombination is more favoured when the length of the replacement is shorter than the native sequence, because chromosome bending is preferred to substrate bending. However, experiments conducted by Song, X. et al. (2017), investigated the correlation between deletion size and editing efficiency. It was found that the single-strand breaking $Cas9^{D10A}$ mediated deletions of 3 kb with 66% efficiency, but when the deletion size was increased to 5 kb the system failed. Although the efficiency of introduced deletions was relatively high when the deletion size was 3 kb, the number of transformants decreased to fewer than 10 colonies. In comparison, the number of colonies when the deletion size was 1.1 kb is described as less than 100 colonies, and 40 colonies were screened for the mutation. This indicates that deletion size strongly influences editing efficiency. In the present study, it was attempted to delete the entire

2.3 kb gene from the genome. In further attempts, perhaps reduction of the region for gene replacement might facilitate the insertion of *NucA*.

5.9 Concluding remarks and future prospects

This thesis describes the successful production and membrane anchoring of the tuberculosis hybrid antigen Ag85B_TB10.4 (AgTB) by the inducible pSIP system in *L. plantarum* WCFS1. Colonies obtained from attempts of constructing a vector for constitutive production of membrane anchored AgTB mostly contained religated vectors. Only one colony contained the insert, but had a mutation in -35 box of the promoter P_5. As problems emerged only in the attempts of constructing the constitutive vectors, it indicates that the constitutive promoter P_5 was functional in the subcloning strain *E. coli*, and that the production of AgTB was toxic. A solution could be to utilize a different subcloning strain, such as *L. lactis*. *L. lactis* has been utilized for production of antigens previously, although not with the same promoters as those utilized in the present study.

One of the goals of this study was to develop the CRISPR/Cas9 system in *L. plantarum*, to mediate integration of AgTB into the genome of the bacteria. As the construction of vectors for constitutive production of AgTB failed, only proof-of-concept experiments was conducted to develop the CRISRP/Cas9 system in *L. plantarum*. However, if construction of constitutive expression systems of AgTB continues to be a problem, another possibility is to integrate AgTB into the genome directly downstream of a native constitutive promoter, such as the promoter controlling production of thymidylate synthase.

The CRISPR/Cas9 system was implemented as a two-plasmid system, and strains of *L. plantarum* harbouring the two plasmids were obtained. Plasmids encoding either the double-strand breaking Cas9 or the single-strand breaking $Cas9^{D10A}$ was constructed, as well as one plasmid only producing the SgRNA and separate plasmid both producing the SgRNA and harbouring a repair template. In total, this resulted in two different systems for gene editing through NHEJ (pSg2645-Cas9 and pSg2645-$Cas9^{D10A}$), and two systems for gene exchange through HDR (pSg2645Ha-Cas9 and pSg2645Ha-$Cas9^{D10A}$). All four systems were utilized to target the *lp_2645* gene, and resulted in colonies displaying the same phenotype as observed for the *L. plantarum* Δ2645. However, none of the colonies had undergone genomic modification, and when grown in MRS without antibiotics for plasmid curing, the phenotype

reversed into the wild type phenotype. These observations strongly indicate that the Cas9/Cas9^{D10A} proteins are able to bind to the target DNA in *L. plantarum* without cutting.

Several strategies should be further explored to develop a successful CRISPR/Cas9 system for genomic modification in *L. plantarum*. One strategy is promoter tuning of the SgRNA plasmid. A possible replacement for the strong, synthetic *L. lactis* promoter P_3 could be the strong, synthetic *L. plantarum* promoter P_{11}. In the present study, the *Cas* genes are expressed through the pSIP system, which leads to high expression. Therefore, promoter tuning might not be as important for this component. Another strategy for successful gene exchange is to reduce the region of the genome to be exchanged, as reduced efficiency of gene exchange has been observed with increased deletion size (Song, X. et al., 2017) . A third strategy to explore in order to obtain successful genome modification, is to overexpress the *L. plantarum* endogenous recombination machinery, or introduce an exogenous recombinase such as RecT, to facilitate homologous recombination equivalent to Leenay et al. (2018) .

The CRISPR/dCas9 system was successfully developed in the present study. The system was characterized using microscopy analyses for detecting morphological changes, and ddPCR to investigate the effect on the transcription level. Depletion of *lp_2645* in *L. plantarum* revealed a significant change in the morphology, while depletion of *lp_1247* and *lp_2217* did not. Importantly, the transcription of the two genes was drastically reduced when the CRISPR/dCas9 system targeting the genes was present, indicating functionality of the CRISPR/dCas9 system despite no detected changes of morphology.

6 References

Antelmann, H., Darmon, E., Noone, D., Veening, J.-W., Westers, H., Bron, S., Kuipers, O. P., Devine, K. M., Hecker, M. & Van Dijl, J. M. (2003). The extracellular proteome of *Bacillus subtilis* under secretion stress conditions. *Molecular Microbiology*, 49 (1): 143-156. doi: doi:10.1046/j.1365-2958.2003.03565.x.

Armitige, L. Y., Jagannath, C., Wanger, A. R. & Norris, S. J. (2000). Disruption of the genes encoding antigen 85A and antigen 85B of *Mycobacterium tuberculosis* H37Rv: effect on growth in culture and in macrophages. *Infection and Immunity*, 68 (2): 767-78.

Aukrust, T. W., Brurberg, M. B. & Nes, I. F. (1995). Transformation of *Lactobacillus* by Electroporation. In Nickoloff, J. A. (ed.) *Electroporation Protocols for Microorganisms*, pp. 201-208. Totowa, NJ: Humana Press.

Balchin, D., Hayer-Hartl, M. & Hartl, F. U. (2016). In vivo aspects of protein folding and quality control. *Science*, 353 (6294): aac4354. doi: 10.1126/science.aac4354.

Baldridge, G. D., Burkhardt, N. Y., Labruna, M. B., Pacheco, R. C., Paddock, C. D., Williamson, P. C., Billingsley, P. M., Felsheim, R. F., Kurtti, T. J. & Munderloh, U. G. (2010). Wide Dispersal and Possible Multiple Origins of Low-Copy-Number Plasmids in Rickettsia Species Associated with Blood-Feeding Arthropods. *Applied and Environmental Microbiology*, 76 (6): 1718. doi: 10.1128/AEM.02988-09.

Bermudez-Humaran, L. G., Cortes-Perez, N. G., Lefevre, F., Guimaraes, V., Rabot, S., Alcocer-Gonzalez, J. M., Gratadoux, J. J., Rodriguez-Padilla, C., Tamez-Guerra, R. S., Corthier, G., et al. (2005). A novel mucosal vaccine based on live Lactococci expressing E7 antigen and IL-12 induces systemic and mucosal immune responses and protects mice against human papillomavirus type 16-induced tumors. *Journal of Immunology*, 175 (11): 7297-302.

Bolhuis, A., Tjalsma, H., Smith, H. E., de Jong, A., Meima, R., Venema, G., Bron, S. & van Dijl, J. M. (1999). Evaluation of Bottlenecks in the Late Stages of Protein Secretion in *Bacillus subtilis*. *Applied and Environmental Microbiology*, 65 (7): 2934-2941.

Braat, H., Rottiers, P., Hommes, D. W., Huyghebaert, N., Remaut, E., Remon, J. P., van Deventer, S. J., Neirynck, S., Peppelenbosch, M. P. & Steidler, L. (2006). A phase I trial with transgenic bacteria expressing interleukin-10 in Crohn's disease. *Clinical Gastroenterology Hepatology*, 4 (6): 754-9. doi: 10.1016/j.cgh.2006.03.028.

Bron, P. A., Grangette, C., Mercenier, A., de Vos, W. M. & Kleerebezem, M. (2004). Identification of *Lactobacillus plantarum* genes that are induced in the gastrointestinal tract of mice. *Journal of bacteriology*, 186 (17): 5721-5729. doi: 10.1128/JB.186.17.5721-5729.2004.

Chen, C., Lu, Y., Wang, L., Yu, H. & Tian, H. (2018). CcpA-Dependent Carbon Catabolite Repression Regulates Fructooligosaccharides Metabolism in *Lactobacillus plantarum*. *Frontiers in Microbiology*, 9 (1114). doi: 10.3389/fmicb.2018.01114.

Crum-Cianflone, N. F. & Sullivan, E. (2017). Vaccinations for the HIV-Infected Adult: A Review of the Current Recommendations, Part II. *Infectious diseases and therapy*, 6 (3): 333-361. doi: 10.1007/s40121-017-0165-y.

de Vos, W. M. (2011). Systems solutions by lactic acid bacteria: from paradigms to practice. *Microbial Cell Factories*, 10 (1): S2. doi: 10.1186/1475-2859-10-s1-s2.

de Vries, M. C., Vaughan, E. E., Kleerebezem, M. & de Vos, W. M. (2006). *Lactobacillus plantarum*—survival, functional and potential probiotic properties in the human intestinal tract. *International Dairy Journal*, 16 (9): 1018-1028. doi: https://doi.org/10.1016/j.idairyj.2005.09.003.

Deltcheva, E., Chylinski, K., Sharma, C. M., Gonzales, K., Chao, Y., Pirzada, Z. A., Eckert, M. R., Vogel, J. & Charpentier, E. (2011). CRISPR RNA maturation by trans-encoded small RNA and host factor RNase III. *Nature*, 471 (7340): 602-7. doi: 10.1038/nature09886.

Desvaux, M., Dumas, E., Chafsey, I. & Hebraud, M. (2006). Protein cell surface display in Gram-positive bacteria: from single protein to macromolecular protein structure. *FEMS Microbiology Letters*, 256 (1): 1-15. doi: 10.1111/j.1574-6968.2006.00122.x.

Desvaux, M., Hébraud, M., Talon, R. & Henderson, I. R. (2009). Secretion and subcellular localizations of bacterial proteins: a semantic awareness issue. *Trends in Microbiology*, 17 (4): 139-145. doi: https://doi.org/10.1016/j.tim.2009.01.004.

Diep, D. B., Mathiesen, G., Eijsink, V. G. & Nes, I. F. (2009). Use of lactobacilli and their pheromone-based regulatory mechanism in gene expression and drug delivery. *Current Pharmaceutical Biotechnology*, 10 (1): 62-73.

Dietrich, J., Aagaard, C., Leah, R., Olsen, A. W., Stryhn, A., Doherty, T. M. & Andersen, P. (2005). Exchanging ESAT6 with TB10.4 in an Ag85B Fusion Molecule-Based Tuberculosis Subunit Vaccine: Efficient Protection and ESAT6-Based Sensitive Monitoring of Vaccine Efficacy. *The Journal of Immunology*, 174 (10): 6332-6339. doi: 10.4049/jimmunol.174.10.6332.

Doron, S. & Snydman, D. R. (2015). Risk and safety of probiotics. *Clinical infectious diseases : an official publication of the Infectious Diseases Society of America*, 60 Suppl 2 (Suppl 2): S129-S134. doi: 10.1093/cid/civ085.

Driessen, A. J. & Nouwen, N. (2008). Protein translocation across the bacterial cytoplasmic membrane. *Annual Review of Biochemistry*, 77: 643-67. doi: 10.1146/annurev.biochem.77.061606.160747.

Fenton, A. K., El Mortaji, L., Lau, D. T., Rudner, D. Z. & Bernhardt, T. G. (2016). CozE is a member of the MreCD complex that directs cell elongation in *Streptococcus pneumoniae*. *Nature Microbiology*, 2: 16237. doi: 10.1038/nmicrobiol.2016.237.

Fredriksen, L., Mathiesen, G., Sioud, M. & Eijsink, V. G. (2010). Cell wall anchoring of the 37-kilodalton oncofetal antigen by *Lactobacillus plantarum* for mucosal cancer vaccine delivery. *Applied Environmental Microbiology*, 76 (21): 7359-62. doi: 10.1128/aem.01031-10.

Fredriksen, L., Kleiveland, C. R., Hult, L. T., Lea, T., Nygaard, C. S., Eijsink, V. G. & Mathiesen, G. (2012). Surface display of N-terminally anchored invasin by *Lactobacillus plantarum* activates NF-kappaB in monocytes. *Applied Environmental Microbiology*, 78 (16): 5864-71. doi: 10.1128/aem.01227-12.

Gong, S., Yu, H. H., Johnson, K. A. & Taylor, D. W. (2018). DNA Unwinding Is the Primary Determinant of CRISPR-Cas9 Activity. *Cell Reports*, 22 (2): 359-371. doi: 10.1016/j.celrep.2017.12.041.

Grissa, I., Vergnaud, G. & Pourcel, C. (2007). The CRISPRdb database and tools to display CRISPRs and to generate dictionaries of spacers and repeats. *BMC Bioinformatics*, 8: 172. doi: 10.1186/1471-2105-8-172.

Haft, D. H., Selengut, J., Mongodin, E. F. & Nelson, K. E. (2005). A guild of 45 CRISPR-associated (Cas) protein families and multiple CRISPR/Cas subtypes exist in prokaryotic genomes. *PLOS Computational Biology*, 1 (6): e60. doi: 10.1371/journal.pcbi.0010060.

Hermans, P. W., van Soolingen, D., Bik, E. M., de Haas, P. E., Dale, J. W. & van Embden, J. D. (1991). Insertion element IS987 from *Mycobacterium bovis* BCG is located in a hot-spot integration region for insertion elements in *Mycobacterium tuberculosis* complex strains. *Infection and Immunity*, 59 (8): 2695-705.

Hindson, C. M., Chevillet, J. R., Briggs, H. A., Gallichotte, E. N., Ruf, I. K., Hindson, B. J., Vessella, R. L. & Tewari, M. (2013). Absolute quantification by droplet digital PCR versus analog real-time PCR. *Nature Methods*, 10: 1003. doi: 10.1038/nmeth.2633

Hiom, K. (2009). DNA Repair: Common Approaches to Fixing Double-Strand Breaks. *Current Biology*, 19 (13): R523-R525. doi: https://doi.org/10.1016/j.cub.2009.06.009.

Ishino, Y., Shinagawa, H., Makino, K., Amemura, M. & Nakata, A. (1987). Nucleotide sequence of the iap gene, responsible for alkaline phosphatase isozyme conversion in *Escherichia coli*, and identification of the gene product. *Journal of Bacteriology*, 169 (12): 5429-33.

Jansen, R., Embden, J. D., Gaastra, W. & Schouls, L. M. (2002). Identification of genes that are associated with DNA repeats in prokaryotes. *Molecular Microbiology*, 43 (6): 1565-75.

Jensen, H., Grimmer, S., Naterstad, K. & Axelsson, L. (2012). In vitro testing of commercial and potential probiotic lactic acid bacteria. *International Journal of Food Microbiology*, 153 (1): 216-222. doi: https://doi.org/10.1016/j.ijfoodmicro.2011.11.020.

Jiang, W., Bikard, D., Cox, D., Zhang, F. & Marraffini, L. A. (2013). RNA-guided editing of bacterial genomes using CRISPR-Cas systems. *Nature Biotechnology*, 31 (3): 233-9. doi: 10.1038/nbt.2508.

Jinek, M., Chylinski, K., Fonfara, I., Hauer, M., Doudna, J. A. & Charpentier, E. (2012). A programmable dual-RNA-guided DNA endonuclease in adaptive bacterial immunity. *Science*, 337 (6096): 816-21. doi: 10.1126/science.1225829.

Jinek, M., Jiang, F., Taylor, D. W., Sternberg, S. H., Kaya, E., Ma, E., Anders, C., Hauer, M., Zhou, K., Lin, S., et al. (2014). Structures of Cas9 endonucleases reveal RNA-mediated conformational activation. *Science*, 343 (6176): 1247997. doi: 10.1126/science.1247997.

Jones, K. L., Kim, S. W. & Keasling, J. D. (2000). Low-copy plasmids can perform as well as or better than high-copy plasmids for metabolic engineering of bacteria. *Metabolic engineering*, 2 (4): 328. doi: 10.1006/mben.2000.0161.

Kandler, O. (1983). Carbohydrate metabolism in lactic acid bacteria. *Antonie van Leeuwenhoek*, 49 (3): 209-224. doi: 10.1007/bf00399499.

Karlskås, I. L., Maudal, K., Axelsson, L., Rud, I., Eijsink, V. G. H. & Mathiesen, G. (2014). Heterologous Protein Secretion in Lactobacilli with Modified pSIP Vectors. *PLOS ONE*, 9 (3): e91125. doi: 10.1371/journal.pone.0091125.

Kim, H. & Kim, J.-S. (2014). A guide to genome engineering with programmable nucleases. *Nature Reviews Genetics*, 15: 321. doi: 10.1038/nrg3686.

Kleerebezem, M., Boekhorst, J., van Kranenburg, R., Molenaar, D., Kuipers, O. P., Leer, R., Tarchini, R., Peters, S. A., Sandbrink, H. M., Fiers, M. W. E. J., et al. (2003). Complete genome sequence of *Lactobacillus plantarum* WCFS1. *Proceedings of the National Academy of Sciences*, 100 (4): 1990-1995. doi: 10.1073/pnas.0337704100.

Kleerebezem, M., Hols, P., Bernard, E., Rolain, T., Zhou, M., Siezen, R. J. & Bron, P. A. (2010). The extracellular biology of the lactobacilli. *FEMS Microbiology Review*, 34 (2): 199-230. doi: 10.1111/j.1574-6976.2010.00208.x.

Kou, Y., Wan, M., Shi, W., Liu, J., Zhao, Z., Xu, Y., Wei, W., Sun, B., Gao, F., Cai, L., et al. (2018). Performance of Homologous and Heterologous Prime-Boost Immunization Regimens of Recombinant Adenovirus and Modified Vaccinia Virus Ankara Expressing an Ag85B-TB10.4 Fusion Protein against *Mycobacterium tuberculosis*. *Journal of Microbiology and Biotechnology*, 28 (6): 1022-1029. doi: 10.4014/jmb.1712.12064.

Kuczkowska, K., Mathiesen, G., Eijsink, V. G. H. & Øynebråten, I. (2015). *Lactobacillus plantarum* displaying CCL3 chemokine in fusion with HIV-1 Gag derived antigen causes increased recruitment of T cells. *Microbial Cell Factories*, 14 (1): 169. doi: 10.1186/s12934-015-0360-z.

Kuczkowska, K., Kleiveland, C. R., Minic, R., Moen, L. F., Øverland, L., Tjåland, R., Carlsen, H., Lea, T., Mathiesen, G. & Eijsink, V. G. H. (2016). Immunogenic Properties of *Lactobacillus plantarum* Producing Surface-Displayed *Mycobacterium tuberculosis* Antigens. *Applied and environmental microbiology*, 83 (2): e02782-16. doi: 10.1128/AEM.02782-16.

Kuczkowska, K., Myrbråten, I., Øverland, L., Eijsink, V. G. H., Follmann, F., Mathiesen, G. & Dietrich, J. (2017). *Lactobacillus plantarum* producing a *Chlamydia trachomatis* antigen induces a specific IgA response after mucosal booster immunization. *PLOS ONE*, 12 (5): e0176401. doi: 10.1371/journal.pone.0176401.

Kuipers, O. P., Beerthuyzen, M. M., de Ruyter, P. G., Luesink, E. J. & de Vos, W. M. (1995). Autoregulation of nisin biosynthesis in *Lactococcus lactis* by signal transduction. *Journal of Biological Chemistry*, 270 (45): 27299-304.

Lambert, J. M., Bongers, R. S. & Kleerebezem, M. (2007). Cre-lox-based system for multiple gene deletions and selectable-marker removal in *Lactobacillus plantarum*. *Applied and environmental microbiology*, 73 (4): 1126-1135. doi: 10.1128/AEM.01473-06.

Leenay, R. T., Vento, J. M., Shah, M., Martino, M. E., Leulier, F. & Beisel, C. L. (2018). Genome Editing with CRISPR-Cas9 in *Lactobacillus plantarum* Revealed That Editing Outcomes Can Vary Across Strains and Between Methods. *Biotechnology Journal*: e1700583. doi: 10.1002/biot.201700583.

Lulko, A. T., Veening, J.-W., Buist, G., Smits, W. K., Blom, E. J., Beekman, A. C., Bron, S. & Kuipers, O. P. (2007). Production and secretion stress caused by overexpression of heterologous alpha-amylase leads to inhibition of sporulation and a prolonged motile phase in *Bacillus subtilis*. *Applied and environmental microbiology*, 73 (16): 5354-5362. doi: 10.1128/AEM.00472-07.

Maizels, N. (2013). Genome engineering with Cre-*loxP*. *Journal of immunology*, 191 (1): 5-6. doi: 10.4049/jimmunol.1301241.

Makarova, K., Slesarev, A., Wolf, Y., Sorokin, A., Mirkin, B., Koonin, E., Pavlov, A., Pavlova, N., Karamychev, V., Polouchine, N., et al. (2006). Comparative genomics of the lactic acid bacteria. *Proceedings of the National Academy of Sciences*, 103 (42): 15611-15616. doi: 10.1073/pnas.0607117103.

Makarova, K. S., Aravind, L., Grishin, N. V., Rogozin, I. B. & Koonin, E. V. (2002). A DNA repair system specific for thermophilic Archaea and bacteria predicted by genomic context analysis. *Nucleic Acids Research*, 30 (2): 482-96.

Mathiesen, G., Sørvig, E., Blatny, J., Naterstad, K., Axelsson, L. & Eijsink, V. G. H. (2004). High-level gene expression in *Lactobacillus plantarum* using a pheromone-regulated bacteriocin promoter. *Letters in Applied Microbiology*, 39 (2): 137-143. doi: doi:10.1111/j.1472-765X.2004.01551.x.

Mathiesen, G., Sveen, A., Piard, J. C., Axelsson, L. & Eijsink, V. G. (2008). Heterologous protein secretion by *Lactobacillus plantarum* using homologous signal peptides. *Journal of Applied Microbiology*, 105 (1): 215-26. doi: 10.1111/j.1365-2672.2008.03734.x.

Mathiesen, G., Sveen, A., Brurberg, M. B., Fredriksen, L., Axelsson, L. & Eijsink, V. G. H. (2009). Genome-wide analysis of signal peptide functionality in *Lactobacillus plantarum* WCFS1. *BMC Genomics*, 10 (1): 425. doi: 10.1186/1471-2164-10-425.

Michon, C., Langella, P., Eijsink, V. G., Mathiesen, G. & Chatel, J. M. (2016). Display of recombinant proteins at the surface of lactic acid bacteria: strategies and applications. *Microbial Cell Factories*, 15: 70. doi: 10.1186/s12934-016-0468-9.

Mierau, I. & Kleerebezem, M. (2005). 10 years of the nisin-controlled gene expression system (NICE) in *Lactococcus lactis*. *Applied Microbiology and Biotechnology*, 68 (6): 705-717. doi: 10.1007/s00253-005-0107-6.

Mohamadzadeh, M., Duong, T., Sandwick, S. J., Hoover, T. & Klaenhammer, T. R. (2009). Dendritic cell targeting of *Bacillus anthracis* protective antigen expressed by *Lactobacillus acidophilus* protects mice from lethal challenge. *Proceedings of the National Academy of Sciences*, 106 (11): 4331-4336. doi: 10.1073/pnas.0900029106.

Mojica, F. J., Ferrer, C., Juez, G. & Rodriguez-Valera, F. (1995). Long stretches of short tandem repeats are present in the largest replicons of the Archaea *Haloferax mediterranei* and *Haloferax volcanii* and could be involved in replicon partitioning. *Molecular Microbiology*, 17 (1): 85-93.

Molenaar, D., Bringel, F., Schuren, F. H., de Vos, W. M., Siezen, R. J. & Kleerebezem, M. (2005). Exploring *Lactobacillus plantarum* genome diversity by using microarrays. *Journal of Bacteriology*, 187 (17): 6119-27. doi: 10.1128/jb.187.17.6119-6127.2005.

Nakata, A., Amemura, M. & Makino, K. (1989). Unusual nucleotide arrangement with repeated sequences in the *Escherichia coli* K-12 chromosome. *Journal of Bacteriology*, 171 (6): 3553-6.

Nelson, K. E., Clayton, R. A., Gill, S. R., Gwinn, M. L., Dodson, R. J., Haft, D. H., Hickey, E. K., Peterson, J. D., Nelson, W. C., Ketchum, K. A., et al. (1999). Evidence for lateral gene transfer between Archaea and bacteria from genome sequence of *Thermotoga maritima*. *Nature*, 399 (6734): 323-9. doi: 10.1038/20601.

Neutra, M. R. & Kozlowski, P. A. (2006). Mucosal vaccines: the promise and the challenge. *Nature Review Immunology*, 6 (2): 148-58. doi: 10.1038/nri1777.

Nguyen, H.-M., Mathiesen, G., Stelzer, E. M., Pham, M. L., Kuczkowska, K., Mackenzie, A., Agger, J. W., Eijsink, V. G. H., Yamabhai, M., Peterbauer, C. K., et al. (2016). Display of a β-mannanase and a chitosanase on the cell surface of *Lactobacillus plantarum* towards the development of whole-cell biocatalysts. *Microbial Cell Factories*, 15 (1): 169. doi: 10.1186/s12934-016-0570-z.

Nguyen, T.-T., Nguyen, T.-H., Maischberger, T., Schmelzer, P., Mathiesen, G., Eijsink, V. G., Haltrich, D. & Peterbauer, C. K. (2011). Quantitative transcript analysis of the inducible expression system pSIP: comparison of the overexpression of *Lactobacillus* spp. β-galactosidases in *Lactobacillus plantarum*. *Microbial cell factories*, 10: 46-46. doi: 10.1186/1475-2859-10-46.

Nieuwenhuizen, N. E., Kulkarni, P. S., Shaligram, U., Cotton, M. F., Rentsch, C. A., Eisele, B., Grode, L. & Kaufmann, S. H. E. (2017). The Recombinant Bacille Calmette–Guérin Vaccine VPM1002: Ready for Clinical Efficacy Testing. *Frontiers in Immunology*, 8: 1147. doi: 10.3389/fimmu.2017.01147.

Oh, J. H. & van Pijkeren, J. P. (2014). CRISPR-Cas9-assisted recombineering in *Lactobacillus reuteri*. *Nucleic Acids Research*, 42 (17): e131. doi: 10.1093/nar/gku623.

Okkels, L. M. & Andersen, P. (2004). Protein-protein interactions of proteins from the ESAT-6 family of *Mycobacterium tuberculosis*. *Journal of Bacteriology*, 186 (8): 2487-91.

Paul, E., Albert, A., Ponnusamy, S., Venkatesan, S. & Govindan Sadasivam, S. (2018). Chromosomal integration of heterologous oxalate decarboxylase in *Lactobacillus plantarum* WCFS1 using mobile genetic element Ll.LtrB. *Archives of Microbiology*. doi: 10.1007/s00203-018-1585-0.

Pinho, M. G., Kjos, M. & Veening, J. W. (2013). How to get (a)round: mechanisms controlling growth and division of coccoid bacteria. *Nat Rev Microbiol*, 11 (9): 601-14. doi: 10.1038/nrmicro3088.

Risøen, P. A., Brurberg, M. B., Eijsink, V. G. H. & Nes, I. F. (2000).

Functional analysis of promoters involved in quorum sensing-based regulation of bacteriocin production in *Lactobacillus*. *Molecular Microbiology*, 37 (3): 619-628. doi: 10.1046/j.1365-2958.2000.02029.x.

Rossi, A., Kontarakis, Z., Gerri, C., Nolte, H., Holper, S., Kruger, M. & Stainier, D. Y. (2015). Genetic compensation induced by deleterious mutations but not gene knockdowns. *Nature*, 524 (7564): 230-3. doi: 10.1038/nature14580.

Rud, I., Jensen, P. R., Naterstad, K. & Axelsson, L. (2006). A synthetic promoter library for constitutive gene expression in *Lactobacillus plantarum*. *Microbiology*, 152 (Pt 4): 1011-9. doi: 10.1099/mic.0.28599-0.

Russell, D. G., Barry, C. E. & Flynn, J. L. (2010). Tuberculosis: What We Don't Know Can, and Does, Hurt Us. *Science*, 328 (5980): 852-856. doi: 10.1126/science.1184784.

Sampson, T. R., Saroj, S. D., Llewellyn, A. C., Tzeng, Y. L. & Weiss, D. S. (2013). A CRISPR/Cas system mediates bacterial innate immune evasion and virulence. *Nature*, 497 (7448): 254-7. doi: 10.1038/nature12048.

Sander, J. D. & Joung, J. K. (2014). CRISPR-Cas systems for editing, regulating and targeting genomes. *Nature Biotechnology*, 32: 347. doi: 10.1038/nbt.2842.

Sartori, A. M. (2004). A review of the varicella vaccine in immunocompromised individuals. *International Journal of Infectious Diseases*, 8 (5): 259-70. doi: 10.1016/j.ijid.2003.09.006.

Sasikumar, P., Gomathi, S., Anbazhagan, K., Baby, A. E., Sangeetha, J. & Selvam, G. S. (2014). Genetically engineered *Lactobacillus plantarum* WCFS1 constitutively secreting heterologous oxalate decarboxylase and degrading oxalate under in vitro. *Current Microbiology*, 69 (5): 708-15. doi: 10.1007/s00284-014-0644-2.

Song, A. A.-L., In, L. L. A., Lim, S. H. E. & Rahim, R. A. (2017). A review on *Lactococcus lactis*: from food to factory. *Microbial Cell Factories*, 16 (1): 55. doi: 10.1186/s12934-017-0669-x.

Song, X., Huang, H., Xiong, Z., Ai, L. & Yang, S. (2017). CRISPR-Cas9(D10A) Nickase-Assisted Genome Editing in *Lactobacillus casei*. *Applied Environmental Microbiology*, 83 (22). doi: 10.1128/aem.01259-17.

Sorek, R., Kunin, V. & Hugenholtz, P. (2008). CRISPR--a widespread system that provides acquired resistance against phages in bacteria and archaea. *Nature Review Microbiology*, 6 (3): 181-6. doi: 10.1038/nrmicro1793.

Sorg, R. A., Kuipers, O. P. & Veening, J.-W. (2015). Gene Expression Platform for Synthetic Biology in the Human Pathogen *Streptococcus pneumoniae*. *ACS Synthetic Biology*, 4 (3): 228-239. doi: 10.1021/sb500229s.

Stamsås, G. A., Myrbråten, I. S., Straume, D., Salehian, Z., Veening, J.-W., Håvarstein, L. S. & Kjos, M. (2018). CozEa and CozEb play overlapping and essential roles in controlling cell division in *Staphylococcus aureus*. *Molecular Microbiology*, 109 (5): 615-632. doi: 10.1111/mmi.13999.

Steidler, L., Neirynck, S., Huyghebaert, N., Snoeck, V., Vermeire, A., Goddeeris, B., Cox, E., Remon, J. P. & Remaut, E. (2003). Biological containment of genetically modified *Lactococcus lactis* for intestinal delivery of human interleukin 10. *Nature Biotechnology*, 21 (7): 785-9. doi: 10.1038/nbt840.

Sternberg, S. H., Redding, S., Jinek, M., Greene, E. C. & Doudna, J. A. (2014). DNA interrogation by the CRISPR RNA-guided endonuclease Cas9. *Nature*, 507: 62. doi: 10.1038/nature13011

Su, T., Liu, F., Gu, P., Jin, H., Chang, Y., Wang, Q., Liang, Q. & Qi, Q. (2016). A CRISPR-Cas9 Assisted Non-Homologous End-Joining Strategy for One-step Engineering of Bacterial Genome. *Scientific Reports*, 6: 37895. doi: 10.1038/srep37895.

Sun, Z., Harris, H. M. B., McCann, A., Guo, C., Argimón, S., Zhang, W., Yang, X., Jeffery, I. B., Cooney, J. C., Kagawa, T. F., et al. (2015). Expanding the biotechnology potential of lactobacilli through comparative genomics of 213 strains and associated genera. *Nature Communications*, 6: 8322. doi: 10.1038/ncomms9322.

Sutcliffe, I. C. & Harrington, D. J. (2002). Pattern searches for the identification of putative lipoprotein genes in Gram-positive bacterial genomes. *Microbiology*, 148 (Pt 7): 2065-77. doi: 10.1099/00221287-148-7-2065.

Sørvig, E., Grönqvist, S., Naterstad, K., Mathiesen, G., Eijsink, V. G. H. & Axelsson, L. (2003). Construction of vectors for inducible gene expression in *Lactobacillus sakei* and *Lactobacillus plantarum*. *FEMS Microbiology Letters*, 229 (1): 119-126. doi: 10.1016/S0378-1097(03)00798-5.

Sørvig, E., Mathiesen, G., Naterstad, K., Eijsink, V. G. H. & Axelsson, L. (2005a). High-level, inducible gene expression in *Lactobacillus sakei* and *Lactobacillus plantarum* using versatile expression vectors. *Microbiology*, 151 (7): 2439-2449. doi: doi:10.1099/mic.0.28084-0.

Sørvig, E., Skaugen, M., Naterstad, K., Eijsink, V. G. H. & Axelsson, L. (2005b). Plasmid p256 from *Lactobacillus plantarum* represents a new type of replicon in lactic acid bacteria, and contains a toxin–antitoxin-like plasmid maintenance system. *Microbiology*, 151 (2): 421-431. doi: doi:10.1099/mic.0.27389-0.

Tauer, C., Heinl, S., Egger, E., Heiss, S. & Grabherr, R. (2014). Tuning constitutive recombinant gene expression in *Lactobacillus plantarum*. *Microbial Cell Factories*, 13 (1): 150. doi: 10.1186/s12934-014-0150-z.

Tenaillon, O., Denamur, E. & Matic, I. (2004). Evolutionary significance of stress-induced mutagenesis in bacteria. *Trends in Microbiology*, 12 (6): 264-270. doi: https://doi.org/10.1016/j.tim.2004.04.002.

Tjåland, R. (2011). *Secretion and anchoring of Mycobacterium tuberculosis antigens in Lactobacillus plantarum*. Ås: Norwegian University of Life Sciences.

Toussaint, B., Chauchet, X., Wang, Y., Polack, B. & Gouëllec, A. L. (2013). *Live-attenuated bacteria as a cancer vaccine vector*, 12: Taylor & Francis. pp. 1139-1154.

van der Els, S., James, J. K., Kleerebezem, M. & Bron, P. A. (2018). Versatile Cas9-Driven Subpopulation Selection Toolbox for *Lactococcus lactis*. *Applied and Environmental Microbiology*, 84 (8). doi: 10.1128/aem.02752-17.

van Pijkeren, J. P. & Britton, R. A. (2014). Precision genome engineering in lactic acid bacteria. *Microbial Cell Factories*, 13 (1): S10. doi: 10.1186/1475-2859-13-S1-S10.

van Roosmalen, M. L., Geukens, N., Jongbloed, J. D., Tjalsma, H., Dubois, J. Y., Bron, S., van Dijl, J. M. & Anne, J. (2004). Type I signal peptidases of Gram-positive bacteria. *Biochimica et Biophysica Acta*, 1694 (1-3): 279-97. doi: 10.1016/j.bbamcr.2004.05.006.

Watson, J. D., Baker, T. A., Bell, S. P., Gann, A. & Losick, R. (2014). *Molecular Biology of the Gene*. Cold Spring Harbor, New York: Pearson.

Wegmann, U., O'Connell-Motherway, M., Zomer, A., Buist, G., Shearman, C., Canchaya, C., Ventura, M., Goesmann, A., Gasson, M. J., Kuipers, O. P., et al. (2007). Complete Genome Sequence of the Prototype Lactic Acid Bacterium *Lactococcus lactis* MG1363. *Journal of Bacteriology*, 189 (8): 3256-3270. doi: 10.1128/jb.01768-06.

Wells, J. M. & Mercenier, A. (2008). Mucosal delivery of therapeutic and prophylactic molecules using lactic acid bacteria. *Nature Review Microbiology*, 6 (5): 349-62. doi: 10.1038/nrmicro1840.

Yang, B., Qi, H., Gu, Z., Zhang, H., Chen, W., Chen, H. & Chen, Y. Q. (2017). Characterization of the triple-component linoleic acid isomerase in *Lactobacillus plantarum* ZS2058 by genetic manipulation. *Journal of Applied Microbiology*, 123 (5): 1263-1273. doi: doi:10.1111/jam.13570.

Yang, P., Wang, J. & Qi, Q. (2015). Prophage recombinases-mediated genome engineering in *Lactobacillus plantarum*. *Microbial Cell Factories*, 14 (1): 154. doi: 10.1186/s12934-015-0344-z.

Yeeles, J. T. P. & Dillingham, M. S. (2010). The processing of double-stranded DNA breaks for recombinational repair by helicase–nuclease complexes. *DNA Repair*, 9 (3): 276-285. doi: https://doi.org/10.1016/j.dnarep.2009.12.016.

Øverland, L. (2013). *Secretion and anhoring of proteins in Lactobacillus plantarum: Studies of a dendritic cell-targeted Mycobacterium tuberculosis antigen*. Ås: Norwegian Unversity of Life Sciences.

7 Appendix

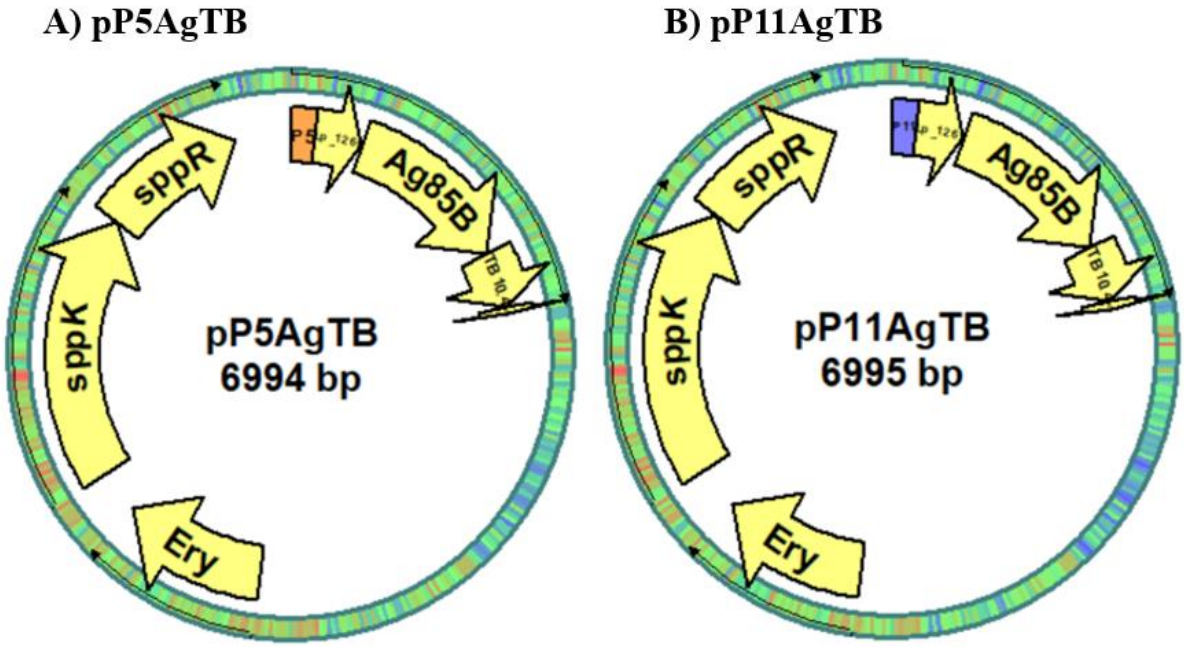

Figure A-1. Plasmid maps of constitutive production of AgTB. The inducible promoter P_{sppA} of the pLp1262_InvS backbone is replaced by A) the weak constitutive promoter P_5 (orange), B) the strong constitutive promoter P_{11} (purple). Downstream of the promoters is the lipo-anchored hybrid antigen Ag85B_TB10.4. The SppK and SppR genes of the inducible system are not removed during construction of the vectors. Both vectors contain an Erythromycin (Ery) resistance gene.

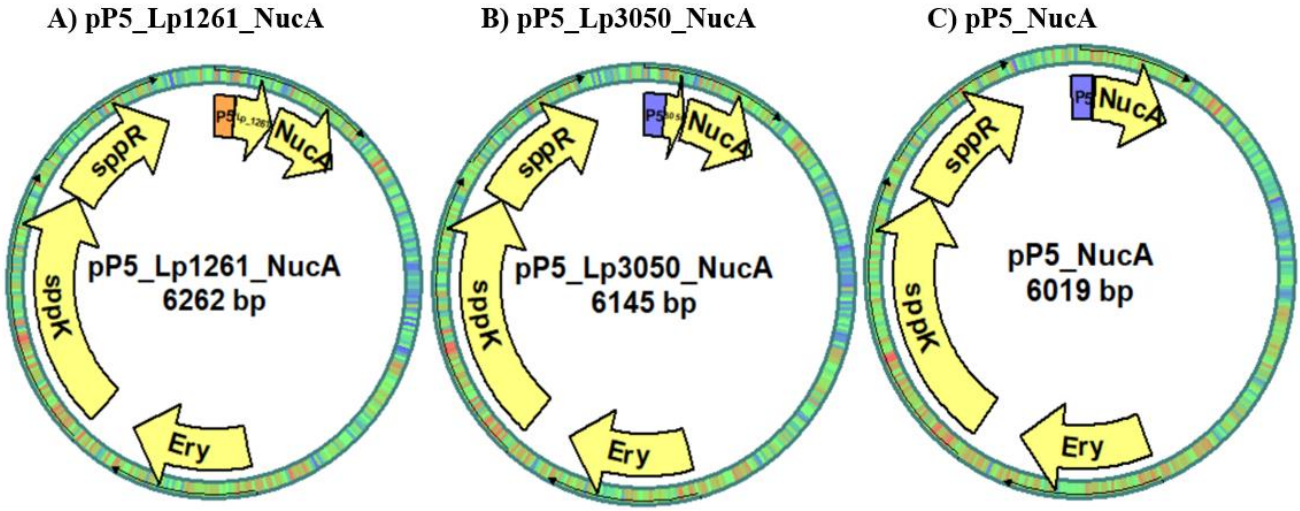

Figure A-2. Plasmid maps of constitutive production of the reporter protein NucA. Constitutive production of A) Lp_1261 anchored NucA, B) Lp_3050 secreted NucA, C) cytoplasmic NucA. The SppK and SppR genes of

the inducible system are not removed during construction of the vectors. Both vectors contain an Erythromycin (Ery) resistance gene.

Norges miljø- og biovitenskapelige universitet
Noregs miljø- og biovitskapelege universitet
Norwegian University of Life Sciences

Postboks 5003
NO-1432 Ås
Norway